K.N.TOOSI UNVERSITY OF TECHNOLOGY

ADVANCED ANALYTICAL AERIAL TRIANGULATION

Written by:
Dr. Hamid Ebadi

Aug 2006

CHAPTER 1

INTRODUCTION

Aerial triangulation is a general term for photogrammetric methods of coordinating points on the ground using a series of overlapping aerial photographs (Faig, 1985). Although the major application of aerial triangulation is for mapping purposes, nowadays it has been applied to a variety of fields such as terrestrial photogrammetry, control densification, and cadastral surveys.

1. 1. History of Aerial Triangulation

Aerial triangulation has gone through different stages in the past; namely, radial, strip, and block triangulation

1. 1. 1. Radial Triangulation

Radial triangulation is a graphical approach and based on the fact that angles measured in a photograph at the iso-centre, located in the middle of line connecting the principal point and photo-nadir, are true horizontal angles and can be used for planimetric triangulation. For a vertical photography, the principal point and the photo-nadir coincide, therefore, the fiducial centre is a suitable approximation of iso-centre for this method. In this approach, the principal points of the neighboring photographs are transferred and the horizontal rays can then be drawn for each photo. These planimetric bundles can be put together along a strip or in a block using two ground control points. The other points can be defined by multiple intersections.

Radial triangulation was used in 1950s in which stereo and slotted templates layouts provided photo-control for mapping purposes. Although this simple technique provided the required accuracy of the day, it was limited by the large physical space required for the layout. Airplane hangars were usually used for this purpose.

1. 1. 2. Strip Triangulation

Strip triangulation was developed in the 1920s, where a Multiplex instrument was used to recreate the aerial photography mission. It is based on dependent pair relative orientation and scale transfer to ensure uniform scale along the strip. The sequential dependent pair relative orientation plus scale transfer starting from a controlled model is known as cantilever extension which is equivalent to an open traverse in surveying. If ground control points are used at the end or in between, the method is called "bridging" which is similar to a controlled traverse in surveying.

Mechanical or graphical interpolation technique were then used to fit the measured strip coordinates to the ground control. Numerical strip adjustments started in the 1960s when electronic digital computers became available. A number of polynomial interpolation adjustment formulations were developed for this purpose(Schut, 1968).

The transition from analog aerial triangulation to analytical procedure was realized with the advent of computers (e.g., analytical relative orientation, absolute orientation, etc). The input for fully analytical aerial triangulation is photo coordinates measured in mono or stereo mode using comparators.

1. 1. 3. Block Triangulation

Block triangulation (bundles or independent models) provides the best internal strength compared to strip triangulation (Ackermann, 1975). The available tie points in consecutive strips assists in the roll angle recovery which is one of the weaknesses inherent in strip triangulation. In terms of the computational aspect, aerial triangulation methods are categorized as: analog, semi-analytical, analytical, and digital triangulation.

1. 1. 3. 1 Analog Aerial Triangulation

This method uses a "first order stereo" plotter to carry out relative and approximate absolute orientation of the first model and cantilever extension. The strip or block adjustment is then performed using the resulting strip coordinates.

1. 1. 3. 2 Semi-Analytical Aerial Triangulation

Relative orientation of each individual model is performed using a precision plotter (e.g., Wild A10). The resulting model coordinates are introduced in a rigorous simultaneous independent model block adjustment. Independent models can also be linked together analytically to form strips which are then used for strip adjustment or block adjustment with strips.

1. 1. 3. 3. Analytical Aerial Triangulation

The input for analytical aerial triangulation are image coordinates measured by a comparator (in stereo mode or mono mode plus point transfer device). A bundle block adjustment is then performed by using all image coordinates measured in all photographs.

An analytical plotter in comparator mode can also be used to measure the image coordinates.

1. 1. 3. 4. Digital Aerial Triangulation

This method uses a photogrammetric workstation which can display digital images. Selection and transfer of tie points and measurement tasks that are performed manually in analytical triangulation are automated using image matching techniques. The procedure is fully automatic, but allows interactive guidance and interference.

1. 1. 4. Control Requirements for Photogrammetric Blocks

Any block consisting of two or more overlapping photographs requires that it be absolutely oriented to the ground coordinate system. The 3D spatial similarity transformation with 7 parameters (3 rotations, 3 translations, 1 scale) is usually employed for absolute orientation and requires at least 2 horizontal and 3 vertical control points. Due to some influences caused by transfer errors (e.g., image coordinate measurements of conjugate points), and extrapolation beyond the mapping area, the theoretical minimum control requirement is unrealistic.

Theoretical and practical studies (Ackermann, 1966, 1974 and Brown, 1979) showed that only planimetric points along the perimeter of the block and relatively dense chains of vertical points across the block are necessary to relate the image coordinate system to the object coordinate system. These measures also ensure the geometric stability of the block as well as control the error propagation.

1. 1. 4. 1. Auxiliary Data as Control Information

Perimeter control for planimetry has reduced the number of control points and required terrestrial work for a photogrammetric block. However, the dense chains of vertical control demand additional surveys. A number of studies (Ackermann, 1984, Blais and Chapman, 1984, Faig, 1979) have been carried out to reduce the number of control points, especially vertical points, using measured exterior orientation parameters at the time of photography. These studies showed that great savings in the number of vertical control points could be achieved .

1. 1. 4. 2. History of Auxiliary Data in Aerial Triangulation

The use of auxiliary data in aerial triangulation goes back to more than half a century. As mentioned by Zorzychi (1972), statoscope, horizon camera, and solar periscope were used to directly measure the exterior orientation parameters of the camera at the time of photography. A statoscope provides the Z coordinate of the exposure stations using differential altimetry. An horizon camera provides the rotation angles of the mapping camera with respect to the horizon. A solar periscope can also determine the rotation angles but they are referred to the sun's location. Airborne ranging was also developed to determine the horizontal positions of the camera stations in order to support the airborne determination of large horizontal networks (Corten, 1960). Except for the statoscope, these instruments were not accepted for practical applications due to accuracy and economic reasons. The Airborne Profile Recorder (APR) was developed in 1960 and used extensively in Canada. This instrument provides the Z coordinate for a number of identifiable features that can be correlated to the profile. This can be achieved by using a statoscope to measure the movements of the aircraft with respect to an isobaric surface and a continuous record of the profile between terrain and aircraft as shown in Figure 1.1.

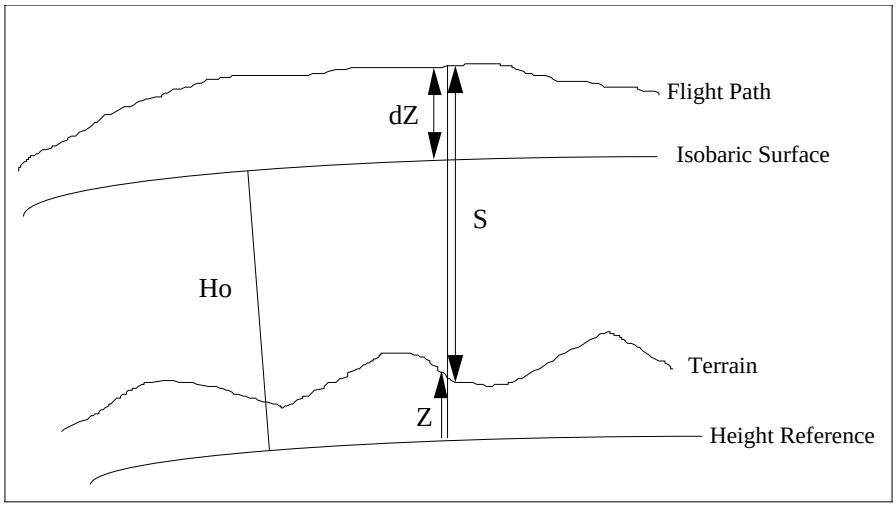

Figure 1. 1. Airborne Profile Recorder Concept

The height information can be derived as:

$$Z = Ho + dZ - S \qquad 1.1$$

Blais (1976) used lake leveling information which makes use of the condition that points along the shoreline of a lake have the same elevation. Gyroscopes were employed to determine the exterior orientation parameters but gained little practical acceptance because of accuracy limitations (Corten and Heimes, 1976). With the advances in inertial and satellite positioning technology, the subject of direct measurements of exterior orientation parameters has gained high attentions in recent years. The Global Positioning System (GPS) can provide the position of the exposure stations while Inertial Navigation System (INS) can determine the attitude of the exposure stations. Ackermann (1984) found that positioning data (X, Y, Z) are more effective than attitude data (ω, Φ, κ) as the latter imply a summation of errors that affect the final object coordinates. The integration of GPS and airborne photogrammetry will be discussed in Chapter 3. The integrated GPS-INS approach to fully recover the exterior orientation parameters is the newest technique (Schwarz, et.al., 1993) but one of the problems is the high cost of INS.

1. 1. 5. GPS Assisted Aerial Triangulation

The Navstar Global Positioning System (GPS) has become generally available and has been considered fully operational on a world wide basis since 1993. It can be used for direct positioning practically anywhere on earth and at any time. GPS has already had a revolutionary impact in various disciplines which are involved with navigation and geodetic positioning. A real time capability is required if GPS is used for navigation purposes. However, it was soon realized that GPS offers a very high accuracy for positioning in combination with post-processing methods.

Since the launch of GPS satellites in early 1980s, photogrammetrists realized the usefulness of GPS for their particular interests (e.g., aerotriangulation). There are four main areas in photogrammetry where GPS can be used (Ackermann, 1994):

1- Establishment of ground control points using terrestrial GPS,
2- GPS controlled survey flight navigation,
3- High precision camera positioning for aerial triangulation,
4- Positioning of other airborne sensors (e.g., laser scanners).

The main purpose of aerial triangulation (AT) is the determination of ground coordinates for a large number of terrain points and the exterior orientation parameters of aerial photographs using as few control points as possible. The best scenario in mapping projects is to determine the exterior orientation parameters accurate enough so that the AT can be neglected. The accuracy for attitude parameters derived from multiple-antenna GPS observations is about 15 arc minutes (Lachapelle et al., 1993) which is still far from what could be obtained from conventional block adjustment. Therefore, aerial triangulation is still one of the important steps in mapping and can not be avoided.

The integration of GPS measurements into photogrammetric blocks allows the accurate determination of coordinates of the exposure stations resulting in a reduction of the number of ground control points to a minimum. Therefore, the goal is to improve the efficiency of aerotriangulation by avoiding ground control points almost completely. The combined adjustment of photogrammetric data and GPS observations can be carried out by introducing GPS observation equations to the conventional block adjustment.

CHAPTER 2

ANALYTICAL AERIAL TRIANGULATION:

In this chapter, conventional aerial triangulation is reviewed. This review encompasses various mathematical models, self calibration technique, additional parameters, and the associated mathematical models.

2. 1. Bundle Blocks

A bundle of rays that originates from an object point and passes through the projective centre to the image points (Figure 2.1) forms the basic computational unit of aerial triangulation. Bundle block adjustment means the simultaneous least squares adjustment of all bundles from all exposure stations, which implicitly includes the simultaneous recovery of the exterior orientation elements of all photographs and the positions of the object points (Faig, 1985).

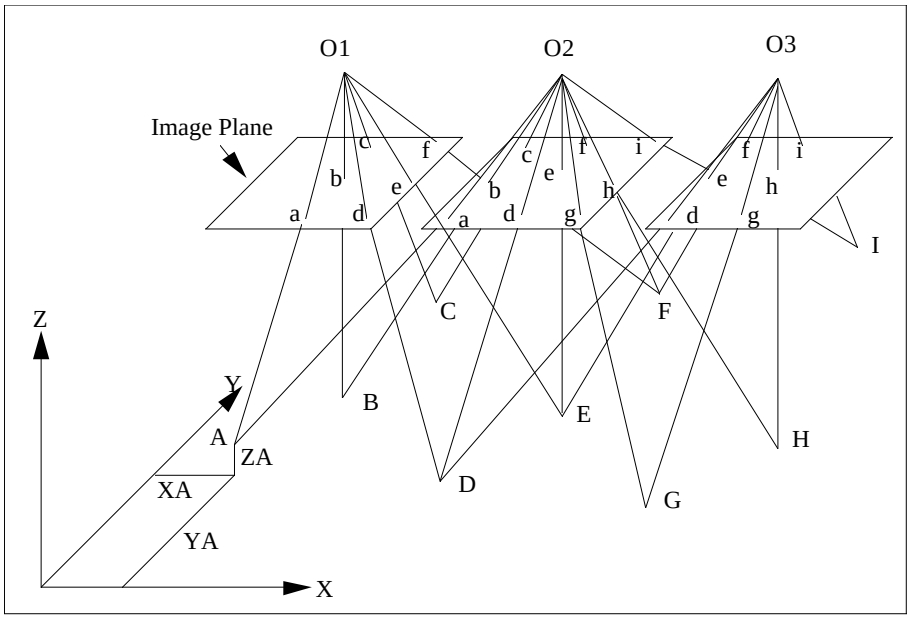

Figure 2.1 Bundle Blocks

The fundamental equation of aerial triangulation is the collinearity equation which states that an object point, its homologous image point, and the perspective centre are collinear (Figure 2.2)

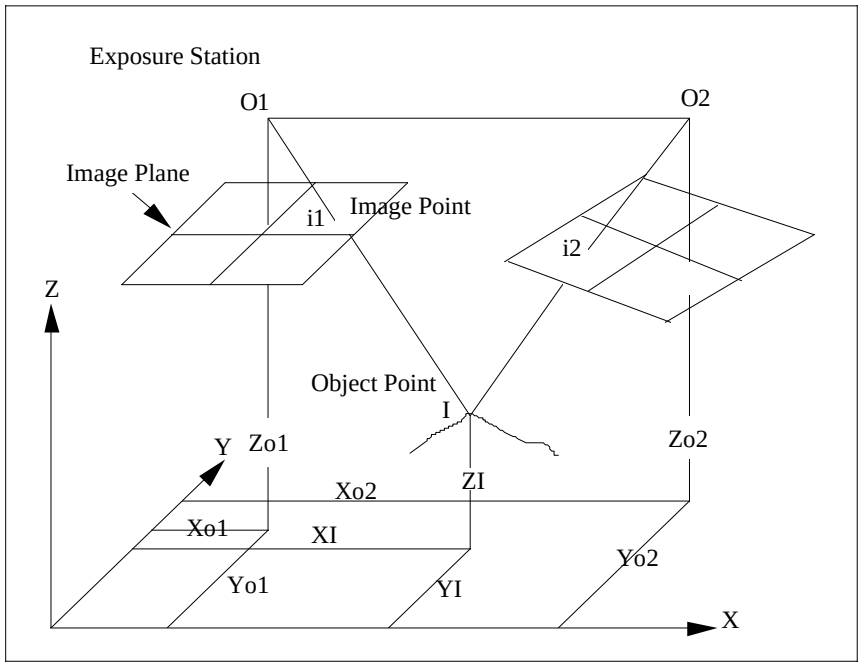

Figure 2.2 Concept of Collinearity Equation

The collinearity equations are given as:

$$F_x = x_i - x_o + c\frac{m_{11}(X_i - X_O) + m_{12}(Y_i - Y_O) + m_{13}(Z_i - Z_O)}{m_{31}(X_i - X_O) + m_{32}(Y_i - Y_O) + m_{33}(Z_i - Z_O)} = 0 \qquad 2.1$$

$$F_y = y_i - y_o + c\,k_y\frac{m_{21}(X_i - X_O) + m_{22}(Y_i - Y_O) + m_{23}(Z_i - Z_O)}{m_{31}(X_i - X_O) + m_{32}(Y_i - Y_O) + m_{33}(Z_i - Z_O)} = 0 \qquad 2.2$$

where

$$M = \begin{bmatrix} m_{11} & m_{12} & m_{13} \\ m_{21} & m_{22} & m_{23} \\ m_{31} & m_{32} & m_{33} \end{bmatrix} = \qquad 2.3$$

$$\begin{bmatrix} \cos(\Phi)\cos(\kappa) & \cos(\omega)\cos(\kappa) + \sin(\omega)\sin(\Phi)\cos(\kappa) & \sin(\omega)\sin(\kappa) - \cos(\omega)\sin(\Phi)\cos(\kappa) \\ -\cos(\Phi)\sin(\kappa) & \cos(\omega)\cos(\kappa) - \sin(\omega)\sin(\Phi)\sin(\kappa) & \sin(\omega)\cos(\kappa) + \cos(\omega)\sin(\Phi)\sin(\kappa) \\ \sin(\Phi) & -\sin(\omega)\cos(\Phi) & \cos(\omega)\cos(\Phi) \end{bmatrix}$$

and

(x_i, y_i)	are the image coordinates,
(x_o, y_o)	are the principal point coordinates,
c	is the camera constant,
m_{ij}	is an element of the rotation matrix,
(X_i, Y_i, Z_i)	are the object point coordinates,
(X_O, Y_O, Z_O)	are the exposure station coordinates,
M	is the rotation matrix,
k_y	is the scale factor for y axis in digital camera (this factor is 1 for film based camera).

There are 6 unknowns in the collinearity equations, namely, the exterior orientation parameters $(X_O, Y_O, Z_O, \omega, \Phi, \kappa)$. The three rotation angles (ω, Φ, κ) are implicit in the rotation matrix M (Equation 2.3). The principal point coordinates (x_o, y_o) and camera constant (c) are considered to be known for the basic bundle approach. However, this might not be true as will be discussed later in this chapter. Strong imaging geometry plus a minimum of three ground control points are needed to solve for the six unknowns per bundle which are then used to determine the unknown object coordinates of other measured image points.

2. 1. 1. Image Coordinate Measurement

A mono or stereo comparator is used to measure the image coordinates (x_i, y_i) which form the basic input into the bundle adjustment. Precision stereo comparators (e.g., Wild STK1) and mono comparators (e.g., Kern MK2) provide an accuracy at the level of 1-3 μm. Analytical plotters such as AC1 in comparator mode can also be used to measure the image coordinates providing 3-5 μm accuracy. It is recommended to observe each point at least twice and to observe the fiducial marks. It is also necessary to transfer points from one image to another when using a mono comparator. However, if the points are targeted on the ground, point transferring is not required.

2. 2. Mathematical Formulations for Bundle Block Adjustment

F_x and F_y in Equations 2.1 and 2.2 may deviate from zero (i.e., perfect case) since the measured image coordinates include random and residual systematic errors. The collinearity equations are non-linear, therefore, they have to be linearized using Taylor's expansion. According to Chapman (1993), 6 different cases can be considered depending on how to treat unknowns and observations.

2. 2. 1 Case # 1

* Observed photo coordinates,

* Known object space coordinates,

* Unknown exterior orientation elements.

The observation equation is given as:

$$W_P = A_{EO}\,\delta_{EO} \tag{2.4}$$

$$W_P = \left(-F_x, -F_y\right)^T \tag{2.5}$$

$$A_{EO} = \begin{bmatrix} \frac{\partial F_x}{\partial X_o} & \frac{\partial F_x}{\partial Y_o} & \frac{\partial F_x}{\partial Z_o} & \frac{\partial F_x}{\partial \omega} & \frac{\partial F_x}{\partial \Phi} & \frac{\partial F_x}{\partial \kappa} \\ \frac{\partial F_y}{\partial X_o} & \frac{\partial F_y}{\partial Y_o} & \frac{\partial F_y}{\partial Z_o} & \frac{\partial F_y}{\partial \omega} & \frac{\partial F_y}{\partial \Phi} & \frac{\partial F_y}{\partial \kappa} \end{bmatrix} \tag{2.6}$$

$$\delta_{EO} = \left(dX_o, dY_o, dZ_o, d\omega, d\Phi, d\kappa\right)^T \tag{2.7}$$

where

W_P is the misclosure vector,

A_{EO} is the design matrix (exterior orientation parameters),

δ_{EO} is the correction vector of exterior orientation parameters,

The correction vector, δ_{EO}, is determined using the least squares approach as:

$$\delta_{EO} = \left(A_{EO}^T P_P A_{EO}\right)^{-1} A_{EO}^T P_P W_P \tag{2.8}$$

$$P_P = C_{l,(P)}^{-1} \tag{2.9}$$

where

P_P is the weight matrix of image coordinates,

$C_{l,(P)}$ is the covariance matrix of image coordinates

The covariance matrix of image coordinates for one image point is defined as:

$$C_{l,(P)} = \begin{bmatrix} \sigma_x^2 & \sigma_{x,y} \\ \sigma_{x,y} & \sigma_y^2 \end{bmatrix} \qquad 2.10$$

Due to non-linearity of the model, an iterative solution method should be exercised until the corrections to the unknown parameters become insignificant. The final exterior orientation parameters can be computed as:

$$X_{EO}^{n} = X_{EO}^{0} + \sum_{i=1}^{n-1} \delta_{EO}^{i} \qquad 2.11$$

where X_{EO}^{n} is the vector of exterior orientation in the nth iteration.

2. 2. 2. Case # 2

* Observed photo coordinates,

* Unknown object space coordinates,

* Unknown exterior orientation elements.

The observation equation is written as:

$$W_P = \overline{A\delta} \qquad 2.12$$

or

$$W_P = \begin{pmatrix} A_{EO} & A_S \end{pmatrix} \begin{pmatrix} \delta_{EO} \\ \delta_S \end{pmatrix} \qquad 2.13$$

where

A_S is the design matrix (object space coordinates),

δ_S is the correction vector of object space coordinates,

$$A_S = \begin{bmatrix} \frac{\partial F_x}{\partial X_i} & \frac{\partial F_x}{\partial Y_i} & \frac{\partial F_x}{\partial Z_i} \\ \frac{\partial F_y}{\partial X_i} & \frac{\partial F_y}{\partial Y_i} & \frac{\partial F_y}{\partial Z_i} \end{bmatrix} \qquad 2.14$$

$$\delta_S = \left(dX_i, dY_i, dZ_i\right)^T \qquad 2.15$$

The correction vector, $\overline{\delta}$, is given as:

$$\begin{pmatrix} \delta_{EO} \\ \delta_S \end{pmatrix} = \left(\begin{bmatrix} A_{EO}^T \\ A_S^T \end{bmatrix} P_P \begin{bmatrix} A_{EO} & A_S \end{bmatrix} \right)^{-1} \begin{bmatrix} A_{EO}^T \\ A_S^T \end{bmatrix} P_P W_P \qquad 2.16$$

or

$$\begin{pmatrix} \delta_{EO} \\ \delta_S \end{pmatrix} = \begin{pmatrix} A_{EO}^T P_P A_{EO} & A_{EO}^T P_P A_S \\ A_S^T P_P A_{EO} & A_S^T P_P A_S \end{pmatrix}^{-1} \begin{pmatrix} A_{EO}^T P_P W_P \\ A_S^T P_P W_P \end{pmatrix} \qquad 2.17$$

2. 2. 3 Case # 3

* Observed photo coordinates,

* Observed object space coordinates,

* Unknown object space coordinates,

* Unknown exterior orientation elements,

The observation equations for observed object space coordinates are written as:

$$f(X_i) = X_i^{observed} - X_i^{unknown} = 0 \qquad 2.18$$

$$f(Y_i) = Y_i^{observed} - Y_i^{unknown} = 0 \qquad 2.19$$

$$f(Z_i) = Z_i^{observed} - Z_i^{unknown} = 0 \qquad 2.20$$

The observation equations in matrix form can be shown as:

$$\begin{pmatrix} A_{EO} & A_S \\ 0 & -I \end{pmatrix} \begin{pmatrix} \delta_{EO} \\ \delta_S \end{pmatrix} = \begin{pmatrix} W_P \\ W_S \end{pmatrix} \qquad 2.21$$

The correction vector, $\overline{\delta}$, is defined as:

$$\begin{pmatrix} \delta_{EO} \\ \delta_S \end{pmatrix} = \begin{pmatrix} A_{EO}^T P_P A_{EO} & A_{EO}^T P_P A_S \\ A_S^T P_P A_{EO} & A_S^T P_P A_S + P_S \end{pmatrix}^{-1} \begin{pmatrix} A_{EO}^T P_P W_P \\ A_S^T P_P W_P - P_S W_S \end{pmatrix} \qquad 2.22$$

where

P_S is the weight matrix of object point coordinates,

W_S is the misclosure vector of object point coordinates.

2. 2. 4 Case # 4

* Observed photo coordinates,

* Observed object space coordinates,

* Unknown object space coordinates,

* Observed exterior orientation elements,

* Unknown exterior orientation elements,

The equations for the observed exterior orientation parameters can be written as:

$$g(X_o) = X_o^{observed} - X_o^{unknown} = 0 \qquad 2.23$$

$$g(Y_o) = Y_o^{observed} - Y_o^{unknown} = 0 \qquad 2.24$$

$$g(Z_o) = Z_o^{observed} - Z_o^{unknown} = 0 \qquad 2.25$$

$$g(\omega) = \omega^{observed} - \omega^{unknown} = 0 \qquad 2.26$$

$$g(\Phi) = \Phi^{observed} - \Phi^{unknown} = 0 \qquad 2.27$$

$$g(\kappa) = \kappa^{observed} - \kappa^{unknown} = 0 \qquad 2.28$$

The observation equations in matrix form can be given as:

$$\begin{pmatrix} A_{EO} & A_S \\ 0 & -I \\ -I & 0 \end{pmatrix} \begin{pmatrix} \delta_{EO} \\ \delta_S \end{pmatrix} = \begin{pmatrix} W_P \\ W_S \\ W_{EO} \end{pmatrix} \qquad 2.29$$

The correction vector is determined as:

$$\begin{pmatrix} \delta_{EO} \\ \delta_S \end{pmatrix} = \begin{pmatrix} A_{EO}^T P_P A_{EO} + P_{EO} & A_{EO}^T P_P A_S \\ A_S^T P_P A_{EO} & A_S^T P_P A_S + P_S \end{pmatrix}^{-1} \begin{pmatrix} A_{EO}^T P_P W_P - P_{EO} W_{EO} \\ A_S^T P_P W_P - P_S W_S \end{pmatrix} \qquad 2.30$$

where

P_{EO} is the weight matrix of exterior orientation parameters,

W_{EO} is the misclosure vector of exterior orientation parameters.

2. 2. 5. Case # 5

* Observed photo coordinates,

* Observed object space coordinates,

* Unknown object space coordinates,

* Observed exterior orientation elements,

* Unknown exterior orientation elements,

* Observed geodetic measurements (e.g., distances)

Observation equation for slope distance is written as:

$$f = d_{ij} - \sqrt{(X_j - X_i)^2 + (Y_j - Y_i)^2 + (Z_j - Z_i)^2} = 0 \qquad 2.31$$

where

d_{ij} is the observed distance between point i and point j,

(X_j, Y_j, Z_j) are the unknown object coordinates of point j,

(X_i, Y_i, Z_i) are the unknown object coordinates of point i.

The observation equations are given as:

$$\begin{pmatrix} A_{EO} & A_S \\ 0 & -I \\ -I & 0 \\ 0 & A_G \end{pmatrix} \begin{pmatrix} \delta_{EO} \\ \delta_S \end{pmatrix} = \begin{pmatrix} W_P \\ W_S \\ W_{EO} \\ W_G \end{pmatrix} \qquad 2.32$$

where

A_G is the design matrix of geodetic observations between points i and j,

$$A_G = \begin{bmatrix} \frac{\partial f}{\partial X_j} & \frac{\partial f}{\partial Y_j} & \frac{\partial f}{\partial Z_j} & \frac{\partial f}{\partial X_i} & \frac{\partial f}{\partial Y_i} & \frac{\partial f}{\partial Z_i} \end{bmatrix} \qquad 2.33$$

and W_G is the misclosure vector of geodetic observation. The correction vector, $\overline{\delta}$, is given as:

$$\overline{\delta} = \begin{pmatrix} \delta_{EO} \\ \delta_S \end{pmatrix} = \begin{pmatrix} A_{EO}^T P_P A_{EO} + P_{EO} & A_{EO}^T P_P A_S \\ A_S^T P_P A_{EO} & A_S^T P_P A_S + P_S + A_G^T P_G A_G \end{pmatrix}^{-1} \times \begin{pmatrix} A_{EO}^T P_P W_P - P_{EO} W_{EO} \\ A_S^T P_P W_P - P_S W_S - A_G^T P_G W_G \end{pmatrix} \qquad 2.34$$

where P_G is the weight matrix of geodetic observations.

2. 2. 6. Case # 6

* Observed photo coordinates,

* Observed object space coordinates,

* Unknown object space coordinates,

* Observed exterior orientation elements,

* Unknown exterior orientation elements,

* Observed geodetic measurements (e.g., distances),

* Unknown interior orientation and additional parameters,

* Observed interior orientation and additional parameters.

The observation equations are written as:

$$\begin{pmatrix} A_{EO} & A_S & A_{IO} \\ 0 & -I & 0 \\ -I & 0 & 0 \\ 0 & A_G & 0 \\ 0 & 0 & -I \end{pmatrix} \begin{pmatrix} \delta_{EO} \\ \delta_S \\ \delta_{IO} \end{pmatrix} = \begin{pmatrix} W_P \\ W_S \\ W_{EO} \\ W_G \\ W_{IO} \end{pmatrix} \qquad 2.35$$

where A_{IO} is the design matrix (derivatives of collinearity equations with respect to interior orientation and additional parameters) and W_{IO} is the misclosure vector of the observed interior orientation and additional parameters.

Interior orientation parameters include the camera constant, principal point coordinates, and Y scale factor for a digital camera scale bias. The equations for observed interior orientation and additional parameters are similar to those of observed exterior orientation parameters (Equations 2. 23 to 2. 28). The correction vector, δ, is computed using the least squares method as:

$$N = \begin{pmatrix} A_{EO}^T P_P A_{EO} + P_{EO} & A_{EO}^T P_P A_S & A_{EO}^T P_P A_{IO} \\ A_S^T P_P A_{EO} & A_S^T P_P A_S + P_S + A_G^T P_G A_G & A_S^T P_P A_{IO} \\ A_{IO}^T P_P A_{EO} & A_{IO}^T P_P A_S & A_{IO}^T P_P A_{IO} + P_{IO} \end{pmatrix} \qquad 2.36$$

$$U = \begin{pmatrix} A_{EO}^T P_P W_P - P_{EO} W_{EO} \\ A_S^T P_P W_P - P_S W_S + A_G^T P_G W_G \\ A_{IO}^T P_P W_P - P_{IO} W_{IO} \end{pmatrix} \qquad 2.37$$

where P_{IO} is the weight matrix of interior orientation and additional parameters.

$$\bar{\delta} = \begin{pmatrix} \delta_{EO} \\ \delta_S \\ \delta_{IO} \end{pmatrix} \qquad 2.38$$

$$\bar{\delta} = N^{-1}U \qquad 2.39$$

In order to compensate for systematic errors such as lens distortion, atmospheric refraction and the digital camera scale bias and improve the collinearity equation model, distortion or additional parameters , $(\Delta x_p, \Delta y_p)$, are introduced into the basic collinearity equations as:

$$x_i - x_o + \Delta x_p = -c\frac{m_{11}(X_i - X_O) + m_{12}(Y_i - Y_O) + m_{13}(Z_i - Z_O)}{m_{31}(X_i - X_O) + m_{32}(Y_i - Y_O) + m_{33}(Z_i - Z_O)} \qquad 2.40$$

$$y_i - y_o + \Delta y_p = -c\,k_y\frac{m_{21}(X_i - X_O) + m_{22}(Y_i - Y_O) + m_{23}(Z_i - Z_O)}{m_{31}(X_i - X_O) + m_{32}(Y_i - Y_O) + m_{33}(Z_i - Z_O)} \qquad 2.41$$

where $(\Delta x_p, \Delta y_p)$ are functions of several unknown parameters and are estimated simultaneously with the other unknowns in the equations. A complete recovery of all parameters (exterior orientation, object space coordinates, interior orientation, and additional parameters) is possible under certain conditions without the need for additional ground control points. This approach is called a "self calibrating bundle block adjustment".

Two general principles should be considered when applying additional parameters (Faig, 1985):

* The number of parameters should be as small as possible to avoid over-parametrization and to keep the additional computational effort small,
* The parameters are to be selected such that their correlations with other unknowns are negligible, otherwise the normal equation matrix becomes ill-conditioned or singular.

Since the same stable and metric aerial camera is used to photograph the entire project area in one flight mission for most topographic mapping projects, the interior orientation parameters and additional parameters can be assumed to be the same for all photos. Brown (1976) calls this approach "block invariant" which is most favorable for computational efficiency. If different cameras are used for the area being mapped, then the " block variant" approach is applied. In this approach, the parameters are only valid for a group of photographs (Ebner, 1976). If a non-metric camera is used for close range applications, a "photo variant " approach can be applied in which there are new additional parameters are considered for each photograph.

2. 2. 7. Mathematical Models for Additional Parameters

There are mainly two types of modeling for additional or distortion parameters; the first approach models the physical causes of image deformation (physical model) while the second approach empirically models the effects of image deformation (algebraic model).

2. 2. 7. 1. Physical Model

Four types of distortions are considered in this approach, namely; radial lens distortion, decentring distortion, and film shrinkage , and non-perpendicularity of the comparator axes in case of film-based imagery. Thus:

$$\Delta x_p = dr_x + dp_x + dg_x \qquad 2.42$$

$$\Delta y_p = dr_y + dp_y + dg_y \qquad 2.43$$

where

$(\Delta x_p, \Delta y_p)$ are total distortions in x and y axes,

(dr_x, dr_y) are the contributions of radial lens distortion,

(dp_x, dp_y) are the contributions of the decentring lens distortions,

(dg_x, dg_y) are the contributions of the film shrinkage and non-perpendicularity of the comparator axes.

The radial lens distortion is expressed as:

$$dr = k_1 r^3 + k_2 r^5 + k_3 r^7 \qquad 2.45$$

or in x and y components:

$$dr_x = \frac{(x - x_o)}{r} dr = (k_1 r^2 + k_2 r^4 + k_3 r^6)(x - x_o) \qquad 2.46$$

$$dr_y = \frac{(y - y_o)}{r} dr = (k_1 r^2 + k_2 r^4 + k_3 r^6)(y - y_o) \qquad 2.47$$

where

k_1, k_2, k_3 are the coefficients of the polynomial,

r is radial distance of the measured point from the principal point,

(x_o, y_o) are the principal point coordinates,

(x, y) are the measured image coordinates.

The decentring lens distortion model is given as (Brown, 1966):

$$dp_x = p_1\left(r^2 + 2(x - x_o)^2\right) + 2\,p_2(x - x_o)(y - y_o) \qquad 2.48$$

$$dp_y = p_2\left(r^2 + 2\left(y - y_o\right)^2\right) + 2\,p_1(x - x_o)(y - y_o) \qquad 2.49$$

where

$\left(dp_x, dp_y\right)$ are the decentring distortions in the x and y directions,

p_1, p_2 are the coefficients of the decentring distortion model.

The affinity model is used to model film shrinkage and non-perpendicularity of the comparator axes (Moniwa, 1977):

$$dg_x = A\left(y - y_o\right) \qquad 2.50$$

$$dg_y = B\left(y - y_o\right) \qquad 2.51$$

where

$\left(dg_x, dg_y\right)$ are the distortions contributed by film shrinkage and non-perpendicularity of the comparator axes,

A, B are the coefficients of the affinity model.

The total number of unknowns per image is 16 (6 for exterior orientation, 3 for interior orientation, and 7 for additional or distortion parameters, $k_1, k_2, k_3, p_1, p_2, A, B$). One more unknown is added to interior orientation parameters, y scale factor k_y, if a digital camera is used.

The disadvantage of using this method is that there could be high correlations between the additional parameters themselves and/or with the interior and exterior orientation parameters. In addition to this, it may not be able to efficiently detect or compensate for irregular image deformations.

2. 2. 7. 2. Mathematical or Algebraic Modeling

In this approach, the combined effects of all systematic errors are modeled using functions that do not necessarily describe the physical nature of the distortions. Orthogonal polynomials have been popular choices of algebraic models. El Hakim (1979) used spherical harmonics to model the systematic errors. His formulations are expressed as:

$$\Delta x_p = (x - x_o)T \qquad 2.52$$

$$\Delta y_p = (y - y_o)T \qquad 2.53$$

where T is the harmonic function

$$T = a_{00} + a_{11}\cos\lambda + b_{11}\sin\lambda + a_{20}r + a_{22}r\cos^2\lambda + b_{22}r\sin 2\lambda + a_{31}r^2\cos\lambda + b_{31}r^2\sin\lambda + a_{33}\cos 3\lambda + b_{33}\sin 3\lambda + \ldots\ldots \qquad 2.54$$

and

$$\lambda = \tan^{-1}\left(\frac{y - y_o}{x - x_o}\right) \qquad 2.55$$

where a_{ij}, b_{ij} are the coefficients of harmonic function T.

Brown (1976) also introduced the following orthogonal functions:

$$\Delta x_P = a_1 x + a_2 y + a_3 xy + a_4 y^2 + a_5 x^2 y + a_6 x y^2 + a_7 x^2 y^2 + \qquad 2.56$$

$$\frac{x}{c}[a_{13}\left(x^2-y^2\right)+a_{14}x^2y^2+a_{15}\left(x^4-y^4\right)]+$$
$$x[a_{16}\left(x^2+y^2\right)^2+a_{17}\left(x^2+y^2\right)^4+a_{18}\left(x^2+y^2\right)^6]$$
$$\Delta y_P = a_8 xy + a_9 x^2 + a_{10} x^2 y + a_{11} x y^2 + a_{12} x^2 y^2 + \qquad 2.57$$
$$\frac{y}{c}[a_{13}\left(x^2-y^2\right)+a_{14}x^2y^2+a_{15}\left(x^4-y^4\right)]+$$
$$y[a_{16}\left(x^2+y^2\right)^2+a_{17}\left(x^2+y^2\right)^4+a_{18}\left(x^2+y^2\right)^6]$$

where

a_1 to a_{18}	are the coefficients of an orthogonal function
c	is the camera constant,
(x, y)	are the measured image coordinates.

The advantage of using this method is that the parameters of these functions are not correlated. Implementing both the physical and algebraic models improves the accuracy of the bundle block adjustment compared to the basic bundle block adjustment.

2. 2. 7. 3. Results from Conventional Self Calibration Blocks

El Hakim (1979) summarized the results of studies carried out by Grün (1978) and Salmenpera et al. (1974) as :

Table 2.1. Self Calibration Block Adjustment Results

	Block Parameters		Without Self Calibration			With Self Calibration		
	Scale	Size	σ_0	μ_{XY}	μ_Z	σ_0	μ_{XY}	μ_Z
Grün	28000	104	5.3	8.8	15.8	3.3	5.2	12.2
Salmenpera	4000	94	5.4	4.5	8.5	5.1	3.4	7.8

All units are given in photo scale in μm and the overlap was 60%. As seen from Table 2.1, an improvement factor in the range of 1.3 to 1. 7 in planimetry and range of 1.05 to 1.3 for height can be achieved for the fully controlled blocks. It can be concluded that bundle block adjustment yields an absolute accuracy which is comparable with conventional terrestrial surveying (Faig, 1985).

2. 2. 8. Introducing Geodetic Observations to the Photogrammetric Block Adjustment

Conventionally, the adjustment of geodetic and photogrammetric measurements has been carried out in two separate steps. First, the terrestrial survey is adjusted to provide a unique set of coordinates and a variance-covariance matrix for the ground control points that are used as control for the photogrammetric solutions.

Combined photogrammetric-geodetic adjustment means rigorous and simultaneous adjustment of all geodetic and photogrammetric observations replacing the two steps solution with one step. This approach makes the error analysis and weighting of the observations more realistic.

2. 2. 8. 1. Mathematical Model used for Photogrammetric and Geodetic Observations

There are 9 types of geodetic measurements that can be handled by GAP, namely; slope distances, horizontal distances, zenith angles, horizontal directions, horizontal angles, 2D coordinate differences, 3D coordinate differences, height differences, and azimuth observations. The observation equation for photogrammetric measurements is given as:

$$F_P\left(\hat{X}_{EO}, \hat{X}_S, L_P\right) = 0 \qquad 2.58$$

where

$\hat{X}_S$ is the object coordinates vector,

$\hat{X}_{EO}$ is the exterior orientation parameters vector,

L_P is the photogrammetric measurements vector.

The observation equation for geodetic measurements can be written as:

$$F_G\left(\hat{X}_S, \hat{X}_{DIR}, L_G\right) = 0 \qquad 2.59$$

where

$\hat{X}_{DIR}$ is the vector of zero directions for horizontal direction observations,

L_G is the geodetic measurements vector.

These equations are non-linear and they have to be linearized. The linearized forms of these equations are:

$$W_P + A_{EO}^{O}\hat{X}_{EO} + A_S^P\hat{X}_S + \hat{B}_P\hat{V}_P = 0 \qquad 2.60$$

$$W_G + A_G^S\hat{X}_S + A_{DIR}^G\hat{X}_{DIR} + \hat{B}_G\hat{V}_G = 0 \qquad 2.61$$

where

W_P is the photogrammetric misclosure vector,

W_G is the geodetic misclosure vector.

A_j^i, B_j are the design matrices,

$\hat{V}_P, \hat{V}_G$ are the residual vectors for image coordinates and geodetic observations.

These observations are combined and adjusted simultaneously using least squares. The solution vector (unknown parameters) are computed using the following formula:

$$\hat{X} = (\overline{A}^T\overline{PA})^{-1}(\overline{A}^T\overline{PW}) \qquad 2.62$$

where

$\overline{A}$ is the design matrix composed of various design matrices,

$\overline{P}$ is the weight matrix and function of covariance matrix of various observations,

$\overline{W}$ is the misclosure vector.

The normal equation matrix becomes more general by including geodetic observations into the block adjustment. Some measures (e.g., reordering of unknowns) have to be taken to keep the computational effort within reasonable limits. One of the advantages of integrating different observation types for coordinating points is that a solution can be achieved even though any one of the approaches alone can be under determined.

2. 3. Control Requirements

Any block comprised of two or more overlapping photographs requires to be absolutely oriented to the ground coordinate system. The 3D spatial similarity transformation with 7 parameters (3 rotations, 3 translations, 1 scale) is most frequently utilized for absolute orientation and require at least 2 horizontal and 3 vertical control points. Due to some influences caused by transfer errors and extrapolations beyond the mapping area, use of only the theoretical minimum control is unrealistic.

Theoretical and practical studies (Ackermann, 1966, 1974 and Brown, 1979) showed that planimetric points along the perimeter of the block and relatively dense chains of vertical points across the block are necessary to relate the image coordinate system to the object coordinate system and also to ensure the geometric stability of the block as well as to control the error propagation .

The control requirements are different for mapping purposes and photogrammetric point determination projects. A spacing of 8-10 base lengths in planimetry along the perimeter of the block and dense cross chains (every 2nd strip) at both ends and 6-8 base lengths in between for vertical control are recommended for regular mapping. Ebner (1972) concluded that dense perimeter control (e.g., every two base lengths) and dense net of vertical points within the block (e.g., every 2 base lengths perpendicular to the strip direction) and every 4 base lengths along the strip direction are required for photogrammetric point determination.

The number of control points can be reduced by changing flight parameters, increasing sidelap, and using multiple coverage. Molenaar (1984) found that if the terrestrial surveys was laid out solely to establish perimeter control (e.g., by a traverse), it may lead to a weak geometric configuration, therefore, some cross connections would strengthen the geometry and absolute accuracy.

2. 3. 1. Auxiliary Data As Control Entities

Perimeter control for planimetry has reduced the number of control points in r equired terrestrial work for a photogrammetric block. However, the dense chains of vertical control demand additional surveys. A number of studies (Ackermann, 1984, Blais and Chapman, 1984, Faig, 1979) have been carried out to reduce the number of control points especially vertical points using measured exterior orientation parameters at the time of photography. These studies showed that great savings in vertical control points could be achieved .

2. 3. 2. Mathematical Models for Auxiliary Data

Auxiliary control can be integrated into a photogrammetric block adjustment as additional observation equations properly weighted and adjusted together with the other equations. Ackermann (1984) used the following observation equations for the statoscope, APR, and attitude data in his independent model block adjustment program (PAT-M):

$$V_j^{Stat} = Z_j^{PC} - Z_j^{Stat} - \left(a_0 + a_1 X_j + \ldots\ldots\right) \qquad 2.64$$

$$V_j^{APR} = Z_j - Z_j^{APR} - \left(b_0 + b_1 X_j + \ldots\ldots\right) \qquad 2.65$$

$$V_j^{\omega} = \omega_j - \omega_j^{Nav} - \left(e_0 + e_1 X_j + \ldots\ldots\right) \qquad 2.66$$

$$V_j^{\Phi} = \Phi_j - \Phi_j^{Nav} - \left(d_0 + d_1 X_j + \ldots\ldots\right) \qquad 2.67$$

$$V_j^{\kappa} = \kappa_j - \kappa_j^{Nav} - \left(e_0 + e_1 X_j + \ldots\ldots\right) \qquad 2.68$$

where

V_j	is the residual,
Z_j^{PC}	is the Z coordinate of exposure station,
Z_j^{Stat}	is the elevation provided by statoscope,
Z_i^{APR}	is the Z coordinate of an identifiable feature in the aerial photo,
ω_j	is the roll angle,
κ_j	is the yaw angle,
Φ_j	is the pitch angle,
X_j	is the X coordinate along strip,
$a_j, \ldots\ldots, e_j$	are the coefficients of the polynomials used to model the systematic errors introduced from auxiliary data.

2. 4. Results Obtained from Previous Studies

Ackermann (1974) used statoscope data for a block of 60 km length without the need for interior vertical control. Studies carried out by Faig (1976 and 1979) and El

Hakim (1979) showed that the use of statoscope with some lake information can completely meet vertical control requirements within a block for small and medium scale mapping. Ackermann (1984) has also used flight navigation data as auxiliary control in block triangulation and demonstrated that the requirements for horizontal control can be reduced for small scale mapping.

2. 5. Reliability Analysis

Aerial triangulation has become a powerful tool for point determination during the last two decades. The main reason is the rigorous application of adjustment theory which enabled simultaneous recovery of exterior orientation parameters and object point coordinates. The refinement of the collinearity model to compensate for systematic errors led to further increase in the accuracy by a factor of two or three. Today, an accuracy of the adjusted coordinates of 2 to $3\,\mu m$, expressed at the photo scale can be achieved if the full potential is used (Förstner, 1985).

The effects of unmodelled errors, especially gross errors, have not been studied thoroughly until a few years ago. Each block adjustment has to handle a certain percentage of gross errors which are generally detected and eliminated via residual analysis. However, there does not exist an accepted criterion about when to stop the process of elimination of possibly erroneous observations. Therefore, undetected gross errors may remain, hopefully, not adversely affecting the results. This leads to the theory of the reliability of adjusted coordinates.

2. 5. 1. The Concept of Reliability

The theory of reliability was developed by Baarda (1968) to evaluate the quality of adjustment results of geodetic networks. According to Baarda, the quality of adjustment includes both precision and reliability (Figure 2. 3)

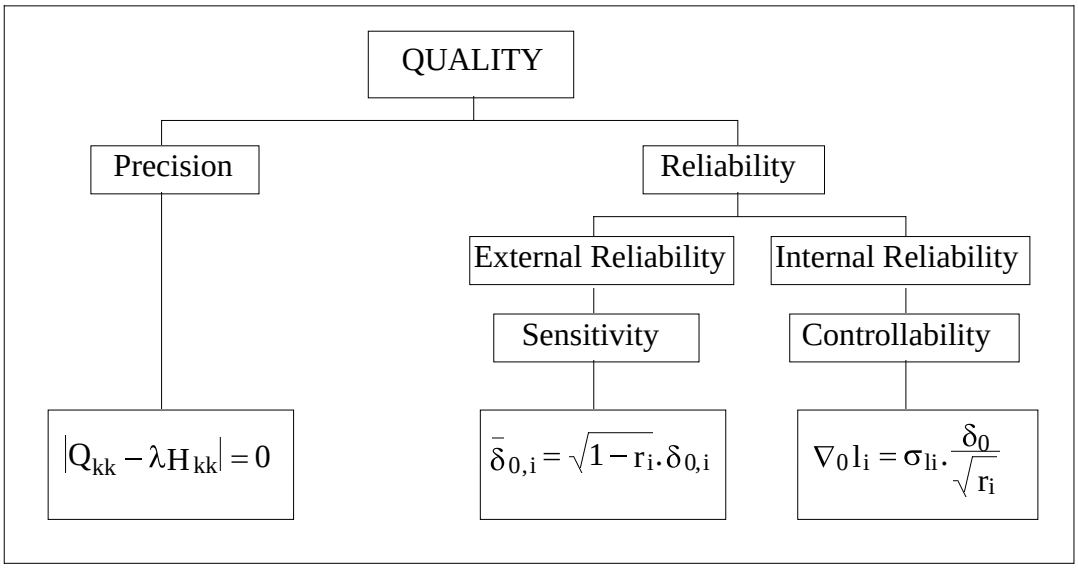

Figure 2. 3. Quality Evaluation of Adjustment (from Förstner , 1985)

Precision evaluation consists of comparing the covariance matrix Q_{kk} of the adjusted coordinates with a given matrix H_{kk} (criterion matrix). The error ellipsoid derived from Q_{kk} should lie inside the error ellipsoid described by H_{kk} and that it is as similar to H_{kk} as possible. This can check whether a required accuracy has been achieved or not.

As for reliability, Baarda distinguishes between internal and external reliabilities. Internal reliability refers to the controllability of the observations described by lower bounds of gross errors which can be detected within a given probability level. The effect of non-detectable gross errors on the adjustment results is described by external reliability factors that indicate by what amount the coordinates may be deteriorated in the worse case.

2. 5. 2 Reliability Measures

The linearized observation equation for a block adjustment can be written as:

$$\bar{l} + \bar{v} = A\hat{X} + a_0 \qquad P_{ll} \qquad 2.69$$

with the vector $\bar{l}$ containing the observations l_i and the residual vector $\bar{v}$ containing the residuals v_i, the design matrix A, the estimated vector $\hat{X}$ of the unknown parameters (e.g., object point coordinates, transformation parameters, additional parameters), a constant vector a_0 resulting from the linearization process, and the weight matrix P_{ll} which is the inverse of the variance-covariance matrix of the observations. The solution vector is derived using least squares method as:

$$\hat{X} = \left(A^T P_{ll} A\right)^{-1} A^T P_{ll} \left(\bar{l} - a_0\right) \qquad 2.70$$

The variance-covariance matrix of the residuals can be obtained from (Förstner, 1985):

$$Q_{vv} = Q_{ll} - A\left(A^T P_{ll} A\right)^{-1} A^T \qquad 2.71$$

and the direct relationship between the residuals and observations is:

$$\bar{v} = -Q_{vv} P_{ll} \left(\bar{l} - a_0\right) \qquad 2.72$$

Because $Q_{vv}P_{ll}$ is idempotent, its rank equals its trace, which are equal to the total redundancy, r = n-u, where n is the number of observations and u is the total number of unknowns.

$$\text{rank}\left(Q_{vv}P_{ll}\right) = \text{trace}\left(Q_{vv}P_{ll}\right) = \sum_{i=1}^{n}\left(Q_{vv}P_{ll}\right)_{ii} = r \qquad 2.73$$

The diagonal elements, $\left(Q_{vv}P_{ll}\right)_{ii}$, reflect the distribution of the redundancy in the observations.

2. 5. 2. 1. Redundancy Numbers

The redundancy number defined as:

$$r_i = \left(Q_{vv}P_{ll}\right)_{ii} \qquad 2.74$$

is the contribution of observation l_i to the total redundancy number r (Förstner , 1985). These numbers range from 0 to 1. Observations which have $r_i = 1$ are fully controllable and observations with $r_i = 0$ can not be checked. The average redundancy number for photogrammetric blocks is about 0.2 to 0.5. A value of 0.5 is an indication of relatively stable block.

The practical application of Baarda's reliability theory is to determine the magnitude of blunders that can not be detected on a given probability level α_0 when accepting a level of risk β_0 of committing Type II error (accepting that there is no blunder present when there is one present) (Van´icek et al., 1991). Assuming that all

observations are burdened with blunders, the objective is to find the minimum size of blunder in each observation that can still be detected.

2. 5. 2. 2 Internal Reliability

Internal reliability represents the maximum blunder in an observation undetectable with selected α_0 (the significance level) and β_0 (power of the test). It is defined as (Li and Jie, 1989):

$$\nabla_0 l_i = \sigma_{li} \cdot \frac{\delta_0}{\sqrt{r_i}} = \sigma_{li} \cdot \delta_{0,i} \qquad 2.75$$

where

σ_{li}	is the standard deviation of the ith observation l_i,
δ_o	is the non-centrality parameter,
$\delta_{0,i} = \delta_0 / \sqrt{r_i}$	is the internal reliability factor for observation l_i,
$\nabla_0 l_i$	is the minimum blunder that can be detected statistically.

2. 5. 2. 3. External Reliability

External reliability measures the effect an undetected blunder ($\nabla_0 l_i$) in the observation has on the unknown parameters obtained through the least squares adjustment. The external reliability factor is defined as (Li and Jie, 1989):

$$\bar{\delta}_{0,i} = \sqrt{1 - r_i} \cdot \delta_{0,i} \qquad 2.76$$

where $\bar{\delta}_{0,i}$ is the external reliability factor for observation l_i.

CHAPTER 3

GPS ASSISTED AERIAL TRIANGULATION: MATHEMATICAL MODELS AND PRACTICAL CONSIDERATIONS

3. 1. Introduction

The main purpose of aerial triangulation (AT) is the determination of ground coordinates for a large number of terrain points and the exterior orientation parameters of aerial photographs using as few control points as possible. The best scenario in mapping projects is that to have the exterior orientation parameters accurate enough so that the AT can be neglected. The GPS accuracy for attitude parameters is about 15 arc minutes (Lachapelle et al., 1993) and still far from what can be obtained from conventional block adjustment (5 arc seconds). Therefore, aerial triangulation is still one of the important steps in mapping and can not be avoided.

The integration of GPS measurements into photogrammetric blocks allows the accurate determination of coordinates of the exposure stations, thus reducing the ground control requirement to a minimum. Therefore, the goal is to improve efficiency by avoiding ground control points almost completely. The combined adjustment of photogrammetric data and GPS observations can be carried out by introducing GPS observation equations to the conventional block adjustment. An empirical investigation by Frieβ (1991), showed that in addition to the high internal accuracy of GPS aircraft positions (σ=2 cm), drift errors may occur due to the ionospheric and tropospheric errors, satellite orbital errors, and uncertainty of the initial carrier phase ambiguities. These drift errors become larger as the distance between the monitor and remote stations increase.

Out of the mentioned errors, incorrect carrier phase ambiguities are the major contributor of the drift errors to the positions.

The following sections concentrate on the application of GPS in aerial triangulation and deal with combined GPS photogrammetric block adjustment, its mathematical models, and practical considerations.

3. 2. GPS Observable Used in the Precise Photogrammetric Applications

There are three types of positioning information that can be extracted from GPS satellite signals: pseudorange (code), carrier phase, and phase rate (Doppler Frequency). Due to the high accuracy required for aerotriangulation, GPS phase measurements are needed to meet the accuracy requirement. In order to eliminate the effects of systematic errors inherent in these observations, double difference GPS phase measurement is used. The reason is that most GPS errors affecting GPS accuracy are highly correlated over a certain area and can be eliminated or reduced. The observation equation for DGPS phase measurement is given as (Lachapelle et al., 1992):

$$\nabla\Delta\Phi = \nabla\Delta\rho + \nabla\Delta\, d_{\rho} + \lambda\nabla\Delta N - \nabla\Delta\, d_{ion} + \nabla\Delta\, d_{trop} + \varepsilon\nabla\Delta\Phi \qquad 3.1$$

where

$\nabla\Delta$ is the double difference notation,

Φ is the carrier beat phase measurement in cycles,

ρ is the distance from satellite to the receiver,

d_{ρ} is the orbital error,

λ is the carrier wave length,

N is the integer carrier beat phase ambiguity,

d_{ion} is the ionospheric error,

d_{trop} is the tropospheric error,

ε is the receiver noise and multipath.

The terms $\nabla\Delta d_{\rho}$, $\nabla\Delta d_{ion}$, and $\nabla\Delta d_{trop}$ are generally small or negligible for short monitor-remote distances (e.g. <10-20 km). However, the term $\nabla\Delta d_{\rho}$ becomes more significant due to Selective Availability (SA) and may introduce some negative effects on integer carrier ambiguity recovery. The satellite and receiver clock errors are eliminated using the DGPS method but the receiver noise is amplified by a factor of 2. The phase observable is used extensively in kinematic mode where the initial ambiguity resolution can be achieved using static initialization or "On The Fly" methods. Accuracy at the centimeter level can be obtained if cycle slips can be detected and recovered (Cannon, 1990). The accuracy of kinematic DGPS is a function of the following factors (Lachapelle, 1992):

- Separation between the monitor and the remote station,
- The effect of Selective Availability,
- The receiver characteristics and ionospheric conditions.

3. 2. Combined GPS-Photogrammetric Block Adjustment

The observation equations for the camera projection centres are added to the conventional block adjustment. The observation equation should take into account the eccentricity vector between the antenna phase centre and the projection centre of the camera. This vector is usually determined using geodetic observations and expressed relative to the camera frame coordinate system (Figure 3. 1). The observation equations are given as (Ebadi and Chapman, 1995):

$$\begin{pmatrix} V_{Xi} \\ V_{Yi} \\ V_{Zi} \end{pmatrix}^{GPS} = \begin{pmatrix} X_i \\ Y_i \\ Z_i \end{pmatrix}^{PC} - \left(\begin{pmatrix} X_i \\ Y_i \\ Z_i \end{pmatrix}^{GPS} + M^T_{\kappa\Phi\omega} \times a \right) \qquad 3.2$$

where

$(X_i, Y_i, Z_i)^{PC}$	are the coordinates of the exposure stations,
$(X_i, Y_i, Z_i)^{GPS}$	are the coordinates of the antenna phase centre,
$(V_{Xi}, V_{Yi}, V_{Zi})^{GPS}$	are the GPS residuals,
a	is the offset vector,
M	is the rotation matrix.

Ackermann (1993) introduced a special approach to take care of GPS errors caused by inaccurate ambiguities. In his approach, ambiguities are resolved using pseudorange observations at the beginning of each strip, therefore , the GPS positions of the exposure stations can be drifted over time. Six linear unknown parameters per strip (3 offsets and 3 drifts) are added to the observation equations of exposure stations to take care of inaccurate ambiguity resolution effects introduced from GPS pseudorange measurements.

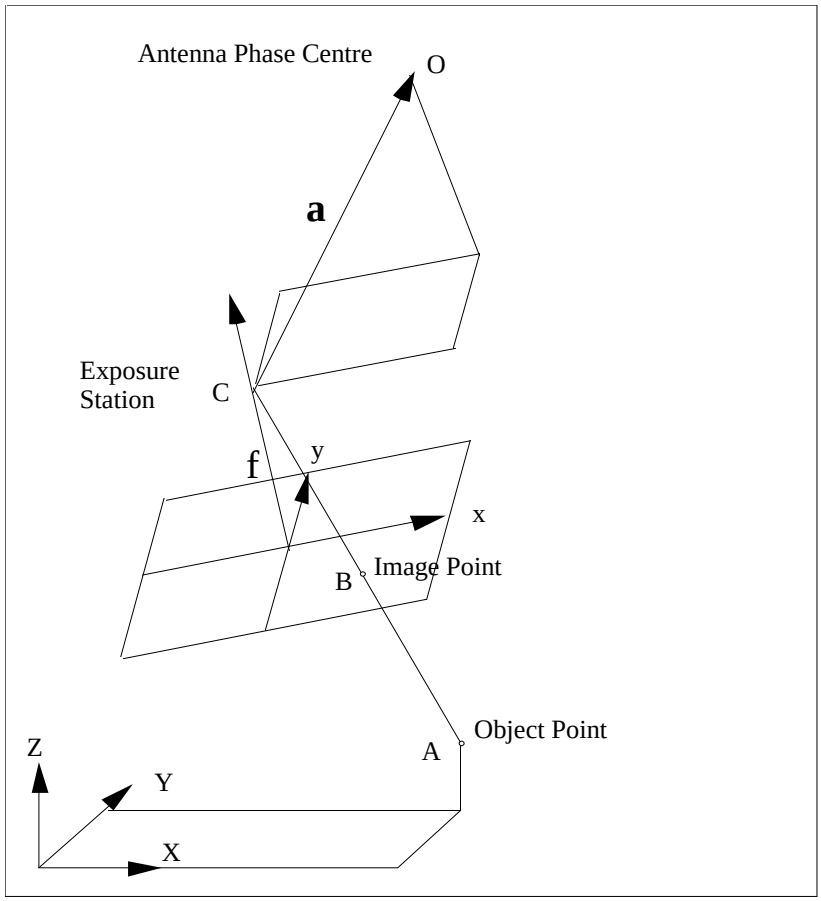

Figure 3. 1. Geometric Model For GPS Observation Equation

These equations are given as:

$$\begin{pmatrix} X_i \\ Y_i \\ Z_i \end{pmatrix}^{GPS} + \begin{pmatrix} V_{Xi} \\ V_{Yi} \\ V_{Zi} \end{pmatrix}^{GPS} = \begin{pmatrix} X_i \\ Y_i \\ Z_i \end{pmatrix}^{PC} - \left(\begin{pmatrix} a_x \\ a_y \\ a_z \end{pmatrix} + \begin{pmatrix} b_x \\ b_y \\ b_z \end{pmatrix} (t - t_o) \right) \qquad 3.3$$

where

$(X_i, Y_i, Z_i)^{PC}$ are the unknown coordinates of the exposure stations,

$(X_i, Y_i, Z_i)^{GPS}$ are the GPS coordinates of the camera exposure stations,

$(V_{Xi}, V_{Yi}, V_{Zi})^{GPS}$	are the GPS residuals,
(a_i, b_i)	are the unknown drift corrections which are common for all observation equations of each strip,
t_i	is the GPS time of each exposure,
t_o	is the reference time for each strip.

The drift parameters approximate and correct the GPS drift errors of the exposure stations in the combined block adjustment. Certain datum transformations can also be taken care by these parameters. Depending on each individual case of a mapping project, drift parameters may be chosen stripwise or blockwise. In the case of stripwise processing, one set of parameters has to be introduced for each strip while in the blockwise case, one set of drift parameters suffices for the entire block. The determinability of these parameters should be guaranteed according to the ground control configuration and flight pattern (Frieβ, 1992). The geometry of the combined GPS-photogrammetric block is determined as in the conventional case (standard overlap and standard tie-pass point distribution).

3. 3. Ground Control Configuration for GPS-Photogrammetric Blocks

Theoretically, as long as datum transformation is known, no control points are needed to carry out the GPS-photogrammetric block adjustment because each exposure station serves as control point. If the coordinate system of the final object coordinates is to be a system other than WGS84, then ground control points are required to define the datum. For this purpose, 4 control points are usually used at the corners of the block.

The situation is different when drift parameters are included. The inclusion of drift parameters weakens the geometry of the block. To overcome this problem, various

ground control configurations can be utilized to strengthen the geometry and recover all unknowns in the block adjustment. The GPS-photogrammetric blocks can be made geometrically and numerically stable and solvable for all unknowns in 3 ways (Ackermann and Schade, 1993):

(a) - If the block has 60% side lap (Figure 3. 2, case a)

(b) - If 2 chains of vertical control points across the front ends of the block are used (Figure 3. 2, case b)

(c) - If 2 cross strips of photography at the front ends of the block are taken (Figure 3. 2, case c)

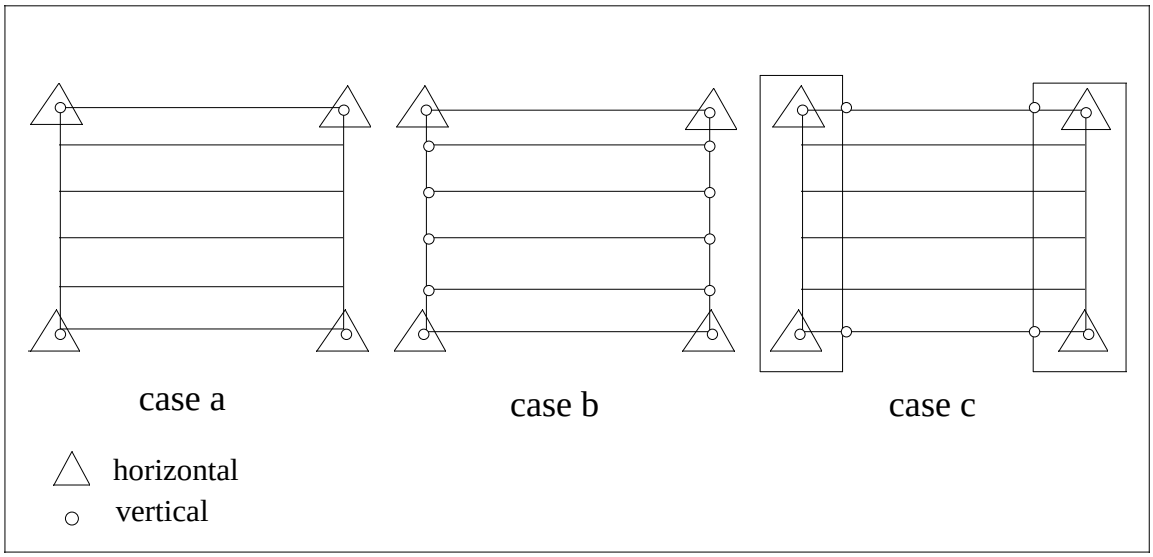

Figure 3. 2. Ground control configurations for GPS assisted blocks

Case (c) with 2 cross strips is usually recommended for GPS aerial triangulation due to its economic efficiency. The use of pairs or triplets of ground control points at the perspective locations in the cross strips is suggested for stronger geometry and higher reliability. Cross strips must be strongly connected to all strips they cover, by measuring and transferring all mutual points, in all combinations. The same procedure applies to ground point which means that they have to be measured in all images where they

appear. It may be required to have more than 2 cross strips and 4 ground control points where the blocks have irregular shape.

3. 4. Problems Encountered and Suggested Remedies

3. 4. 1. Antenna-Aerial Camera Offset

GPS provides the coordinates of the antenna phase centre and not, as desired, the projection centre of the camera (Frieβ, 1987). This happens because the phase centre of the antenna and the rear nodal point of the aerial camera lens can not occupy the same point in space (Lucas, 1987). If the camera is operated on a locked down mode, the relative motion of the camera's projective centre with respect to the antenna can be avoided. In this case, the offset between the camera projection centre and the antenna phase centre is constant with respect to the camera fixed coordinate system (Figure 3. 1)

The offset vector can be surveyed using geodetic methods and measured with respect to the image coordinate system or treated as an unknown quantity and solved together with other unknowns in a block adjustment. However, the latter case requires more extensive control.

The GPS positions of the antenna phase centre have to be reduced onto the camera exposure stations. Since an external coordinate system is considered for the coordinate reduction, the attitude of the camera must be known. The attitude parameters can be obtained by an initial block adjustment run.

3. 4. 2. Synchronization Between Exposure And GPS Time

To interpolate exposure station positions from GPS positions, the instants of exposure must be recorded using the receiver time scale with precise synchronization to GPS time (Frieβ, 1987). The measuring rate for GPS observations must be 1 Hz or more as the speed of survey aircraft is in order of 50 to 100 m per second (Ackermann and Schade, 1993). The photogrammetric camera should be equipped with a shutter synchronized electronic signal, providing an accuracy better than 1 ms.

3. 4. 3. Geodetic Datum

GPS provides coordinates in the WGS84 which is a geocentric Cartesian coordinate system centred at the mass centre of the earth. However, the reference systems usually used in aerial triangulation are the local coordinate systems referring to the local ellipsoids. Planimetric coordinates may be obtained by transforming from WGS84 to the local coordinate system (e.g., UTM) meaning that there is still a need for minimum ground control points to carry out the transformation. The transformation between these two coordinate systems can also be based on published formulas (Colomina, 1993). The transformation of height requires knowledge of specific geoid and its undulation (Faig and Shih, 1989). It is also possible to carry out the GPS aerial triangulation in a localized vertical coordinate system and apply the transformation thereafter (Ackermann and Schade, 1993).

3. 4. 4. Ambiguity Resolution

This problem can be handled in a number of ways. It can be approximately determined from the pseudorange observed in the C/A or P codes. Calibrating N (by going over a known point at the airport) is another solution. The unknown N can also be determined using "On The Fly" ambiguity resolution methods (Hatch, 1990, Abidin,

1993, Dencheng, 1994). Inaccurate approximation of ambiguity creates drift errors in the GPS positions of exposure stations. Ambiguity resolution is still one of the most challenging parts of kinematic GPS positioning. No matter what method is chosen for ambiguity resolution, GPS drift errors can not be avoided.

3. 4. 5. Cycle Slip

Cycle slips are discontinuities in the time series of a carrier phase as measured in the GPS receiver. It is occurred when:

- parts of the aircraft obstruct the inter visibility between the antenna and satellite
- multipath from reflection of some parts of the aircraft (Krabill, 1989)
- Receiver power failure
- Low signal strength due to the high ionospheric activity or external source (e.g., radar)

Some approaches for cycle slip detection and correction are:

- Using receiver with more than 4 channels to obtain redundant observations
- Integrating GPS with INS or other sensors (Schwarz et al., 1993)
- Using dual frequency receivers
- Applying OTF ambiguity resolution techniques
- Locking on new course GPS positions derived from C/A code pseudorange after signal interruption (Ackermann and Schade, 1993)

3. 5. Accuracy Performance of the GPS-Photogrammetric Blocks

GPS-photogrammetric blocks yield high accuracy due to the fact that these blocks are effectively controlled by the GPS air stations acting practically as control entities. The advantages are that there is little error propagation and the accuracy distribution is quite uniform throughout the block. Accuracy does not also depend on the block size. The accuracy of these blocks are determined by intersection accuracy of the rays having measurement accuracy of σ_0 (Ackermann and Schade, 1993).

Ground control points are no longer required for controlling the block accuracy. They may provide the datum transformation in which a few points are sufficient. The geometry of the block may be weakened by introducing GPS shift and drift parameters but the required accuracy is still maintained. Such general accuracy features have been confirmed by theoretical accuracy studies (Ackermann and Schade, 1993) based on the inversion of the normal equation matrices. These studies showed that the standard deviations of the tie points for a simulated block controlled with 4 ground control points and only one set of free datum parameters is quite uniform and the overall RMS accuracies are $1.4\sigma_0$.S (horizontal) and $1.9\sigma_0$.S (vertical) where S is the scale of photography.

Ackermann and Schade (1993) found that the block accuracy deteriorates if the GPS camera positioning accuracy decreases. GPS assisted blocks do not strongly depend on high GPS camera positioning accuracy except for very large scale blocks. Similar accuracies could be achieved in conventional aerial triangulation only with a large number of ground control points. The theoretical studies (Ackermann, 1992, Burman and Tolegård, 1994) have established the very high accuracy performance of GPS blocks even in the case of additional parameters. The results are valid for the whole range of photo scales which are used in practice for mapping purposes except for very large scale and photogrammetric point determination. According to Ackermann (1994), GPS assisted

blocks for large scale mapping warrants further investigation. Part of this research deals with this case and its associated problems and recommended solutions.

3. 6. Practical Considerations in GPS Airborne Photogrammetry

There are some practical problems to be considered before the process can be fully operational. These problems consist of selecting and mounting of a GPS antenna on the aircraft, receiver and camera interface, and the determination of the antenna-aerial camera offset. A solid consideration of the operational requirements and their effect on flight plan will lead to a successful photogrammetric mission.

3. 6. 1. GPS Antenna

The GPS antenna should be mounted on the aircraft in such a way that it can receive the GPS signals with a minimum of obstruction and multipath. Potential places include the fuselage directly over the camera or the tip of the vertical stabilizer (Curry and Schuckman, 1993).

The advantage of fuselage location is that the antenna phase centre can be located along the optical axis of the camera which simplifies the measurements of the offset vector. However, the fuselage location is more subject to multipath and shadowing of the antenna depending on wing placement. The vertical stabilizer location is usually less sensitive to multipath and shadowing. Another advantage is that the actual mount of the antenna can be simplified since some aircrafts have already a strobe light mount in the same location which can be used for antenna mounting. However, the measurements of the antenna offset vector is more complicated. Once the antenna and camera have been

mounted in the aircraft, it is not necessary to remeasure the offset vector for subsequent flight missions. As a rule of thumb, the best location for the GPS antenna is the one which can receive the GPS signals. This location varies in different aircraft types. It should also be noted that making any kind of holes in the aircraft for antenna mounting must be done by a certified aircraft mechanic. Possible locations for antenna are shown in Figure 3. 3.

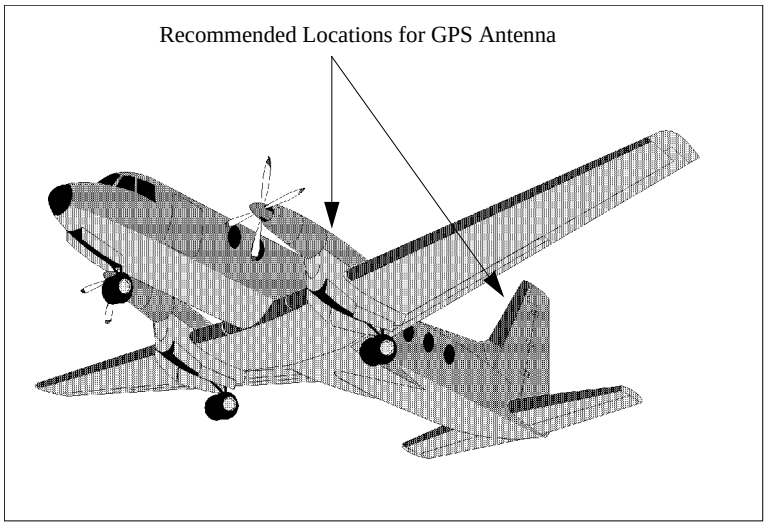

Figure 3. 3. GPS antenna locations on the aircraft

3. 6. 2. Receiver and Camera Interface

The photogrammetric camera and the GPS receiver must be connected in such a way that exposure times can be recorded and correlated with the GPS time of antenna phase centres. Modern aerial cameras can send a pulse corresponding to the so called "centre of exposure" to the receiver. These pulses are repeatable to some tens of nanoseconds. Older cameras can also be modified to send an exposure pulse to the receiver but the repeatability is not as good as modern cameras. There may be some pulse lag which will need calibration.

A GPS receiver records signals at regular epochs set by the user such as every one second. However, camera exposure can occur at any time and therefore the camera position at the instant of exposure should be interpolated from the GPS position of the antenna phase centre. Theoretically, the aerial camera can record exposure times with a high accuracy and the interpolation can be performed using these times. However, GPS receivers have an extremely accurate time base, therefore, it is preferred to record exposure times in the receiver. Most receivers have a simple cable connection from the camera. The camera pulse is sent to the receiver whenever an exposure occurs. The event time and an identifier are recorded in the receiver data file. GPS receivers can also send an accurate Pulse-Per-Second (PPS) signal that is used to trigger the camera at the even second pulse nearest to the designed exposure time. In order to use the exposure pulse to mark the occurrence of an event, the instant of a camera exposure should be exactly defined. The pulse is usually triggered when the fiducials are exposed onto the film in forward motion compensation cameras. An image is created as soon as enough photons hit the silver halide crystals to cause the ground control targets to begin to be exposed (Curry and Schuckman, 1993). The errors caused by these timing issues are small but can be modeled by introducing correction parameters to the bundle block adjustment program.

After the flight mission and film processing, the individual frames and the GPS event markers should be correlated. Some cameras can accept data from the receiver by imprinting the time and approximate coordinates onto the film. Lacking such a system, the camera clock can be set to GPS time so that GPS time is recorded for every frame simplifying the match to event markers.

3. 6. 3. Antenna-Aerial Camera Offset

The GPS receivers record position data for the GPS antenna phase centre at the instant of the exposure, but the coordinates of the exposure stations are required for the block adjustment. The offset vector between these two points should, therefore, be determined. If the location of the antenna is directly along the camera optical axis, the offset vector includes a single vertical component. If not, a more sophisticated measurement method is required. The antenna offset can be surveyed using geodetic techniques (e.g., angular and distance measurements to the fiducial marks of the camera and to estimated location of the antenna phase centre). The antenna manufacturer is usually able to provide the location of the antenna phase centre with centimeter level accuracy. The measurements of the offset vector is carried out in the aircraft or camera coordinate system. The coordinates of the antenna phase centre are given in a geocentric coordinate system (e.g., WGS84). The bundle block adjustment is performed in a ground-based coordinate system using the exposure station coordinates as weighted observations. Since the aircraft attitude changes with respect to the ground coordinate system, three orientation parameters known as roll, pitch, and yaw should be available in order to transfer the 3D antenna position to the camera's exposure stations. The bundle block adjustment program can be modified in such a way that it resolves the offset vector into the ground coordinate system at every iteration based on the calculated values of the attitude parameters. Coordinates for the exposure stations can then be updated. A formulation for this modification is given in Section 3. 6. 2. It is the antenna position that it is actually held fixed with appropriate weight while the camera exposure station moves about in ground space with respect to the antenna.

If the camera is not operated in locked mode, the components of the antenna offset vector in the camera coordinate system will change. Therefore, the orientation angles in flight, for each frames should be recorded and used later in the block adjustment. A gyro-stabilizer camera mount can be used for this purpose.

3. 6. 4. Planning and Concerns for Flight Mission

The key to a successful GPS photogrammetry flight is careful mission planning. All GPS receiver manufactures provide planning software which helps to determine satellite constellation for a particular day, time, and location. Flights should be planned for period during which at least six or seven satellites are available so that if phase lock between one or two satellites is lost during a turn, carrier phase processing can still continue. Even if only C/A code pseudorange is collected and processed, additional satellites improve the geometry and increase the redundancy. The location of the master station has to be carefully planned to minimize multipath and obstruction effects.

Another parameter to be considered is the satellite cut-off elevation angle. It is recommended to record data from satellites which are 15 degrees or more above the horizon to reduce the errors introduced by atmosphere. The elevation mask can be programmed in the receiver or set in the planning software. However, it is advantageous to set a lower mask on the receivers during data acquisition which will help later to detect and correct for cycle slips during turns. Low elevation satellites can usually be ignored by post processing software.

All GPS receivers provide PDOP which is the Positional Dilution of Precision which indicates the accuracy of position from the satellite geometry view point. PDOP should be less than 5. A flight should not be planned and executed when this parameter is greater than 7 or 8 during any portion of the mission. There could be brief spikes in PDOP when satellites rise and set. It may be possible to process through a PDOP spike and achieve good results on either side of spike.

GPS data rate should be chosen according to the required accuracy of the photogrammetric project. Normally, a one second or half-second rate is sufficient. Many GPS receivers can record data from five to six satellites at a half-second rate for three to five hours in dual frequency mode. Data can be logged to an external device (e.g., PC) for longer flights.

The receivers at both the master and remote stations should start logging at approximately the same time. Only data collected simultaneously at both receivers can be post-processed.

Static initialization for the aircraft receiver is required in carrier phase mode. This can be done by sitting on the runway for 5-10 minutes and performing a fast static survey to compute the base line between master and remote stations or by physically lining up the aircraft antenna over a known point on the runway, measuring the height of the antenna and collecting a few seconds of data. It has to be remembered that continuous phase lock must be maintained on at least 4 satellites once the static initialization has been done. The ambiguity can also be resolved using so called "On The Fly" techniques. If possible, data should be collected in such a way that both carrier and code post processing methods can be applied.

It is advisable to check the camera before the take-off by shooting a few test exposures with the camera connected to the receiver. Most receivers can indicate that an event has been recorded.

The banking angle of the aircraft should be restricted to 20-25 degrees during a turn, depending on the satellite geometry. If carrier phase data are being collected, smaller banking angles will extend the flight duration. The receiver itself has to be monitored for sufficient battery power and satellite tracking.

The maximum distance allowable between monitor and remote stations should be chosen in such a way that the errors contributed from atmosphere are negligible.

After completing the flight, it is useful to align the antenna over a known point and collect a few seconds of data or to carry out a second fast static survey if continuous kinematic data are being collected. In this way, the data can be processed backward, if necessary. The data should also be immediately downloaded to a computer and checked for loss of lock. The photo coverage of the project area has to be evaluated upon completion of the flight.

CHAPTER 4

EMPIRICAL RESULTS OF GPS ASSISTED AERIAL TRIANGULATION

This chapter deals with the results of GPS-photogrammetric block adjustments obtained from simulated and real data. Results from a simulated block triangulation incorporating GPS-observed exposure stations are presented first after which the results from a medium scale mapping are discussed.

4. 1 Simulated Large Scale Mapping Project

The required GPS accuracy for the camera exposure stations for large scale mapping projects is less than 0.5 m. Therefore, reduction and elimination of GPS errors (e.g., timing errors and atmospheric errors) and especially errors introduced from wrong ambiguities are important to be considered for large scale GPS-photogrammetric blocks.

There are mainly two reasons that GPS has not been used for large scale mapping in the past; the satellite configuration was not complete until 1993 and also intelligent and advanced ambiguity resolution techniques were not developed until recent years.

Both the precision and reliability of bundle block adjustment with GPS data were theoretically investigated using simulated data. The variance-covariance matrix of unknown parameters (Q_{XX}) and variance-covariance matrix of residuals (Q_{VV}) and

weight matrix of observations (P_{ll}) as well as independent check points were used to aid both precision and reliability analyses.

This study demonstrates the potential of GPS even for large scale mapping projects. The simulated block was made up 10 strips. The block parameters are shown in Table 4. 1.

Table 4. 1. Information of Simulated Block

Number of Photos	230
Number of Strip	8 + 2 Cross Strips
Terrain Elevation Difference	150 m
Photo Scale	1: 5,000
Focal Length	152 mm
Average Flying Height	900 m
Forward Overlap	60%
Side Overlap	30% & 60%
Photograph Format	23 cm x 23 cm
Precision of Image Coordinates	0.005 mm
Precision of GPS Data	0.02 - 1.0 m
Precision of Ground Control Points	0.02 m & 0.1 m

4. 1. 1. Methodology

Image coordinates for all pass points and tie points were derived from collinearity Equations 2. 1 and 2. 2, based on simulated values for camera exposure station coordinates and attitude and ground coordinates of tie or pass points. The image coordinates were contaminated with pseudo-random noise in order to better simulate the real situation. The test design of GPS camera exposure stations is composed of different accuracies ranging from 2 cm to 1 m. Configurations of ground control points are shown in Figure 4. 1.

A - No ground control points,

B - 4 Ground control points at the corners of the block,

C - Full ground control Points

D - Four pairs of ground control points and cross strips.

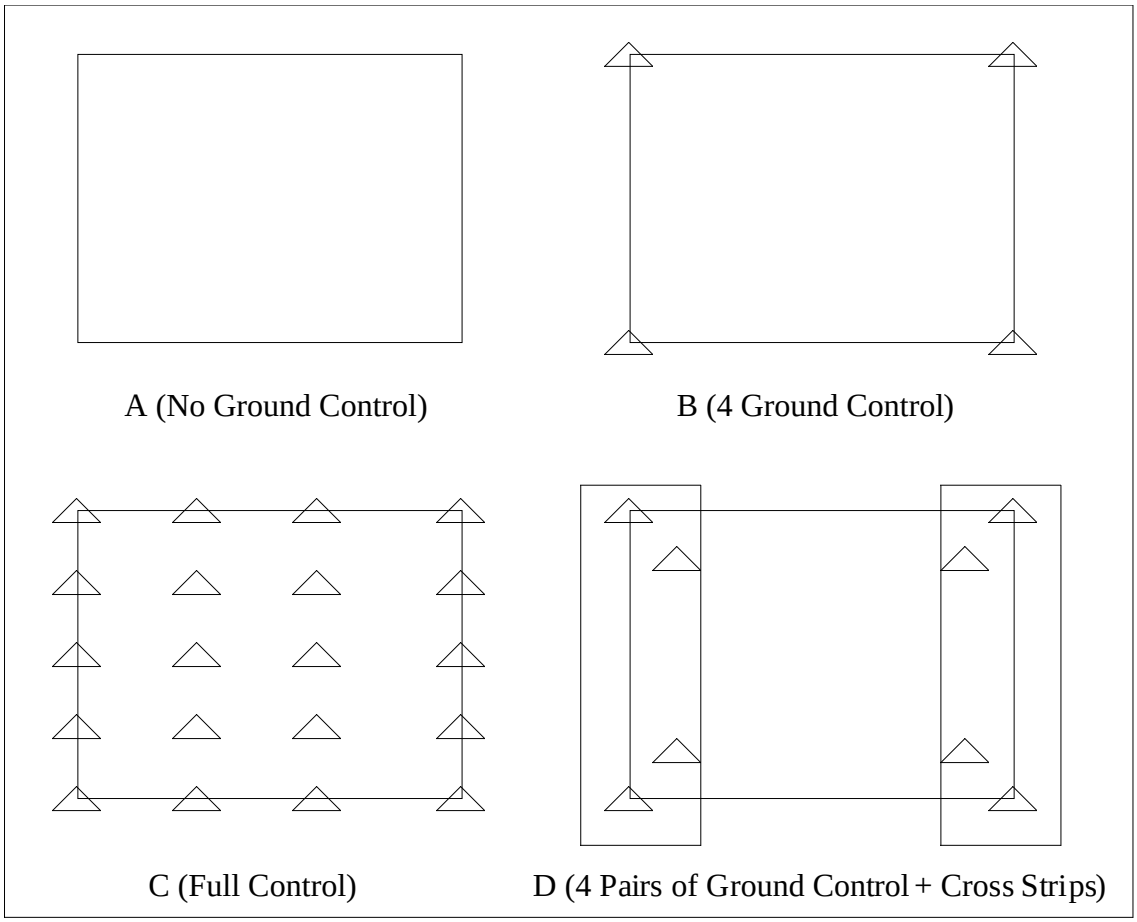

Figure 4. 1. Ground Control Configurations

There are two more configurations, E and F, which are the same as D and B except with 60% sidelap. Among these configurations, version C refers to a conventional block adjustment and was considered for comparison.

The block adjustments were performed with a newly developed program GAP (Appendix A). For both precision and reliability analysis, the matrices Q_{XX} and $Q_{VV}P$ are computed by this program. A local coordinate system was adopted for the datum of the object points.

4. 1. 2. The Precision Analysis of Simulated GPS-Photogrammetric Block

The covariance matrix of object points is generally considered as a measure of theoretical precision:

$$D(X) = \sigma_0^2 Q_{XX} \qquad 4.1$$

where Q_{XX} is the cofactor matrix of the object points and σ_0^2 is the *a priori* variance factor. The theoretical precision in one coordinate direction of the ith object point is given by:

$$m_i = \sigma_0 \sqrt{(Q_{XX})_{ii}} \qquad 4.2$$

The average theoretical precision of n object points is computed as:

$$\overline{m} = \sigma_0 \sqrt{tr(Q_{XX}) / 3n} \qquad 4.3$$

The average practical precisions in X, Y, and Z coordinate directions are:

$$\overline{\mu}_X = \sqrt{\frac{\sum \Delta X^2}{n}} \qquad 4.4$$

$$\overline{\mu}_Y = \sqrt{\frac{\sum \Delta Y^2}{n}} \qquad 4.5$$

$$\overline{\mu}_Z = \sqrt{\frac{\sum \Delta Z^2}{n}} \qquad 4.6$$

where $\Delta X, \Delta Y,$ and ΔZ are differences between the adjusted and simulated coordinates of an object point. The simulated object points serve as check points in this simulated block.

Figures 4. 2 - 4.4 show the practical precisions of all object points and Figures . 4. 5 - 4. 7 depict the theoretical precisions obtained from the inversion of normal matrix respectively. In all these Figures, ground control accuracy was assumed to be 0.02 m. The program GAP was executed for various configurations of ground control with different GPS accuracy of camera exposure stations. The following conclusions can be derived from the analysis of these Figures.

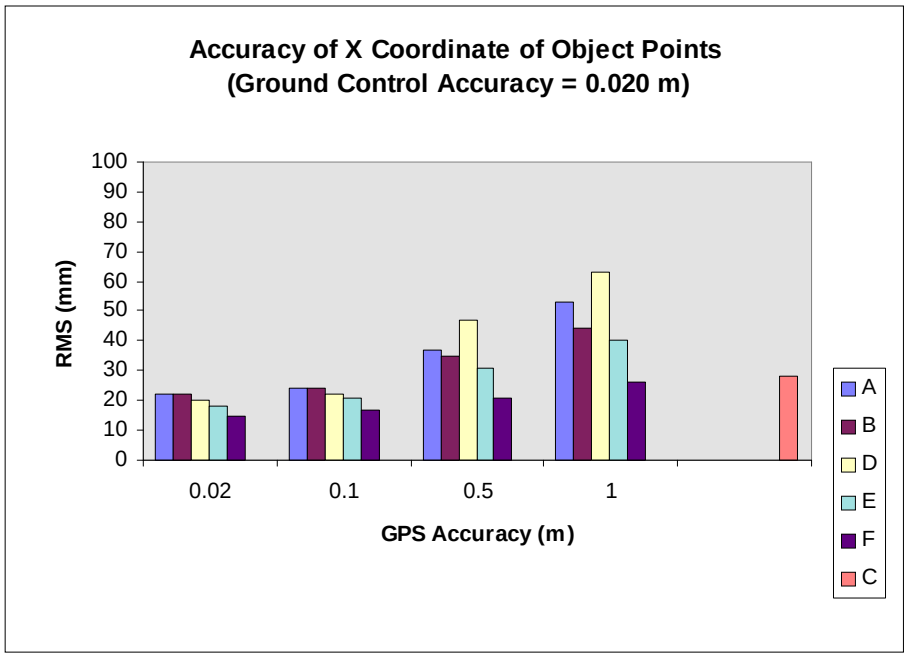

Figure 4. 2. Practical Precision of Simulated Block

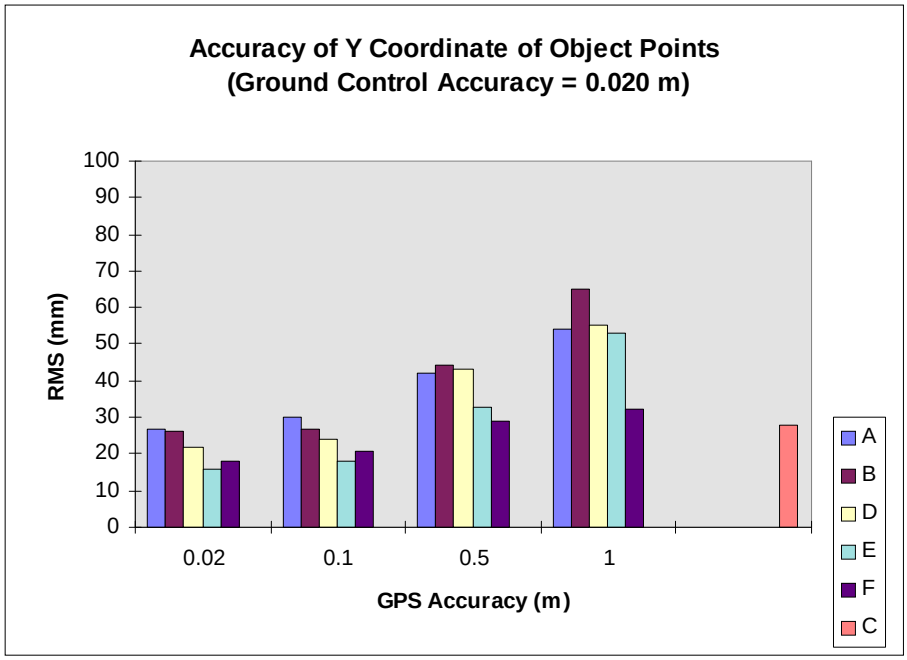

Figure 4. 3. Practical Precision of Simulated Block

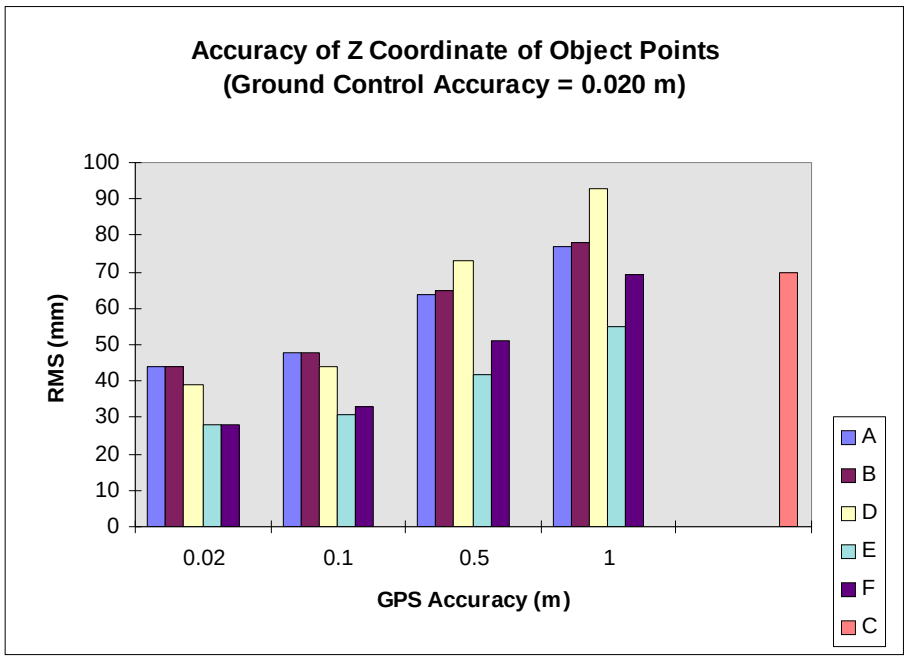

Figure 4. 4. Practical Precision of Simulated Block

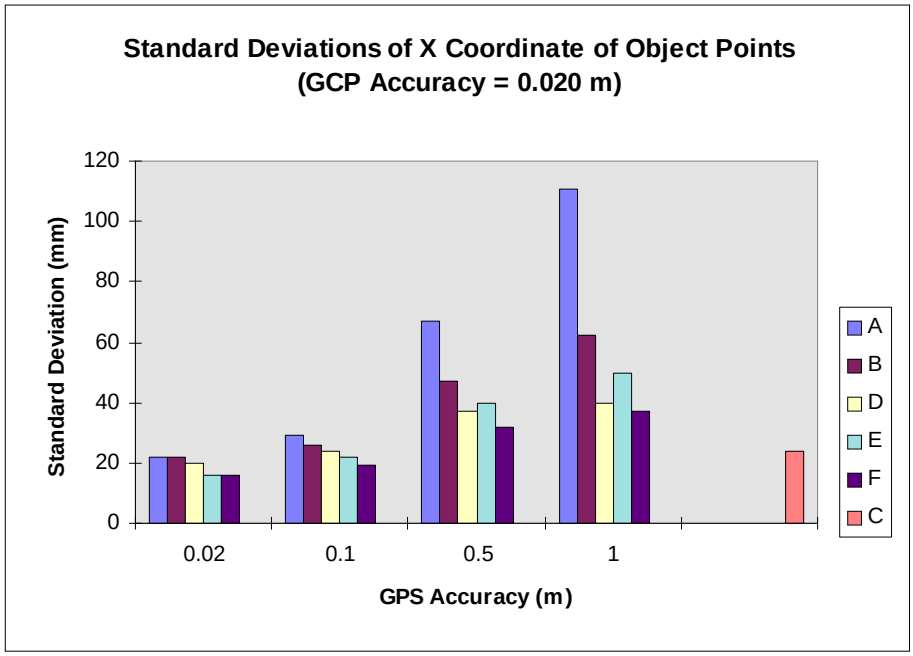

Figure 4. 5. Theoretical Precision of Simulated Block

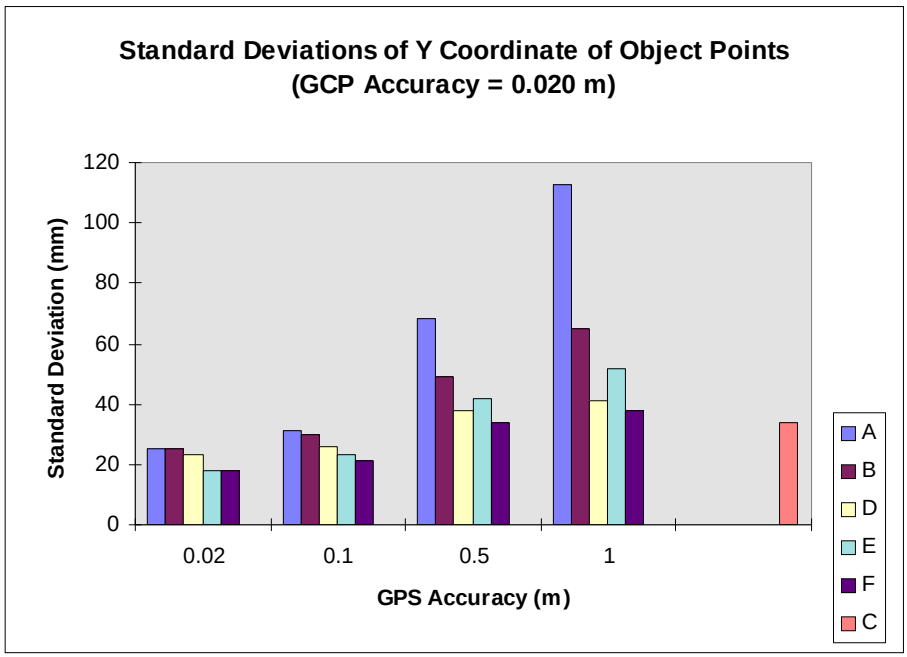

Figure 4. 6. Theoretical Precision of Simulated Block

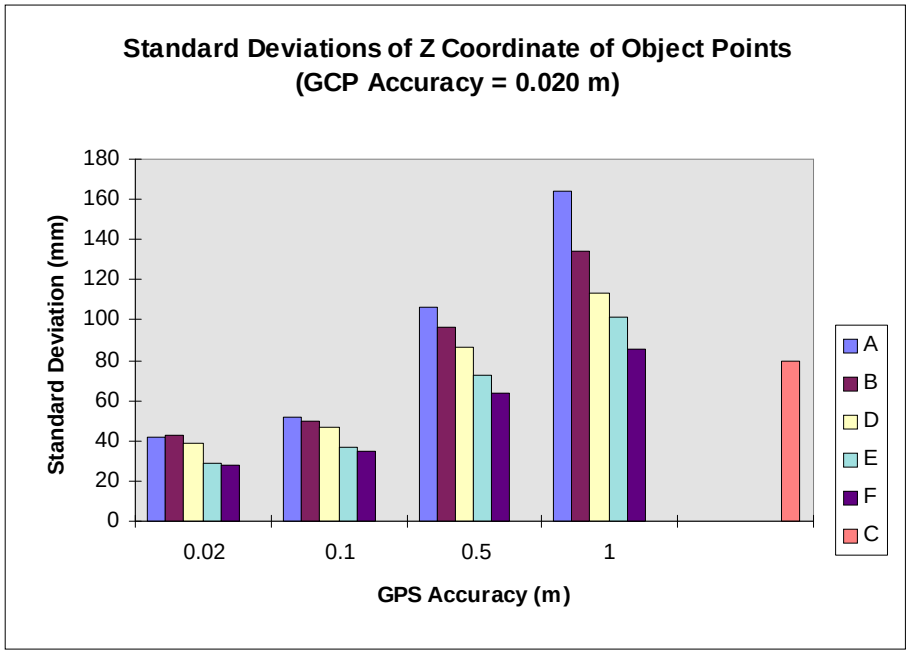

Figure 4. 7. Theoretical Precision of Simulated Block

* If the accuracy of the camera exposure stations is better than 0.5 m, especially in height, then the adjusted coordinates are better than those obtained from conventional block adjustment (configuration C) no matter whether the ground control points are used or not.

* The adjusted points are more precise than GPS data with which the adjustment was performed. This means the precision of point determination can reach centimeter level if the camera station accuracy is at decimeter level.

* The accuracy of the adjusted object points reduces as the accuracy of GPS-derived camera exposure stations deteriorate. The rate of deterioration is high for configurations A, B, and D but increasing sidelap overcomes this problem (configurations E and F).

* The best results were obtained from configuration F, which includes 4 pairs of control points at the corners of the block and 60% sidelap, and cross strip.

* The accuracy obtained from configuration A (no ground control) and version B (4 Ground control) are quite the same. It should be mentioned that there was no datum deficiency for this simulated block. Therefore, it can be concluded that the GPS-photogrammetric block adjustments can be executed without ground control points provided that the datum transformation is known. The planimetric transformation between WGS84 and local coordinate system involves a straight forward procedure but height transformation requires the knowledge of the geoid.

Figures 4.8 - 4. 10 show the accuracy for the same block when ground control point accuracy has changed from 0.02 m to 0.1 m. As shown in these Figures, there is no significant deterioration in accuracy, which implies to some extent the insensitivity of the GPS controlled blocks to ground control points.

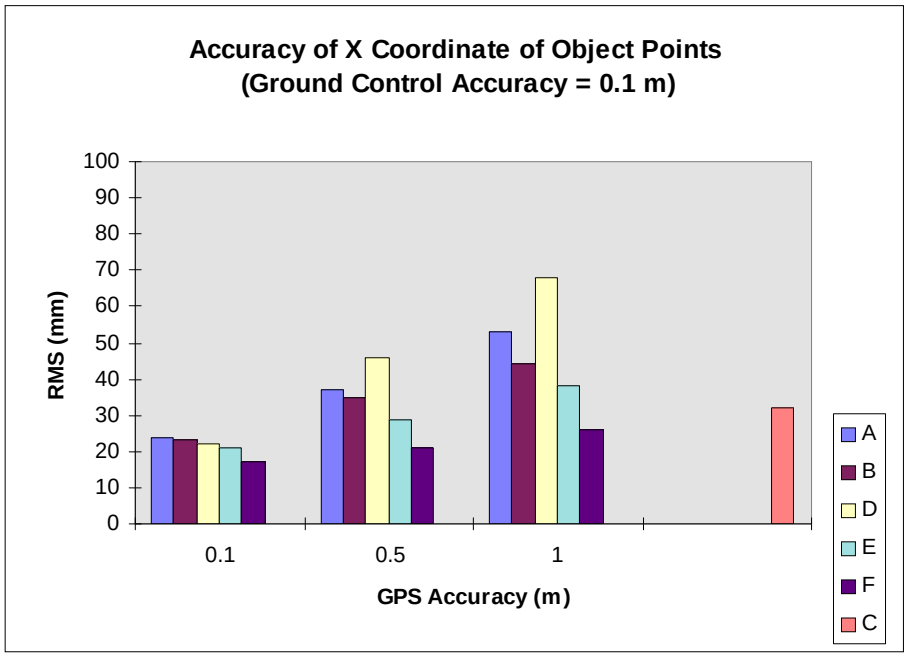

Figure 4. 8. Practical Precision of Simulated Block

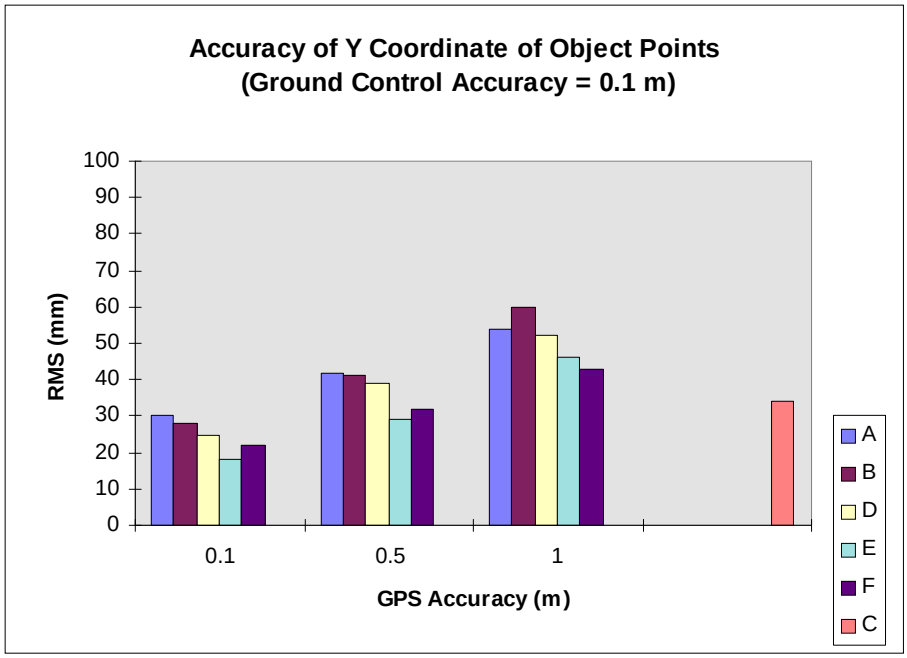

Figure 4. 9. Practical Precision of Simulated Block

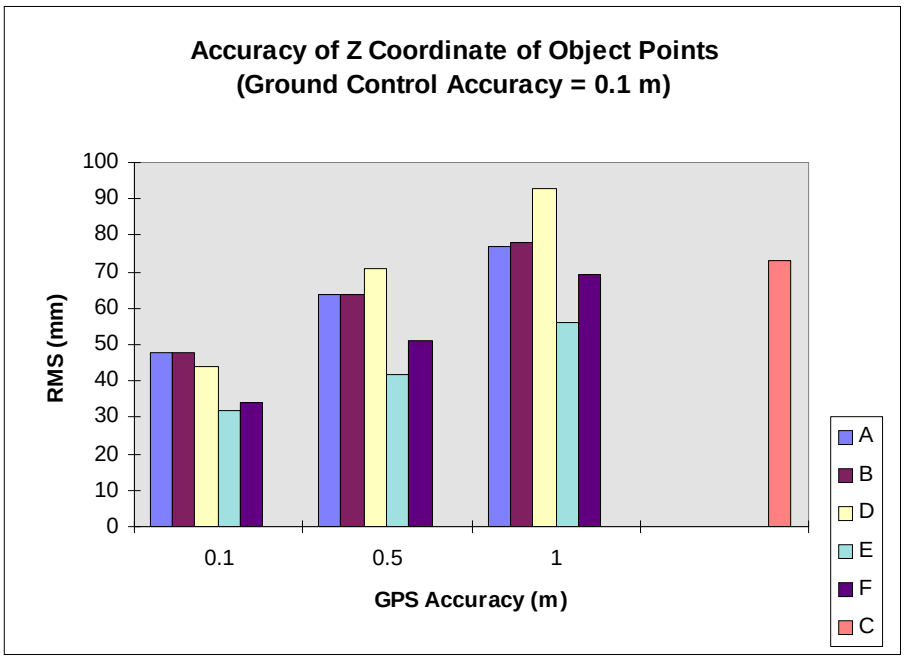

Figure 4. 10. Practical Precision of Simulated Block

The precision distribution of the object points obtained from inversion of the normal matrix for upper right part of the block and for various configurations are shown in Figures 4. 11 through 4. 19. The following statements can be developed from these Figures:

* For GPS-photogrammetric blocks, the precision is worse both at corners and edges of the blocks(especially for blocks with no ground control). Therefore, the flight strategy of extra strips and photos are recommended.

* The precision of adjusted object points in the interior part of the GPS-photogrammetric block is quite homogenous both in planimetry and height(configuration A or F) but this is

not true for conventional blocks (configuration C). Thus, there is no need for vertical control points inside the GPS-controlled blocks.

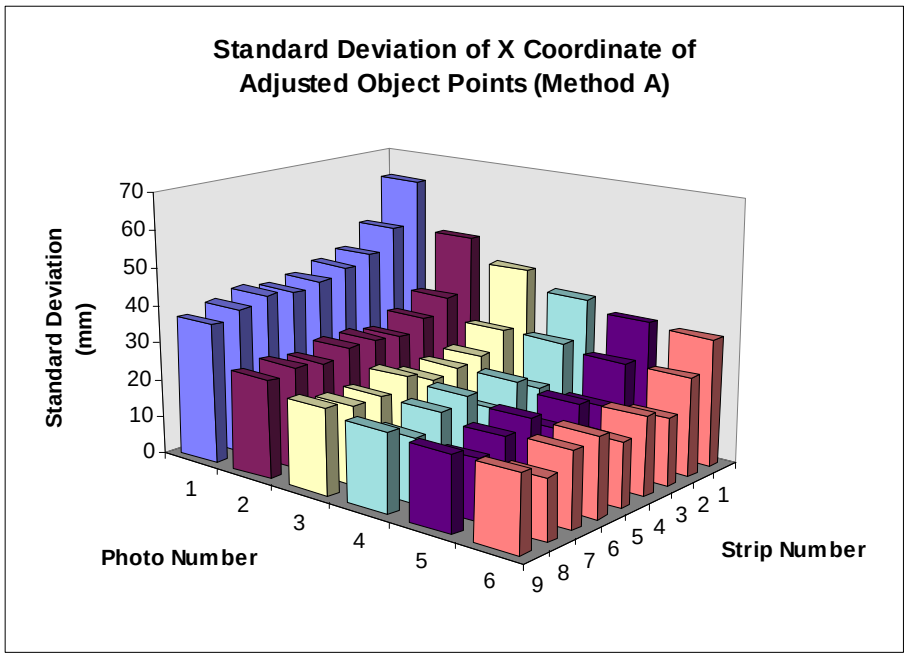

Figure 4. 11. Precision Distribution of Object Points (Method A)

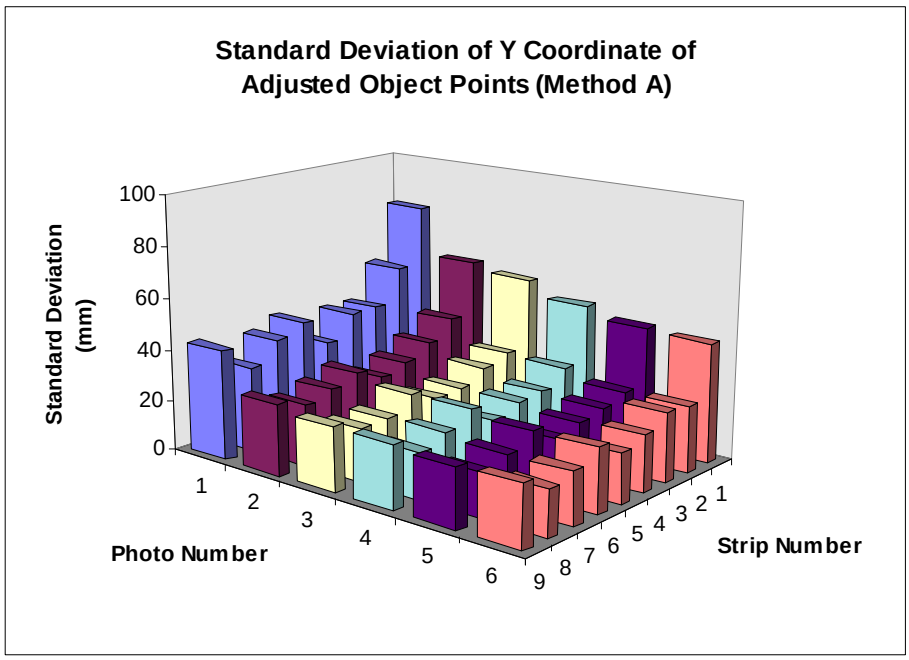

Figure 4. 12. Precision Distribution of Object Points (Method A)

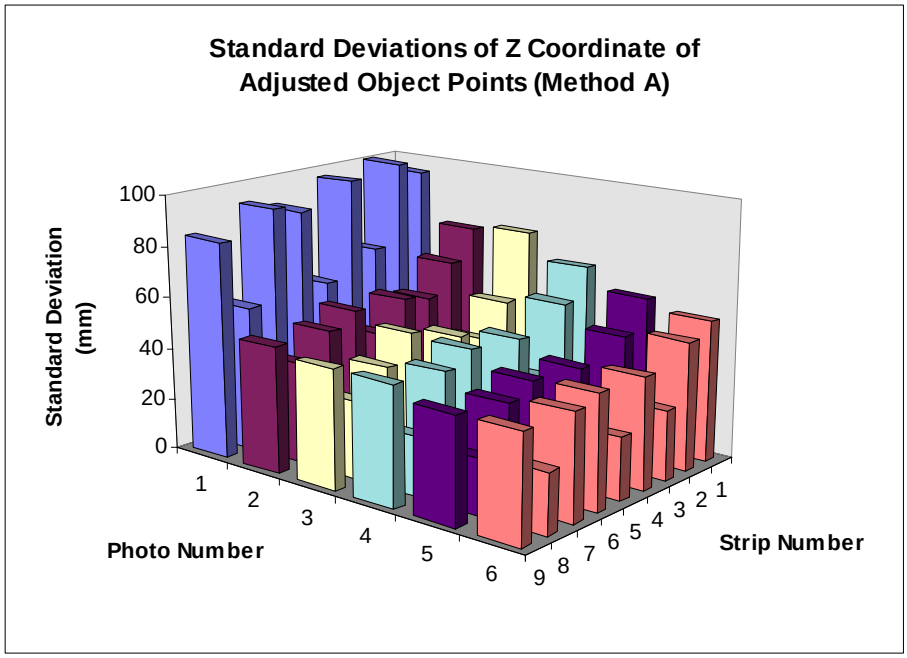

Figure 4. 13. Precision Distribution of Object Points (Method A)

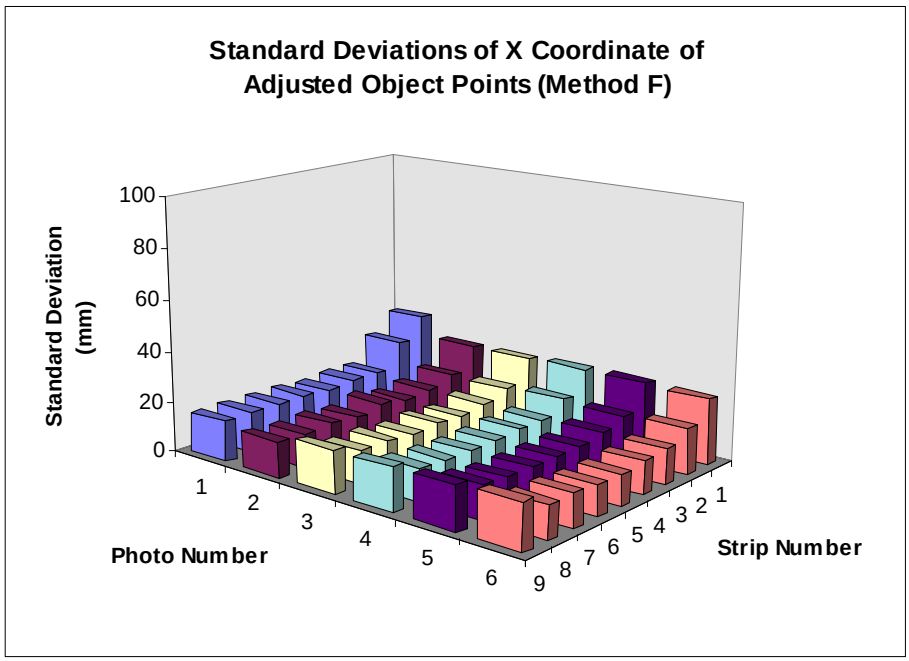

Figure 4. 14. Precision Distribution of Object Points (Method F)

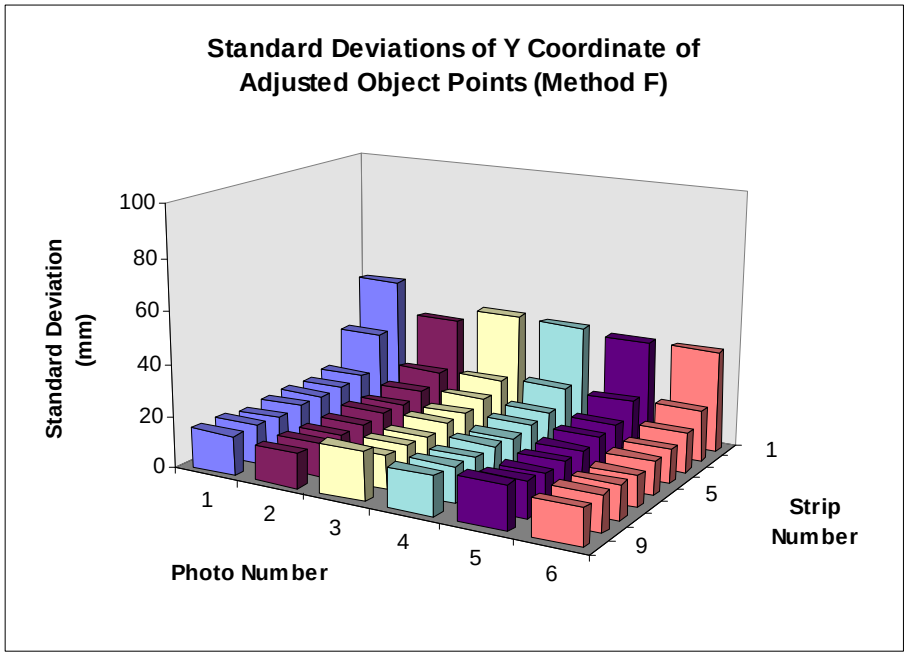

Figure 4. 15. Precision Distribution of Object Points (Method F)

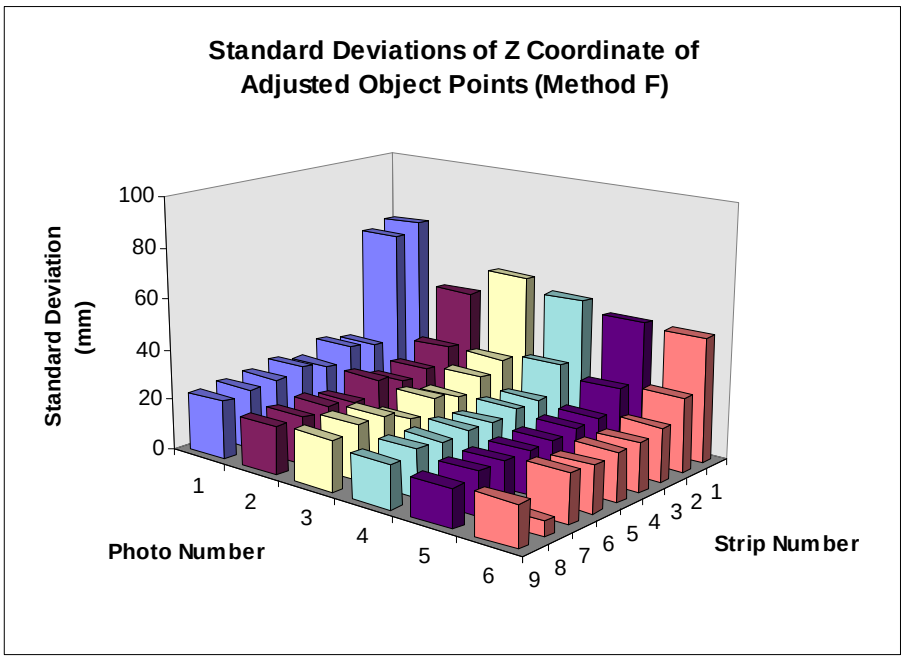

Figure 4. 16. Precision Distribution of Object Points (Method F)

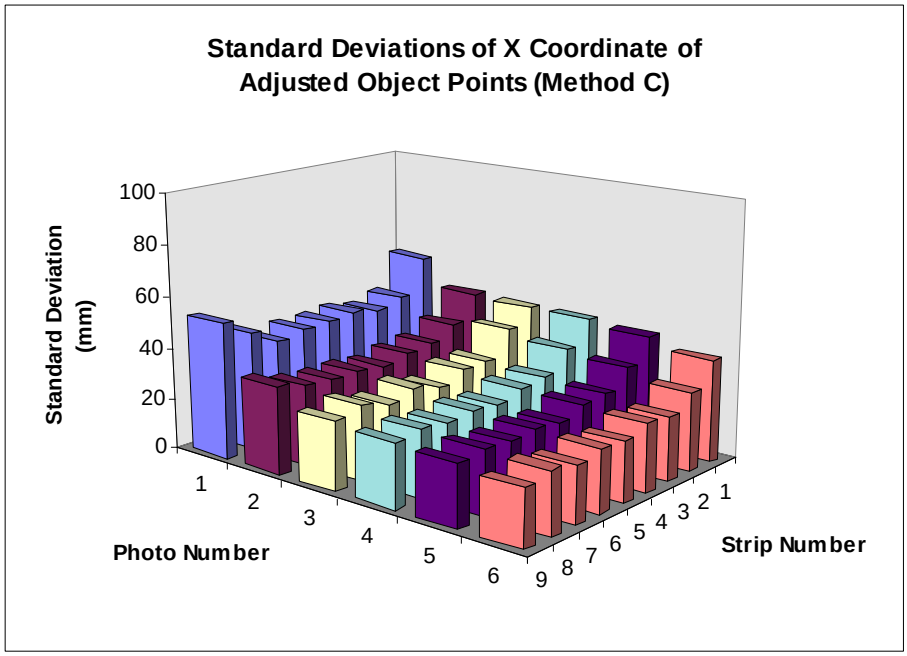

Figure 4. 17 Precision Distribution of Object Points (Method C)

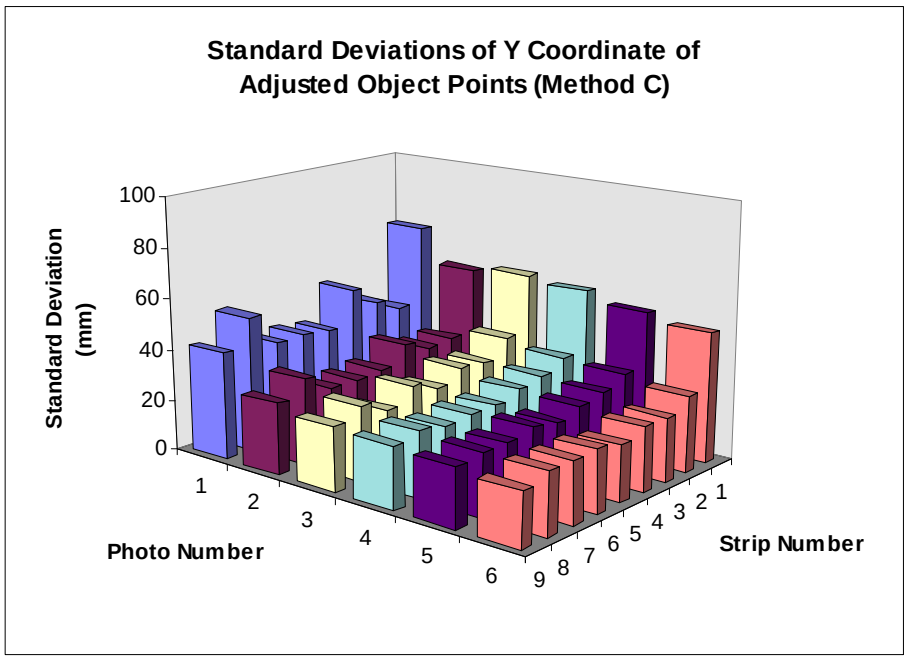

Figure 4. 18. Precision Distribution of Object Points (Method C)

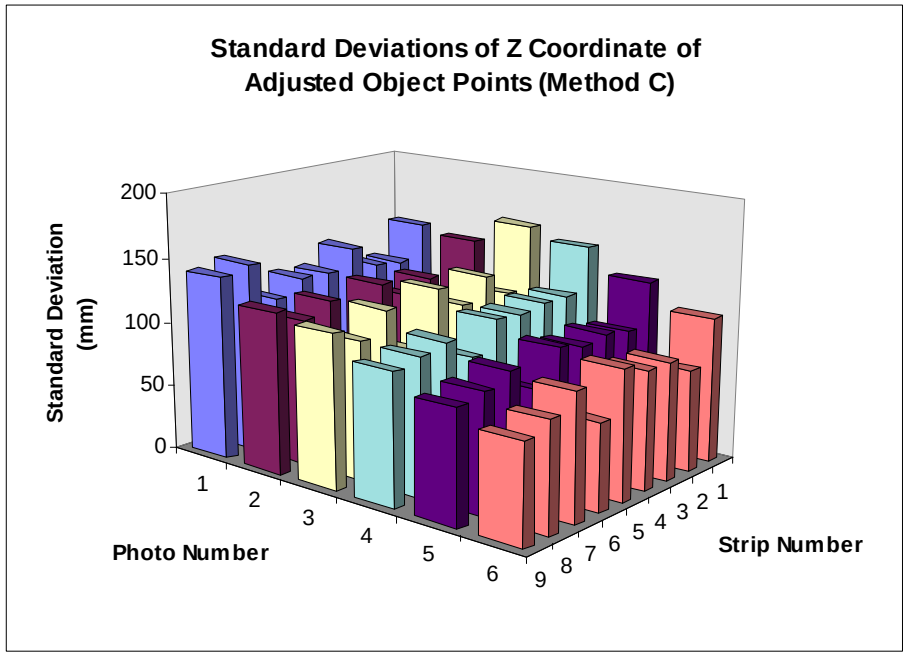

Figure 4. 19. Precision Distribution of Object Points (Method F)

4. 1. 3. The Reliability Analysis of Simulated GPS-Photogrammetric Block

Three measures of reliability; redundancy numbers, internal reliability factors, and external reliability factors, were derived. With a significant level, α=0.1% and a power of the test, β = 93%, the non-centrality parameters δ_0 is equal to 4. The average local redundancy is considered as a measure of the overall reliability of one group of observations. It is defined as (Li and Jie, 1989):

$$r_k = \sum_{j=1}^{n_k} r_j \Big/ n_k \qquad 4.7$$

where n_k is the number of members in the kth group of observations and r_j is the local redundancy of the jth observation in the kth group. Table 4. 2 gives an indication of how to evaluate the different reliability measures.

Table 4. 2. On The Evaluation of The Reliability Measures (From Förstner, 1985)

	Good	Acceptable	Bad	Not Acceptable
r_i	$r_i > 0.5$	$0.1 < r_i \leq 0.5$	$0.04 < r_i \leq 0.1$	$r_i \leq 0.04$
$\delta_{0,i}$	$\delta_{0,i} < 6$	$6 \leq \delta_{o,i} < 12$	$12 \leq \delta_{o,i} < 20$	$\delta_{o,i} \geq 20$
$\overline{\delta}_{0,i}$	$\overline{\delta}_{o,i} < 4$	$4 \leq \overline{\delta}_{0,i} < 10$	$10 \leq \overline{\delta}_{0,i} < 20$	$\overline{\delta}_{o,i} \geq 20$

Figures 4. 20 through 4. 27 show the average local redundancy numbers for image coordinates, GPS observations, and ground control points derived for various ground control configurations. Based on these Figures, the following statements can be made:

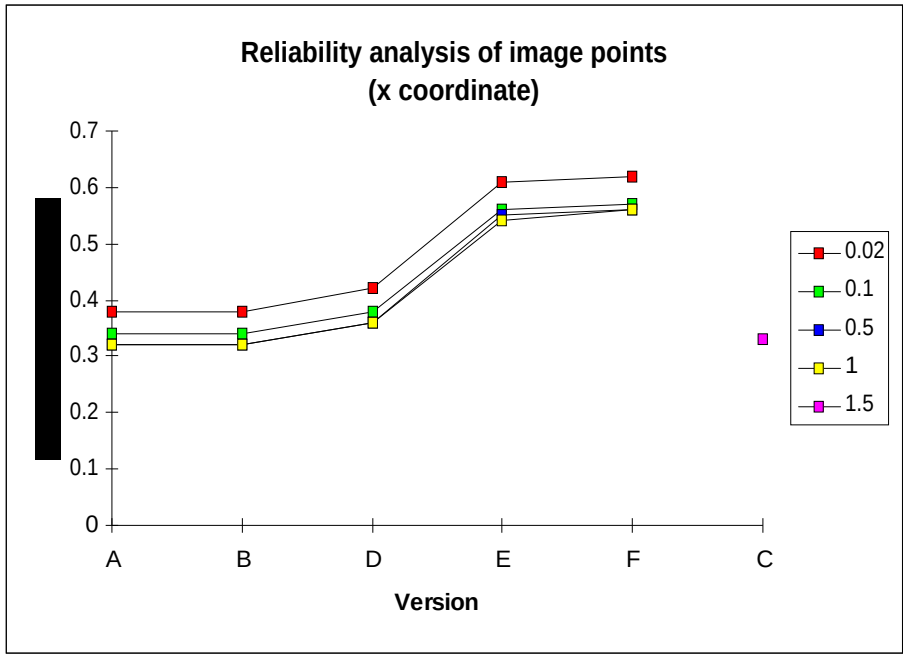

Figure 4. 20. Redundancy Numbers of Image Coordinates

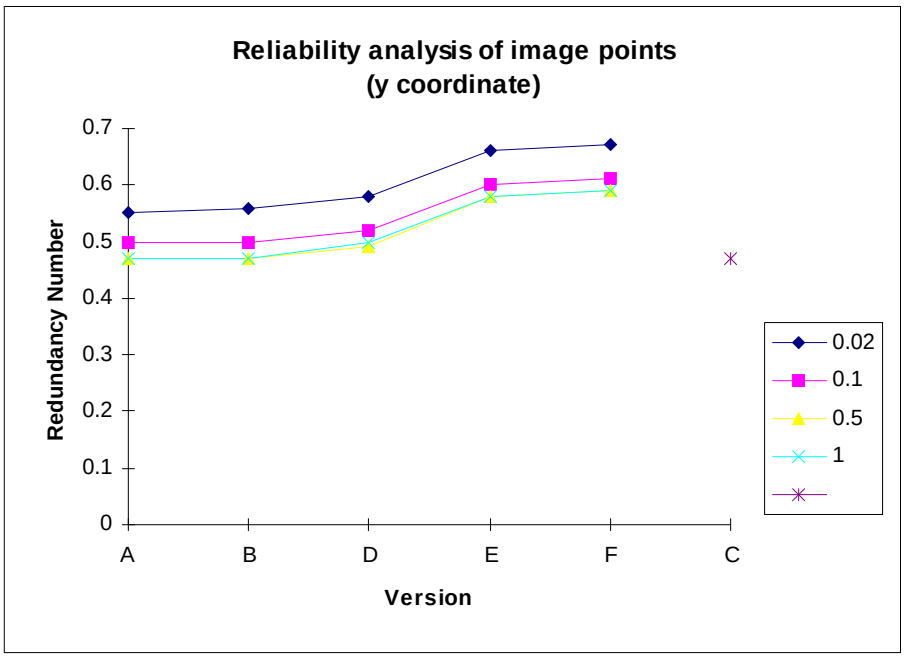

Figure 4. 21. Redundancy Numbers of Image Coordinates

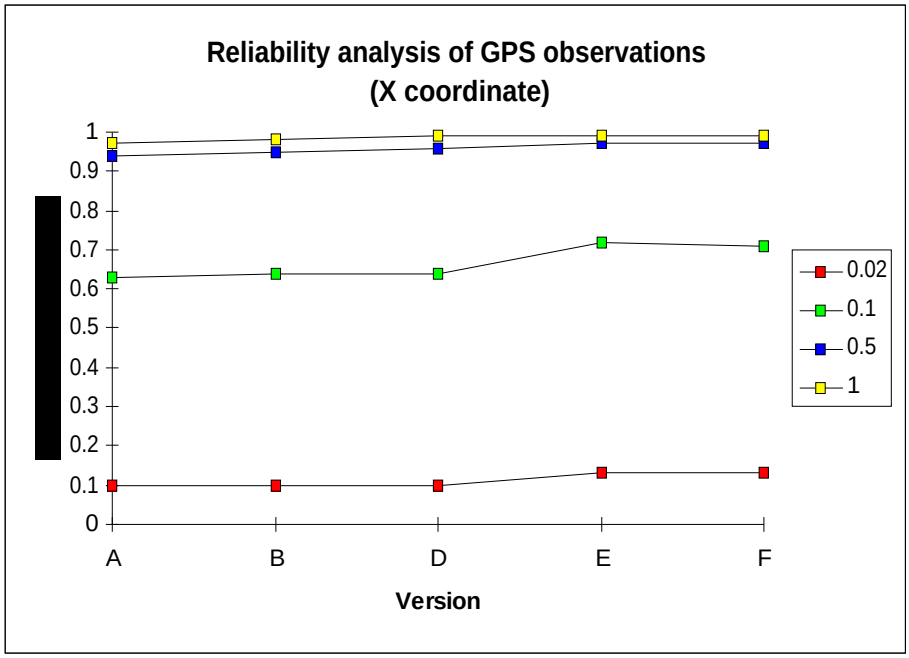

Figure 4. 22. Redundancy Numbers of GPS Observations

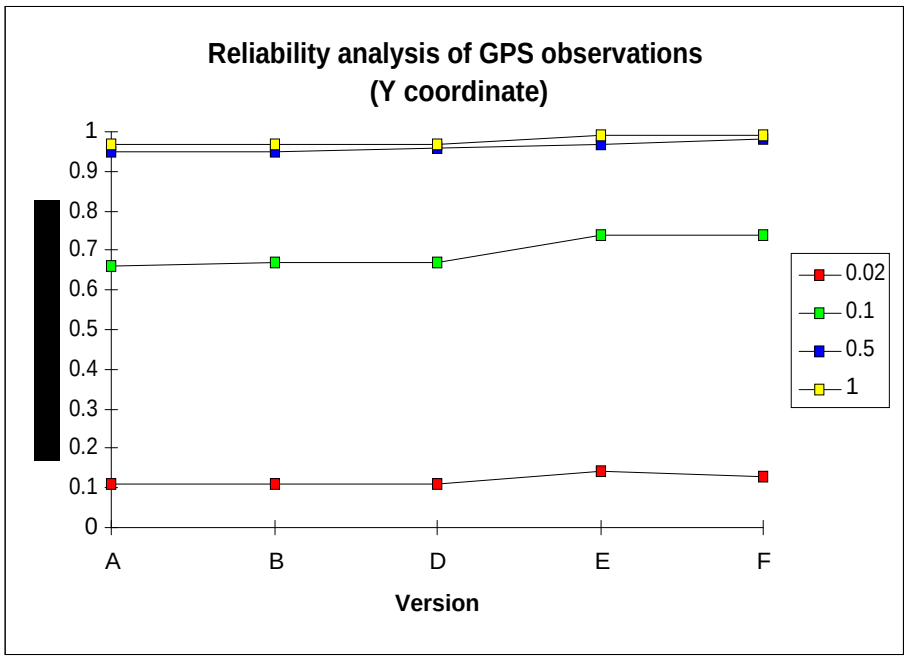

Figure 4. 23. Redundancy Numbers of GPS Observations

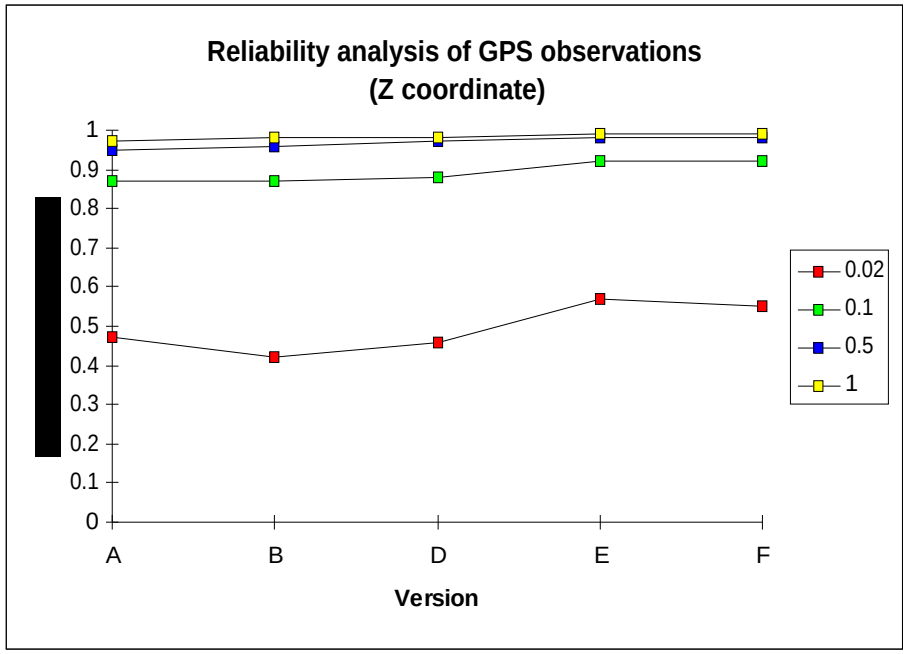

Figure 4. 24. Redundancy Numbers of GPS Observations

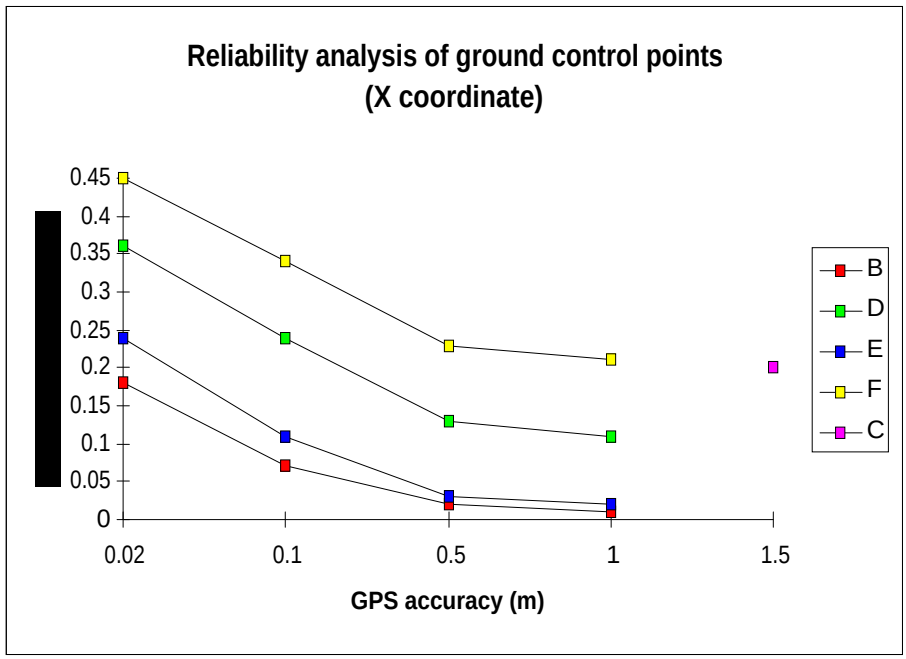

Figure 4. 25. Redundancy Numbers of Ground Control Points

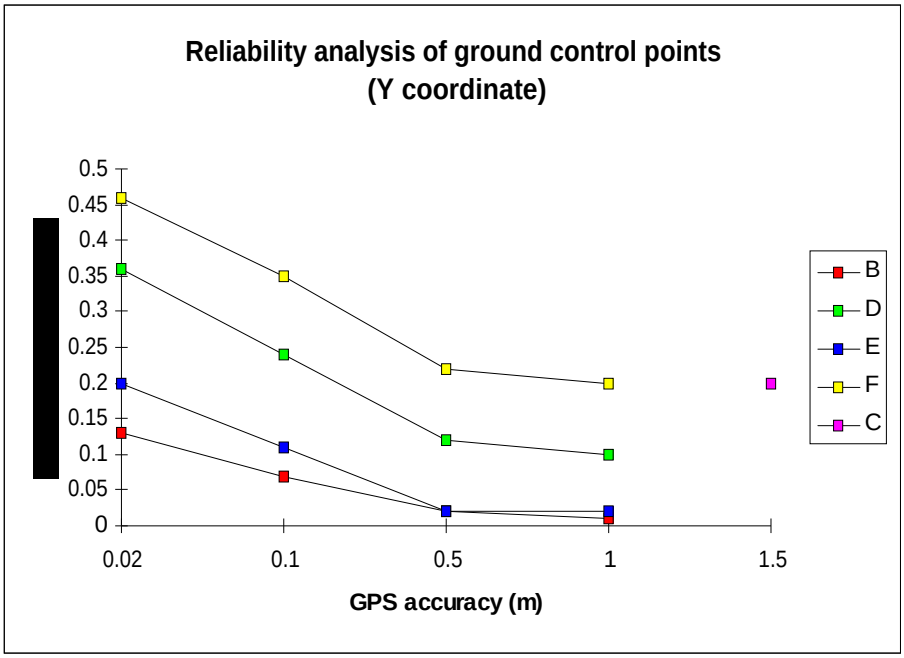

Figure 4. 26. Redundancy Numbers of Ground Control Points

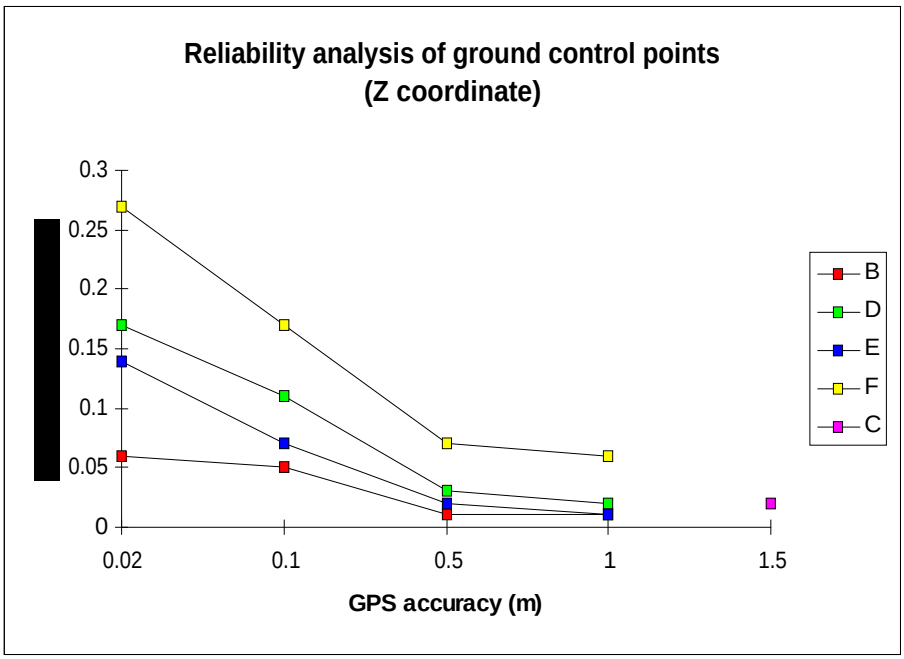

Figure 4. 27. Redundancy Numbers of Ground Control Points

* In an aerial triangulation block incorporating GPS data, the reliability of image coordinates does not depend on the ground control points at the corners of the block. Therefore, from the reliability point of view, GCPs are not needed in a GPS assisted aerial triangulation.

* In a GPS assisted aerial triangulation, the average reliability of image points is not less than that in the conventional block adjustment. The image points become more reliable with more precise GPS data.

* The more precise the GPS data, the smaller their local redundancy numbers become. But compared with the poor reliability of the control points (0.02-0.4) in the conventional block, the reliability of GPS data is better and more homogeneous over the entire block.

* It is well known that the reliability of ground control points in a conventional block adjustment is dependent on the location of the ground control points (Förstner, 1985). Therefore, the replacement of the GCPs with GPS data can alleviate the poor reliability of the control points in a conventional block adjustment.

The effect of an undetected blunder in the observation on unknown parameters can be measured by external reliability. Figures 4. 28 through 4. 35 show the external reliability factors for various groups of observations. Blunders in GPS data, that can not be detected statistically, do not significantly affect the adjusted object points. The external reliability of GPS data is almost better than that of the ground control points

located at the edges of the conventional block. The external reliability factors of image coordinates obtained from all ground control configurations are almost equal or better than those obtained from conventional block adjustment (Figures 4. 28 and 4. 29). The best results were achieved from configurations E and F where 60% sidelap and cross strips have been added. If GPS provides accuracies ranging from 0.1 m to 0.5 m, then the external reliability factors of GPS data are between 1 and 3 producing reliable results (Figures 4. 30, 4. 31, and 4. 32).

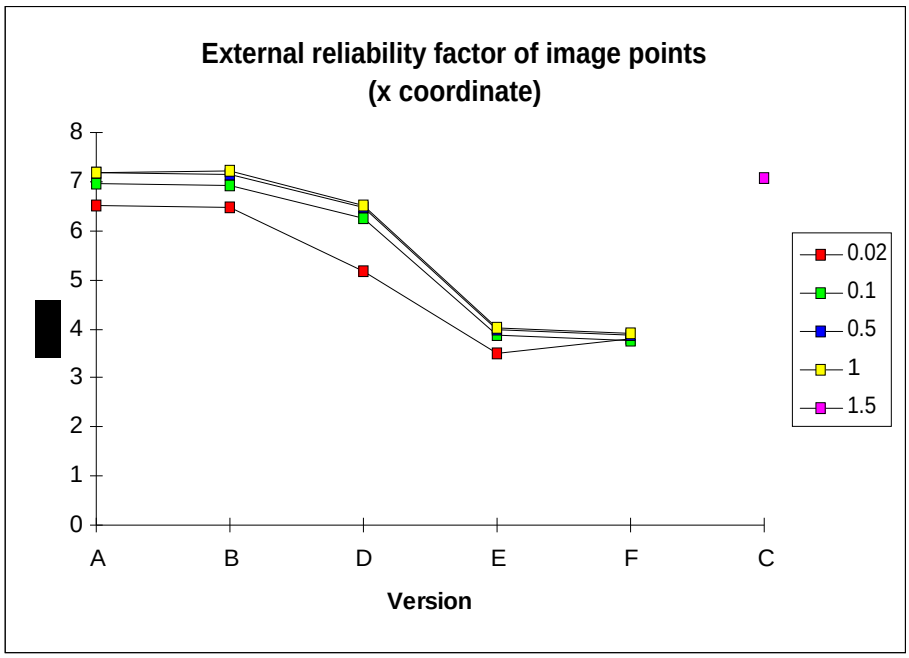

Figure 4. 28. External Reliability Analysis of Image Coordinates

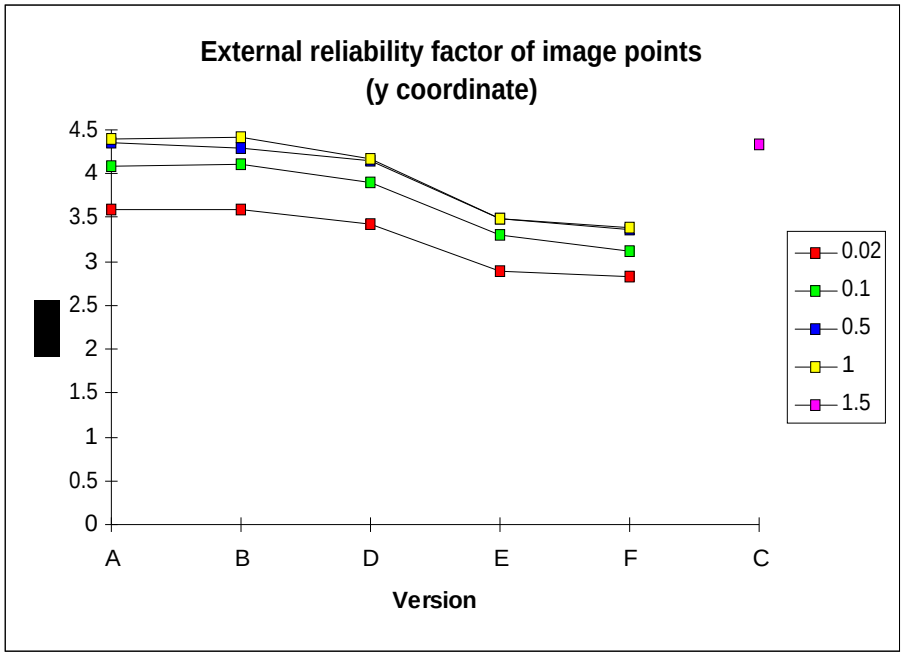

Figure 4. 29. External Reliability Analysis of Image Coordinates

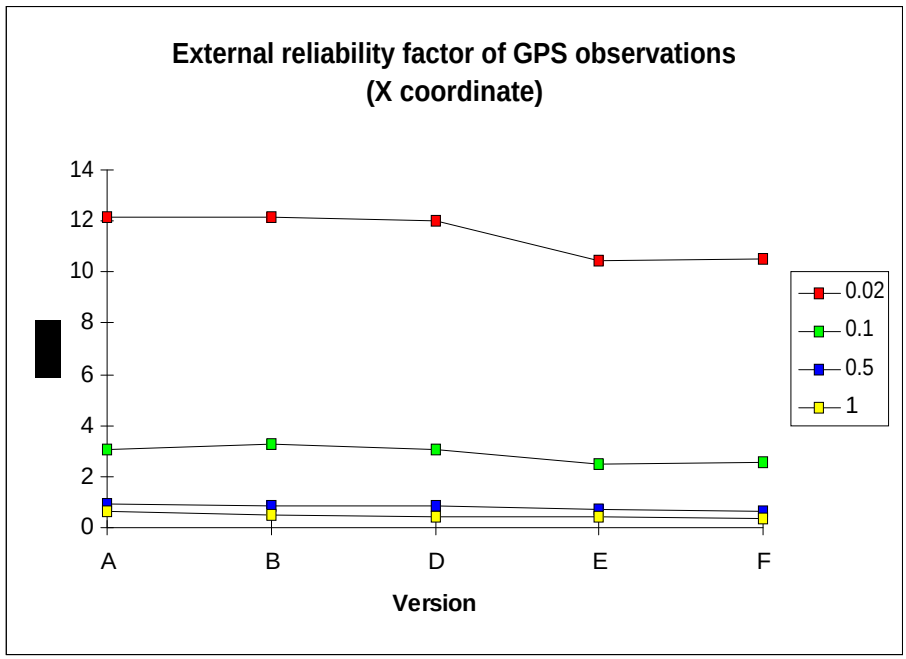

Figure 4. 30. External Reliability Analysis of GPS Observations

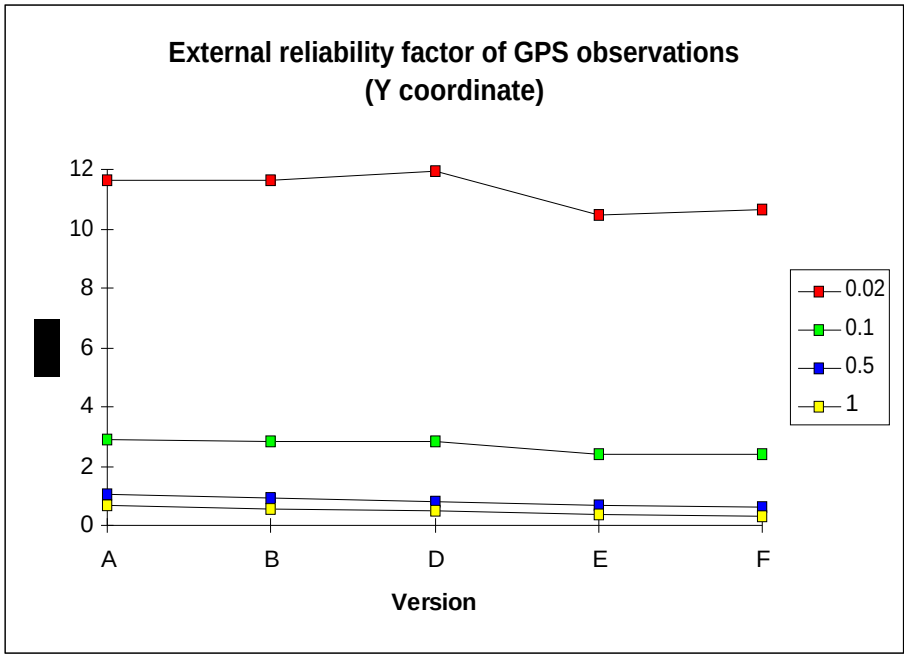

Figure 4. 31. External Reliability Analysis of GPS Observations

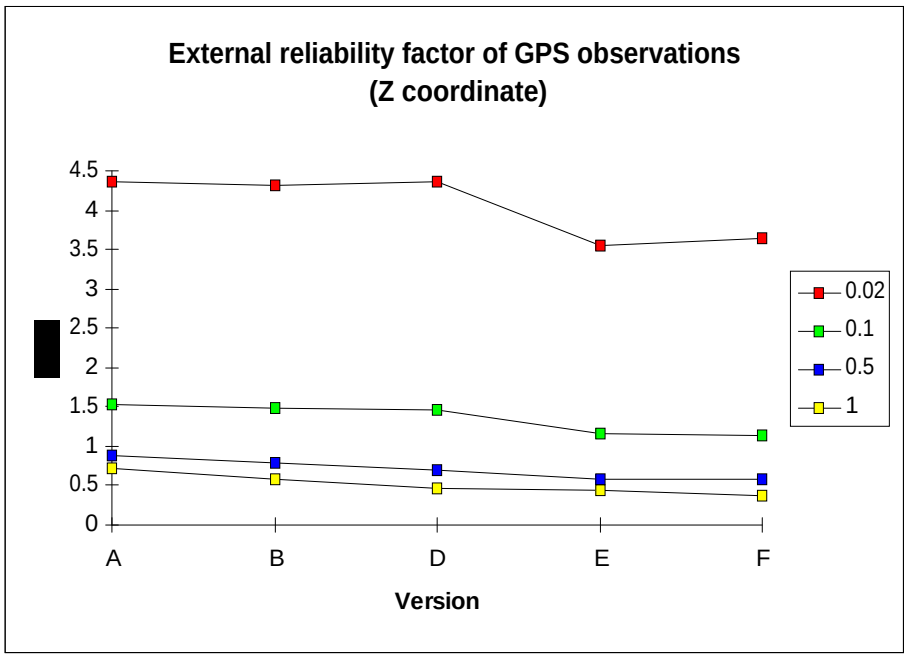

Figure 4. 32. External Reliability Analysis of GPS Observations

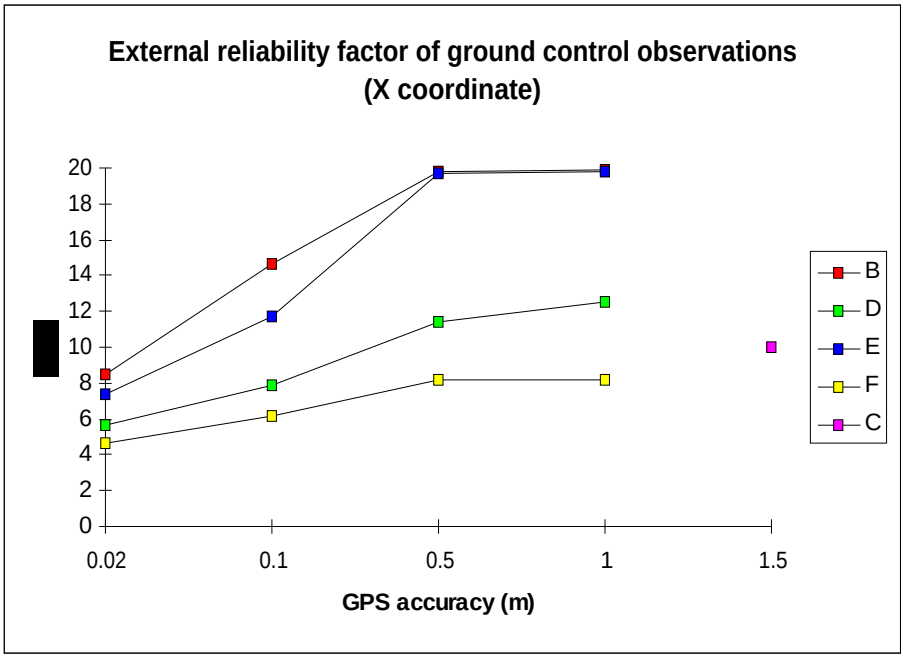

Figure 4. 33. External Reliability Analysis of Ground Control Points

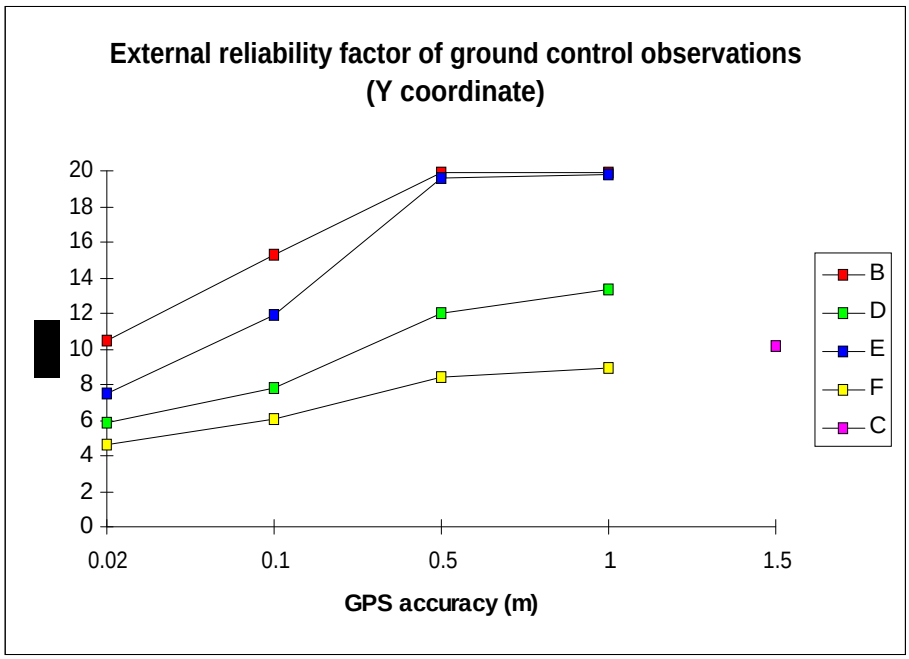

Figure 4. 34. External Reliability Analysis of Ground Control Points

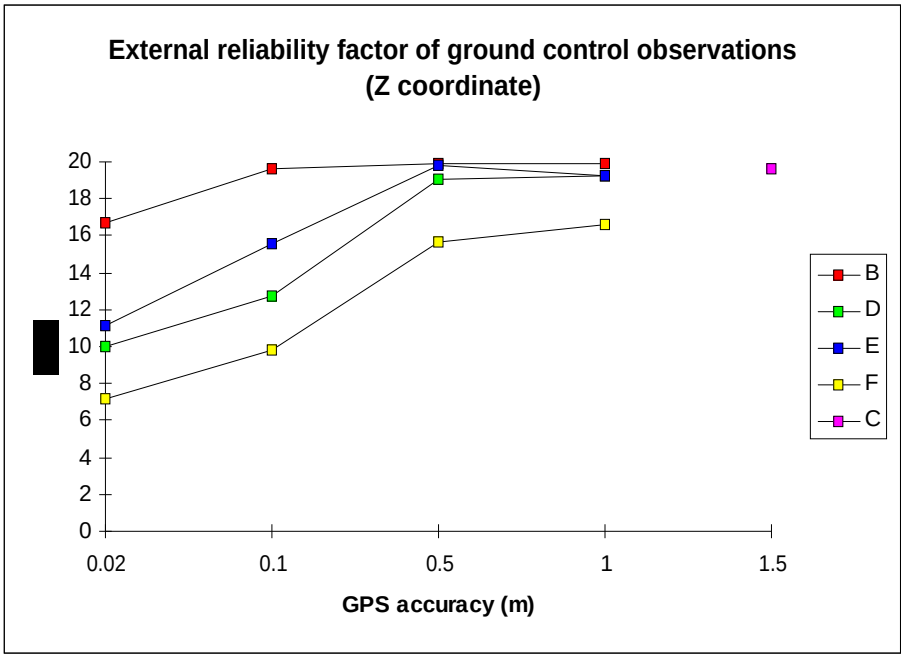

Figure 4. 35. External Reliability Analysis of Ground Control Points

The external reliability factors of image coordinates obtained from configurations A and B are the same, meaning that the ground control points do not have a significant effect on this factor. In all previous Figures for reliability analysis, global (average) values of various reliability measures were shown. Now, local redundancy and reliability factors of image points are considered. For this purpose, the local redundancy numbers and reliability factors of image coordinates for configurations A and B are shown in Figures 4. 36 and 4. 37.

Comparing Figures 4. 36 and 4. 37, shows that the local redundancy numbers and reliability factors obtained from GPS-photogrammetric block adjustment are better than those achieved from the conventional block adjustment. This means that even if these

measures of reliability are looked at locally, the GPS assisted aerial triangulation provides more reliable results.

Configuration A

Corner of the block

	x	y	x	y
r_i	0.35	0.33	0.11	0.43
$\bar{\delta}_{0,i}$	5.45	5.72	11.22	4.62
r_i	0.37	0.43	0.14	0.56
$\bar{\delta}_{0,i}$	5.23	4.58	9.85	3.58
r_i	0.38	0.34	0.35	0.50
$\bar{\delta}_{0,i}$	5.11	5.57	5.52	3.98

Centre of the block

	x	y	x	y	x	y
r_i	0.67	0.57	0.68	0.58	0.67	0.57
$\bar{\delta}_{0,i}$	2.83	3.48	2.77	3.42	2.62	3.48
r_i	0.59	0.60	0.60	0.61	0.67	0.60
$\bar{\delta}_{0,i}$	3.30	3.23	3.28	3.20	3.31	3.20
r_i	0.67	0.57	0.68	0.58	0.67	0.57
$\bar{\delta}_{0,i}$	2.83	3.48	2.77	3.42	2.82	3.48

Figure 4. 36. Local Redundancy Numbers and Reliability Factors of Image Points

Configuration C

Corner of the block

	x	y	x	y
r_i	0.11	0.17	0.10	0.16
$\bar{\delta}_{0,i}$	11.78	8.96	12.05	9.23
r_i	0.12	0.37	0.14	0.51
$\bar{\delta}_{0,i}$	11.01	5.17	9.98	3.95
r_i	0.25	0.18	0.27	0.32
$\bar{\delta}_{0,i}$	6.91	8.47	6.61	3.95

Centre of the block

	x	y	x	y	x	y
r_i	0.56	0.44	0.58	0.44	0.57	0.44
$\bar{\delta}_{0,i}$	3.54	4.55	3.40	4.46	3.47	4.54
r_i	0.57	0.55	0.57	0.58	0.56	0.54
$\bar{\delta}_{0,i}$	3.50	3.60	3.44	3.39	3.54	4.69
r_i	0.56	0.44	0.58	0.44	0.57	0.44
$\bar{\delta}_{0,i}$	3.54	4.55	3.40	4.47	3.49	4.52

Figure 4. 37. Local Redundancy Numbers and Reliability Factors of Image Points

4. 2. Jackson Project

This project was designed to support planimetric mapping at the scale of 1” = 10,000’. The project area is located in and around the city of Jackson, Tennessee, U.S.A. (Figure 4. 38.). Aerial triangulation was required to achieve ± 0.75 m horizontal accuracy for the facility and land-based elements on the derived orthophotos and to support the generation of 5 m contours within the area covered by photography. The project parameters are given in Table 4. 3.

Table 4. 3. Project Parameters

Region: Jackson Utility Division, TN
Purpose: Planimetric Mapping at 1:10,000 Size of Project Area: 40 Km by 20 km Terrain Elevation Difference: 150 m Photo Scale: 1:24,000 Number of Strips: (7 + 2 Cross Strips) Number of Photos: 179 Number of Ground Control Points: 20 (Full) Forward Overlap: 60% Side Overlap: 30%

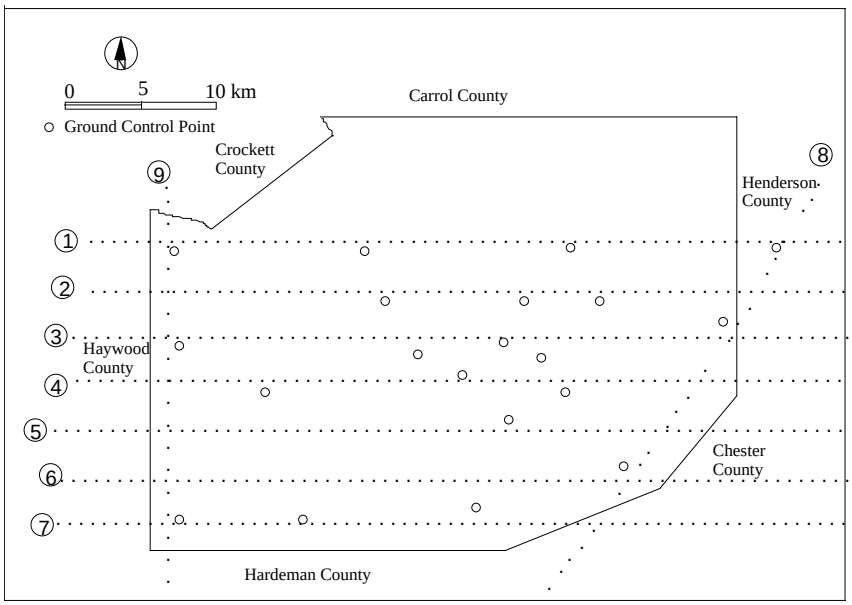

Figure 4. 38. The Study Area (from Ebadi and Chapman, 1995)

4. 2. 1. GPS Data Collection and Processing

GPS data were collected at 1 MHz data rate using Trimble Navigation, Ltd. 4000 SSE dual frequency receiver. Two receivers were used; one as master station located approximately in the centre of the block and the other one as remote station onboard the aircraft. Various methods were used to process these data due to the receiver capability of receiving both L1 and L2 carriers. Double difference GPS processing techniques were applied in all methods in order to eliminate or reduce the effects of some of the GPS errors (e.g., timing errors and atmospheric errors). Static data were collected prior to take-off and after landing for initial ambiguity resolution, which also made possible the processing of data in reverse mode. The coordinates of the antenna phase centre at each epoch were determined using a Kalman filtering techniques, and “On The Fly” ambiguity

resolution technique, whenever needed. The initial cycle ambiguities were determined using the fixed baseline technique, and the data were then processed in a continuous kinematic mode. The GPS data set was continuous throughout the flight mission, except for one loss of lock at the beginning of the mission (while in static mode). The re-initialization was performed after flight mission to verify the correct determination of the ambiguities, and provide independent check on the GPS data processing.

Twenty ground control points were established during an independent survey using conventional DGPS static and rapid static processing. The accuracy of these points is within the range (10 mm + 10 ppm). Elevations (orthometric heights) were computed from the GPS-derived ellipsoidal heights by means of geoid undulations.

4. 3. GRAFNAV

GRAFNAV software, developed by Waypoint Consulting Inc., (1994), was utilized to process the GPS data. This software is a Window and menu based and allows informatic switch from static to kinematic data processing. The Quick Static ambiguity resolution method can be applied to resolve the ambiguities for medium and short baselines (e.g., <7 km) in 5 to 15 minutes, depending on availability of L2 carrier phase data, the length of baseline, and satellite geometry. A fixed static solution can be used for medium length baselines (7-15 km). A float static solution is available for long and/or noisy baselines. “On The Fly” ambiguity resolution allows the user to start up in kinematic mode and/or fix otherwise unrecoverable cycle slips. The software accepts data

in .GPB format which is a binary GPS format. Utilities are available to convert from other formats to this format, enabling the software to process data collected with a multitude of receivers.

Differential processing determines a three dimensional baseline between two stations. There are three types of static solutions supported by GRAFNAV; float solution, fixed solution, and quick static solution. Kinematic processing is usually started with a static survey or from a known point. All GPS computations are carried out in differential mode (double difference) meaning that the pseudorange, carrier phase, and doppler values are subtracted twice. The first subtraction removes the range/phase/doppler value of the baseline, while the second subtraction removes these values from the master station.

4. 3. 1. Overview of Various Processing Modes in GRAFNAV

Static processing is the default mode, however the program can switch automatically from static to kinematic by inspecting a flag in the binary data.

4. 3. 1. 1. Float Static Solution

Positions and velocities (X, Y, Z, Vx, Vy, Vz) and ambiguities (number of satellites - 1) are computed in this mode. During static processing mode, the program goes into a “learning” mode, and positions and ambiguities are solved simultaneously.

Any deviation of the position over time is an indication of the accuracy. The ambiguities are not fixed to integer values. For a good data set with long observation time (e.g., >30 minutes), the ambiguities will converge to integer values which is an indication of stability in the data. Carrier phase RMS is also an indication of a clean data set when it is less than 0.05 m. Accuracy of 5 ppm (parts per millions) can be expected using this solution for baselines with 45 minutes of observation time.

4. 3. 1. 2. Fixed Static Solution

In the first step, the optimal observation time span is found by scanning the static data section, and selecting the longest interval without any cycle slips or loss of satellites on the selected satellites. The next step is to determine a fairly good approximate position of the remote station with one pass of the float solution. The float solution is assumed to be accurate enough for subsequent processing (± 20 cm). An ambiguity search technique is initiated next ± 1.5 cycles around the float solution, assuming that the ambiguities must be integer values. These intersections are then tested on the data by applying a sequential technique. The result is an averaged solution using the fixed ambiguities and an RMS value which shows how well this intersection fits the data. It is recommended that this solution be used for baselines smaller than 15 km or for time spans more than 15 minutes.

The fixed solution uses a phase trend cycle slip method to detect and correct cycle slips. This method fits a polynomial through a few epochs of phase measurements to

detect slips. The accuracy of fixed static solution is approximately 2 ppm provided that at least 30 minutes of data are collected.

4. 3. 1. 3. Quick Static Solution

This method commences with a float solution, which performs a single pass to determine an initial starting position, about which the search cube is centred. In the second pass, the quick static takes over, and determines a search cube at the beginning and the end of the time span. The method uses a cosine function test. Acceptable intersections are tested at the second epoch at the end of the quick static period. An RMS is computed and used to sort the intersections and extract optimal values. A third pass is carried out to finally find the best solution. The size of the search cube depends on the accuracy of the solution from the first pass, therefore, narrow correlator receivers or P-code receivers offer more accurate solution after 10 minutes than C/A code receivers. This method requires a minimum of 5 minutes of observation time. It is advised that quick static techniques be used on baselines shorter than 7 km.

The third pass tests ambiguity values using the positions of the best intersections. This method is independent of cycle slips, because of using position other than ambiguities. During this pass, the ambiguities should be stable if they are correct. The accuracy of this method is about 5 ppm of the baseline length..

4. 3. 2. GPS Kinematic Processing using GRAFNAV

The processing techniques are the same as the float static solution. The only difference is that the program is not in a “learning” mode. Position (X, Y, Z), velocity (Vx, Vy, Vz) and ambiguities (n-1) are computed. When a cycle slip is detected, the ambiguities become unknown and their variances are increased. In this case, the ambiguity of the relevant satellite becomes unstable, and may cycle around for a few epochs. The ambiguity unknowns may also be adjusted to compensate for multipath or ionosphere. The following techniques can be used to start the kinematic GPS survey:

a - starting from a known control point,

b - initializing with static or quick static solution,

c - “On The Fly” kinematic ambiguity resolution which requires 5 or more satellites.

4. 3. 2. 1. On The Fly Ambiguity Resolution

“On The Fly” (OTF) kinematic ambiguity resolution searches the ambiguities and evaluates relative quality of each intersection (RMS). This technique can be used in kinematic mode because it examines ambiguities instead of positions. OTF uses many minutes of kinematic and static data following a serious loss of lock. OTF is only applied if the program is started in kinematic mode or a serious loss of lock occurs (i.e., the receiver is tracking less than four satellites).

OTF searches the data following the loss of lock. A suitable time span is chosen in such a way that it maximizes the number of satellites, maximizes the length of the time

span, and minimizes the time between the loss of lock and the start of the OTF. The search cube is defined based on whether the receiver has precise pseudorange available. An instantaneous C/A code position may not fall within this cube size. Due to the fact that OTF uses many seconds of data following the loss of lock, a more precise position is derived. It is very beneficial to OTF if L2 phase measurements are also available.

Unreliable results may be obtained if the RMS value is more than 0.05 cycles and the reliability value is less than 1.5. This can happen due to the following:

* poor initial approximate,
* the long distance between master and remote stations,
* unavailability of L2 carrier phase data,
* Large ionospheric or multipath error,
* poor geometry or not enough satellites.

4. 4. Kinematic GPS Processing of Jackson Data Set

The Jackson data set was processed using various methods due to the availability of both L1 and L2 Carrier frequencies. These methods are described in the following sections. The satellite geometry was derived using PDOP formula and shown in Figure 4. 39. As shown in Figure 4. 39, for most of the time, the PDOP is less than 3 which is an acceptable value for airborne-GPS applications.. Six to eight satellites were tracked for the entire mission. The master station was set up in the centre of the photogrammetric block to minimize the atmospheric effects. The distance between the monitor and remote

stations did not exceed 30 km. In all methods of processing, GPS data rate was 1 MHz. The options used for each method are shown in Table 4. 4.

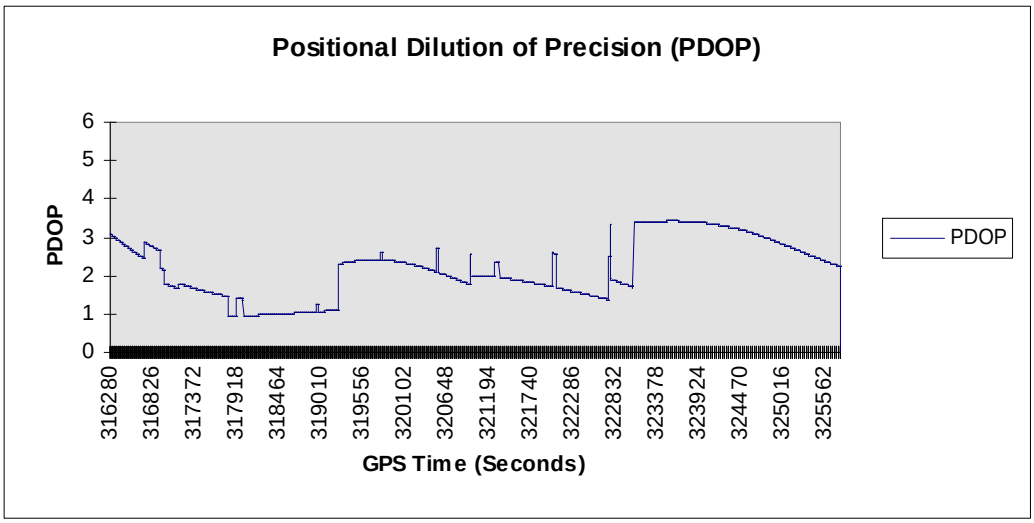

Figure 4. 39. PDOP for Jackson Data Set

Table 4. 4. Processing Methods of Jackson Data Set

	Dual Frequency	Single Frequency	OTF	Solution	Processing Mode
Method 1	Yes	No	Yes	Float	Forward
Method 2	No	Yes	Yes	Float	Forward
Method 3	Yes	No	Yes	Float	Reverse

According to the standards for medium scale mapping, the required accuracy for camera exposure stations is less than 1 m. Therefore, in all GPS processing methods, float solution was chosen. “On The Fly” ambiguity resolution option was activated to take care of loss of lock in the case of less than 4 satellites. This could happen when the aircraft is turning. Forward and backward processing procedures were used, and the

forward and backward trajectories compared to examine the repeatability of GPS data. Both dual and single frequencies were used to compare the results and find out how much accuracy degrades due to the lack of L2 carrier phase. Relative ionospheric correction did not improve the results, thus, this option was turned off.

RMS values for L1 carrier phase data obtained from the three methods are shown in Figure 4. 40 - 4. 42. There are just 4 spikes of 6 cm in all cases which are assumed to be caused mainly by multipath. RMS values are about 2 cm for all methods . There is a slight degradation in RMS when single frequency was used (Method 2). Comparison between Figures 4. 40 and 4. 42 show that the forward and reverse trajectories are compatible and repeatable. One of the advantages of using dual frequency technique is that it helps to resolve ambiguity values quicker, because of widelane carrier phase processing techniques. The mean of RMS values for these three methods are 16.4, 17.1, and 16.9 mm and their standard deviations are 12.0, 13.5, and 12.5 mm, respectively. Method 1 provides better results by comparing these values. Although there is 1 mm degradation in the mean and 2 mm in standard deviation when single frequency was being used, it is still an acceptable accuracy for medium scale mapping.

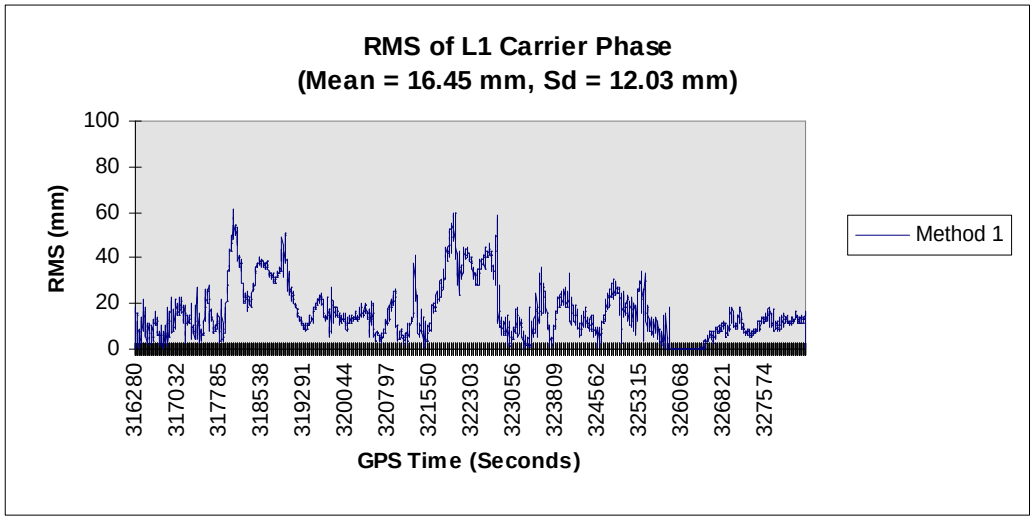

Figure 4. 40. RMS of L1 Carrier Phase Obtained from Method 1

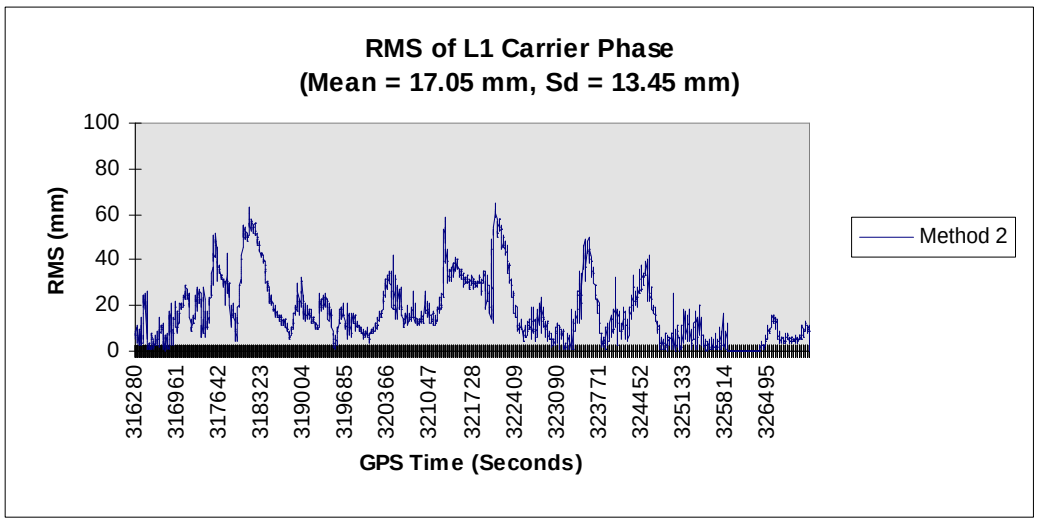

Figure 4. 41. RMS of L1 Carrier Phase Obtained from Method 2

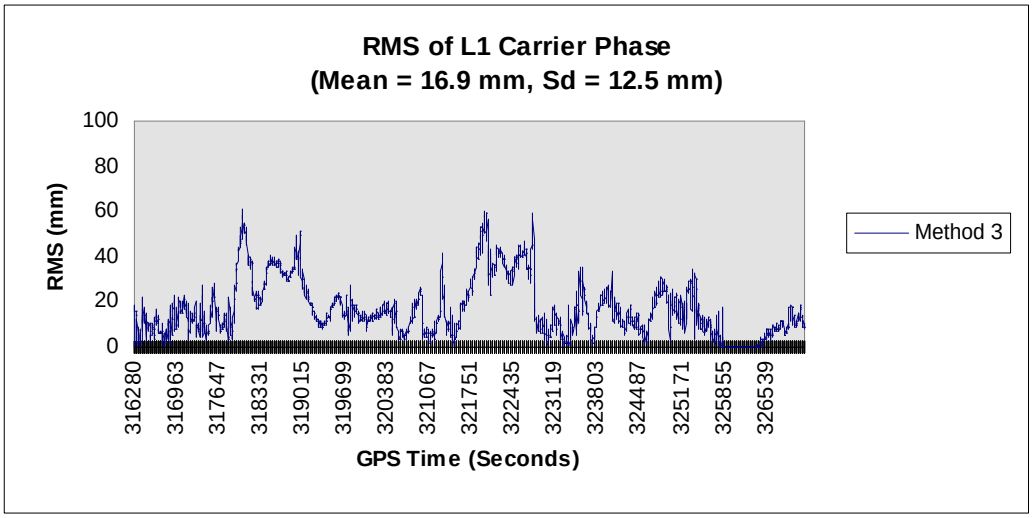

Figure 4. 42. RMS of L1 Carrier Phase Obtained from Method 3

GRAFNAV also generates a quality number ranging from 1 to 6 as a function of the geometry of the satellites, and RMS of the L1 carrier phase (1 is best and 6 is worst). The quality numbers for the three processing methods are shown in Figures 4. 43 - 4. 45. The quality number is 1 for almost the entire flight mission when using both L1 and L2 carrier frequencies. It was degraded a little when single frequency was chosen to process the data (Method 2). This number for Method 3 (reverse processing mode) is the same as that of Method 1.

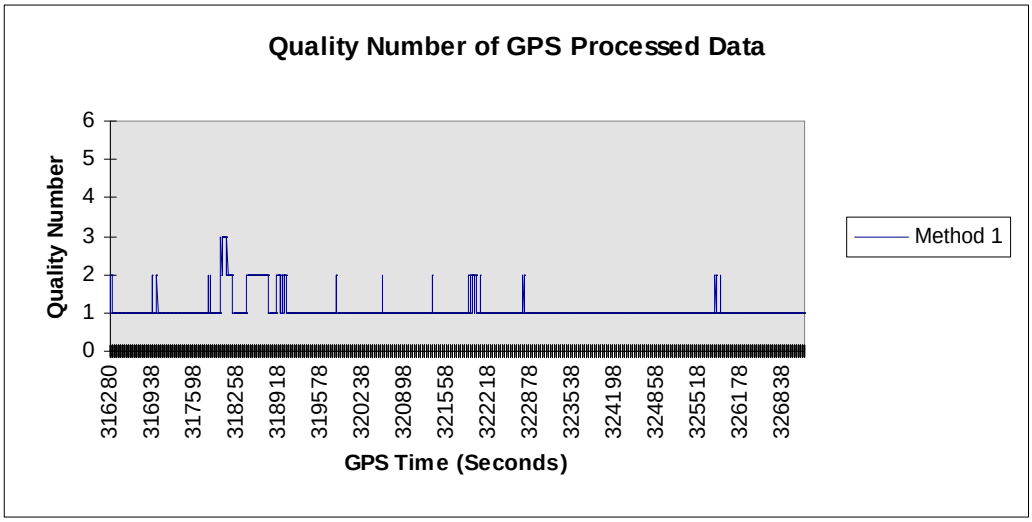

Figure 4. 43. Quality Number Obtained from Method 1

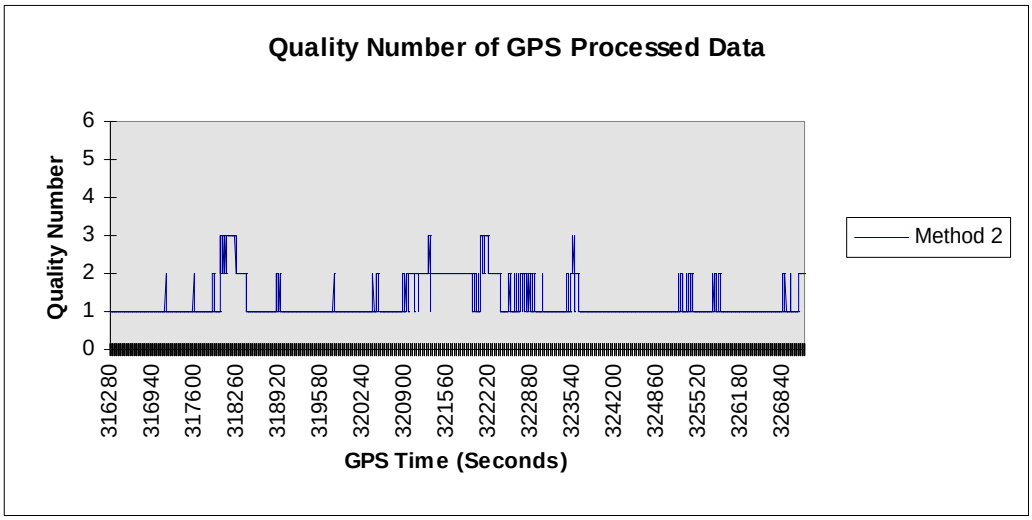

Figure 4. 44. Quality Number Obtained from Method 2

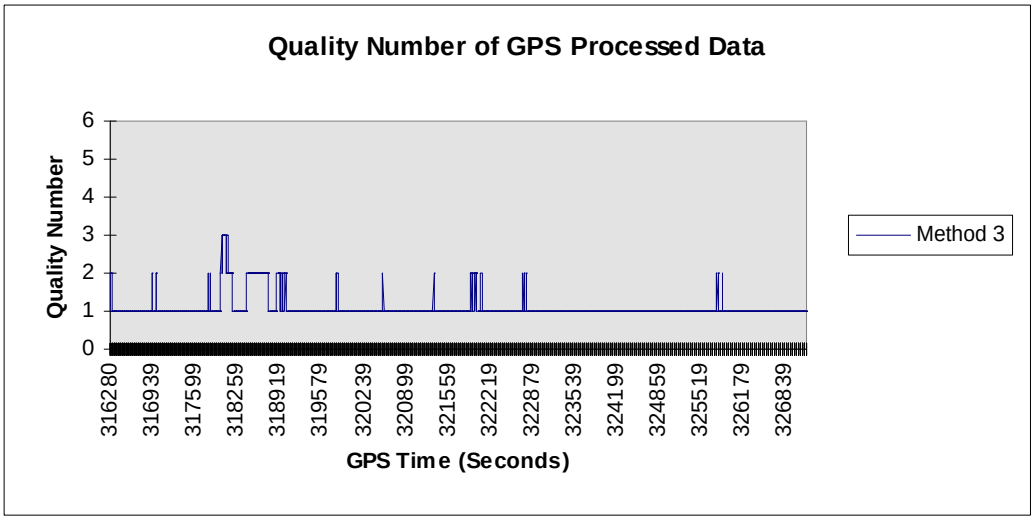

Figure 4. 45. Quality Number Obtained from Method 3

In order to see the behavior of ambiguities for the entire mission, ambiguity drifts were computed and are shown in Figures 4. 46 - 4. 48. The mean values of ambiguity drifts for Methods 1, 2, and 3 are 0.0008, 0.0018, and 0.0009 cycles per second. The standard deviations of ambiguity drifts are 0.001, 0.0019, and 0.001, respectively. These values show that ambiguities were relatively constant after resolving them for the entire flight mission. Although there are some spikes due to loss of lock on a particular satellite during banking in Figure 4. 47, but these drifts are still acceptable.

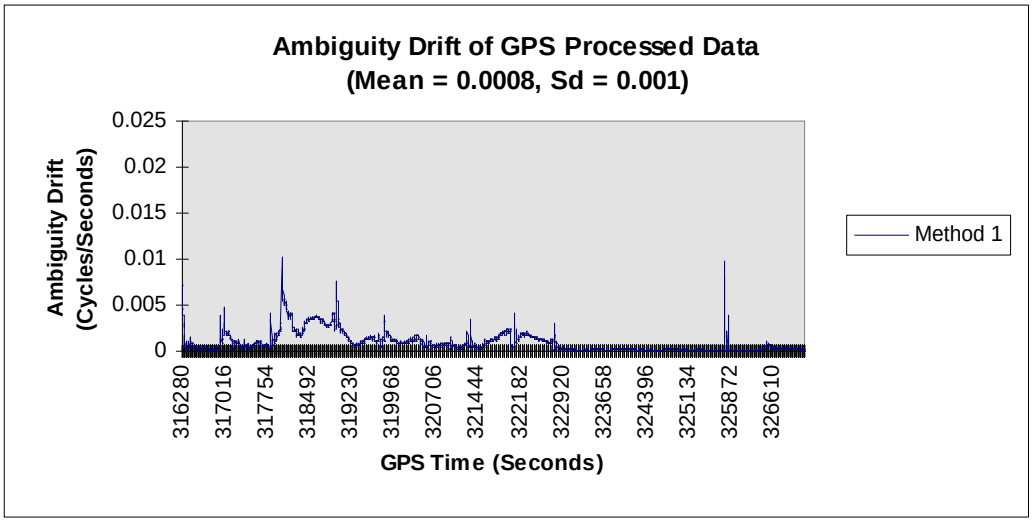

Figure 4. 46. Ambiguity Drift obtained from Method 1

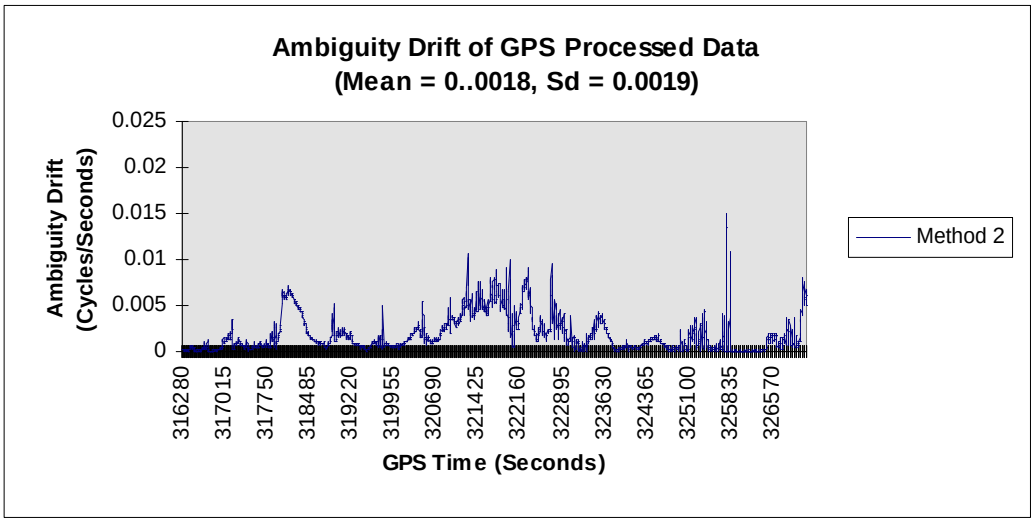

Figure 4. 47. Ambiguity Drift obtained from Method 2

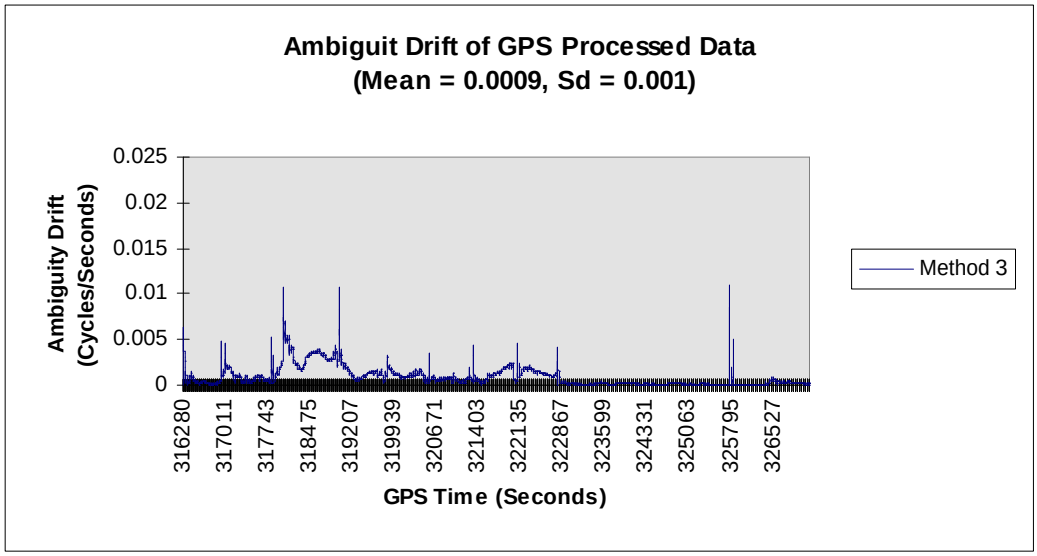

Figure 4. 48. Ambiguity Drift obtained from Method 3

The differences in X, Y, and Z from forward and reverse trajectories were computed to compare the repeatability of airborne-GPS data. These differences are shown in Figure 4. 49. The X, Y, and Z differences are less than 10 cm for almost entire mission except one spike of 30 cm which happened at the middle of mission due to the abrupt change in satellite geometry.

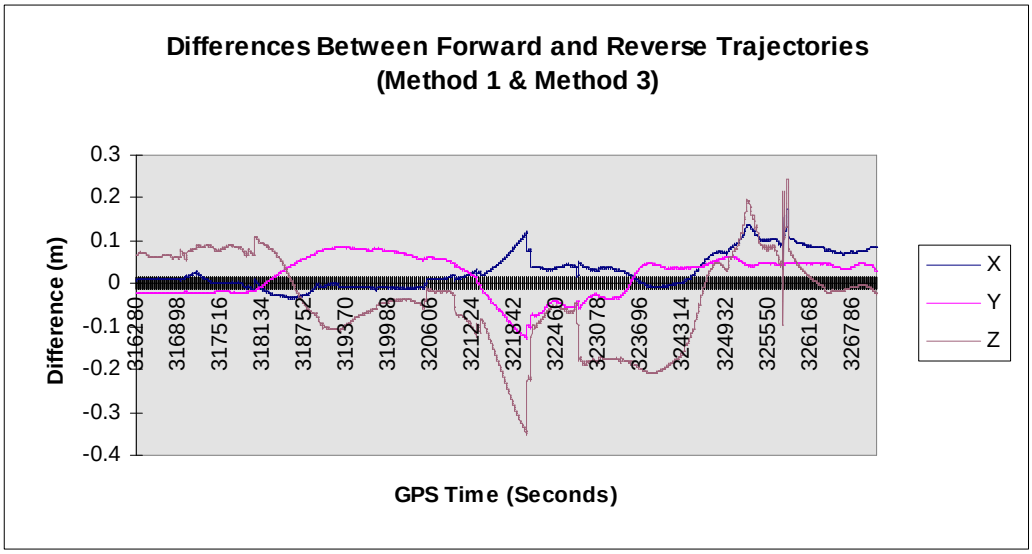

Figure 4. 49. Difference Between Forward and Reverse Trajectories

4. 5. Photogrammetric Processing of Jackson Data Set

The flowchart of the processing methodology for GPS-assisted aerial triangulation is shown in Figure 4. 50.

This rigorous and integrated approach to the GPS-assisted aerial triangulation has been successfully implemented on Jackson project. As known, the GPS-photogrammetric bundle block adjustment includes the simultaneous, rigorous, and 3-dimensional adjustment comprising reduced image coordinates, GPS camera exposure station coordinates, and ground control points as well as other auxiliary information which may be available. These observation should be appropriately weighted.

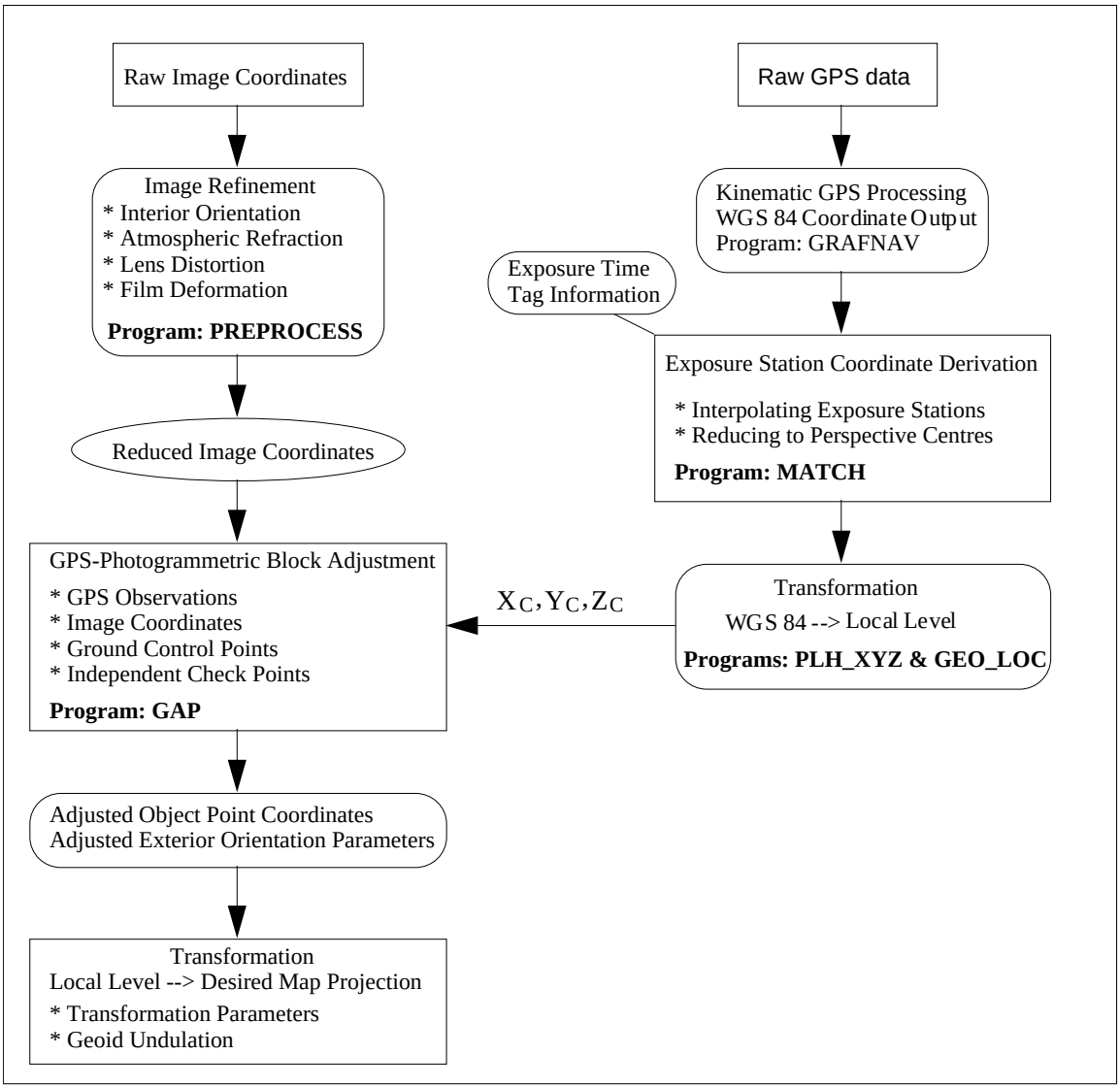

Figure 4. 50. Processing Methodology of GPS-Assisted Aerial Triangulation

4. 5. 1. Methodology

All photogrammetric measurements were carried out on a Wild BC 1 analytical plotter, with point transfer being under taken with a Wild PUG device (Trevor et al., 1994). All measured image coordinates were reduced to the fiducial coordinate system and corrected for systematic errors such as, principal point displacement , radial lens

distortions, film deformations, and atmospheric refraction. Image coordinates were not corrected for earth curvature effects since the block adjustment was to be executed in a Local Level Cartesian coordinate system (LL). The reduced image coordinates serve as input into the adjustment.

Coordinates of antenna phase centre were obtained from airborne kinematic GPS processing described in previous sections (Method 1). All camera exposures were stored as time-tagged events within the GPS data file during the photographic mission. Each instant of exposure was interpolated from the GPS processed data using both linear and polynomial interpolation techniques and subsequently reduced to the camera exposure stations knowing the antenna-camera offset and the attitude of the aircraft. The WGS84 coordinates of camera exposure stations were then transformed to the local level Cartesian coordinate system by 3-dimensional, rigorous transformation before being introduced to the adjustment. The origin of this system was chosen to be in the centre of the project area such that X_L, Y_L, Z_L coordinate axes were closely oriented with respect to the Northing-Easting-Up system.

The ground control point coordinates were determined using GPS static processing technique and the baseline vectors were rigorously adjusted through 3-dimensional least squares adjustment software. These coordinates in WGS84 were also transformed to the LL system.

The bundle adjustment was executed in the local level coordinate system. Various configurations of GPS-photogrammeric block adjustment were run based on the following factors:

* Observational weighting ,
* Block geometry,
* Ground control configuration,
* Self calibration

4. 5. 1. 1. Observational Weighting

The role of observational weighting in GPS-photogrammetric block adjustment has not been received adequate attention (Fraser, 1995). This is more important in the presence of systematic error initiated from GPS and datum related error sources, as well as errors in camera interior orientation parameters. Three types of observational data are typically present in the GPS-photogrammetric bundle block adjustment, namely; image coordinates observations, GPS exposure stations, and ground control points. The observational weight of the image coordinates refers to the relative orientation of the block and to block shape in free space, while the weight of GPS camera exposure stations and ground control points relate directly to positions. Relative weighting of observations has a direct impact on the precision of aerial triangulation, especially in the presence of biases. A good example could be where both GPS and ground control observations have low weights. In this case, the block is allowed to float to fit its best position for an

optimal level of triangulation misclosure. The problem here is that the coordinate system is not sufficiently defined, particularly with biases, block shifts of a significant amount can not be avoided.

Assuming that σ_{GPS} and σ_{GCP} are the positional standard errors of GPS observations and ground control points, and σ_{XYZ} and σ^{C}_{XYZ} be the standard errors of object point coordinates and exposure station coordinates, respectively obtained from a full control block. If $\sigma_{GPS} >> \sigma^{C}_{XYZ}$, the object space datum is defined by weight matrix of GPS observations (P_{GPS}) and the relative geometry of the block triangulation will be determined by photogrammetric observations. The situation is different when $\sigma_{GPS} \leq \sigma^{C}_{XYZ}$, in this case, weight matrix of GPS observations, P_{GPS}, serves as a constraint on the relative and absolute orientation of the block. Incorporating ground control can improve the absolute accuracy of the block depending on the relative contributions of P_{GPS} and P_{GCP} (i.e., weight matrix of ground control points) and the presence of systematic errors (Fraser, 1995). For a block with small number of control points, the effect of ground control points is negligible unless $\sigma_{GCP} << \sigma_{GPS}$.

Photogrammetric blocks controlled by GPS air stations and no control points could have some unfortunate results if interior orientation parameters are contaminated by systematic errors. For example, a systematic error in focal length will have a direct impact on the Z coordinate of object points.

In order that the ground control points play the dominant role on the absolute orientation of the block, the conventional block adjustment with just control points and very small weights for GPS observations should be carried out.

A favourable procedure found in this study is that the bundle block adjustment can be executed using GPS exposure stations with appropriate weights through P_{GPS} and available ground control points with a simultaneous 3D similarity transformation. This preserves the shape of the bundle network, compensates for any systematic errors introduced from interior orientation of the camera, and accounts for small differences in origin or orientation between the ground coordinate system and airborne GPS system.

Inclusion of stripwise drift parameters allows for compensation of these systematic errors and, therefore, GPS signal interruption between strips can be tolerated (Fraser, 1995). However, this requires certain GPS processing techniques to be used.

4. 5. 1. 2. Block Geometry

Loss of satellite lock, with subsequent cycle slips and difficulties in recovering the GPS ambiguity resolutions, have been viewed as a significant problem and error source for airborne kinematic GPS applications (Fraser, 1995). Error modeling through inclusion of drift parameters in the block adjustment allows us to model the errors introduced by the approximate ambiguity solutions through stripwise shifts and time-dependent linear drift terms (Ackermann and Schade, 1993). These six parameters per

strip will destabilize the geometry of the block, and might have some negative impacts on recovery of all unknowns in the adjustment (e.g., singularity of normal matrix). Therefore, cross strips are employed to overcome this problem, and make it possible to recover all unknown parameters. It has to be mentioned that the airborne GPS data should be processed in a special way in order to use drift parameters in a block adjustment (i.e., locking on new pseudorange at the beginning of each strip and tracking L1 carrier phase continuously for each strip).

4. 5. 1. 3. Self Calibration

In order to further improve the accuracy of combined GPS-photogrammetric bundle block adjustment, the self calibration approach was also considered. Self-calibration bundle block adjustments were carried out with and without additional parameters. GAP uses three different techniques to formulate the additional parameters; conventional lens distortion formulas, Brown's formulas, and Harmonic functions.

4. 5. 2. Combined GPS-Photogrammetric Block Adjustment Results

Based on GPS-derived coordinates of the exposure stations, various ground control configurations (Figure 4. 1), and image coordinates of all tie and control points, combined GPS-photogrammetric block adjustment were carried out for different scenarios according to Table 4. 5. As depicted in this table, different ground control distributions, self calibration, and cross strips were considered.

Table 4. 5. Methodologies For Combined GPS-Photogrammetric Block Adjustment

Method	Ground Control Configuration	Self Calibration (Basic Interior Orientation)	Cross Strips	3D Transformation	σ_{GPS} (m)	σ_{GCP} (m)
1	A	No	NO	NO	0.25	0.1
2	B	No	NO	NO	0.25	0.1
3	B	YES	NO	NO	0.25	0.1
4	C	NO	YES	NO	1000.0	0.1
5	C	YES	YES	NO	1000.0	0.1
6	D	NO	YES	NO	0.25	0.1
7	D	YES	YES	NO	0.25	0.1
8	D	YES	YES	YES	0.25	0.1

The Root Mean Square Error (RMSE) of the check points for Jackson project is shown in Figure 4. 51 for all scenarios. As shown in this Figure, there is a systematic error associated with Z (two times greater than that of X or Y coordinate) when applying no self-calibration and using no cross strips. Applying self-calibration (basic interior orientation parameters) and including cross strips removes this systematic error, and implies that fixing the wrong focal length in a bundle block adjustment has a direct impact on the Z coordinate. Another conclusion is that there is still a need for vertical control across the block which can be replaced by cross strips. The common conclusion is that using self-calibration techniques, and including cross strips, improved the accuracy of the block especially in Z coordinate. The theoretical accuracy obtained from inversion of normal matrix was also compatible to the practical accuracy obtained from check point coordinates (Figure 4. 52).

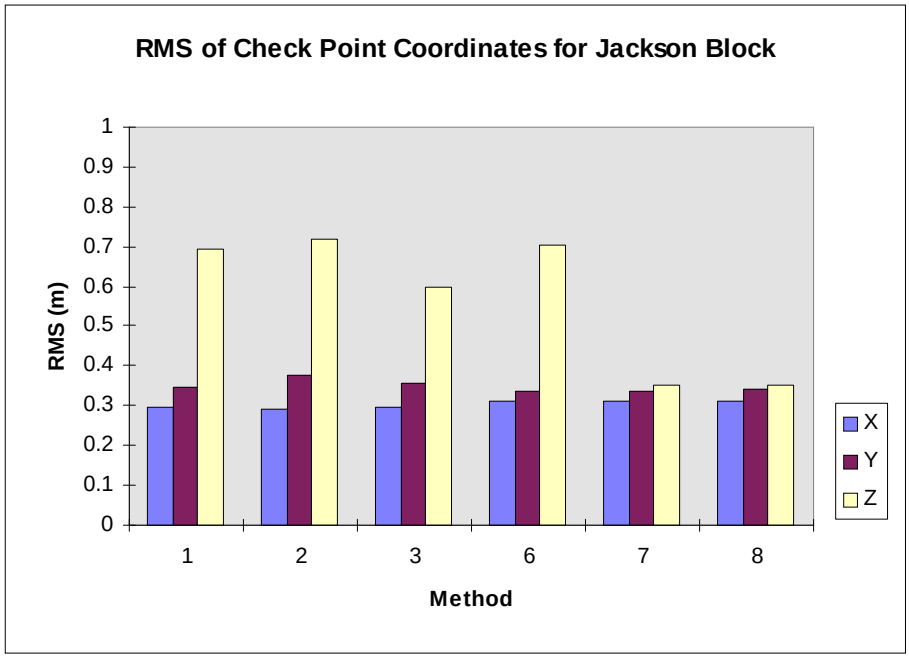

Figure 4. 51. RMSE of All Check Points

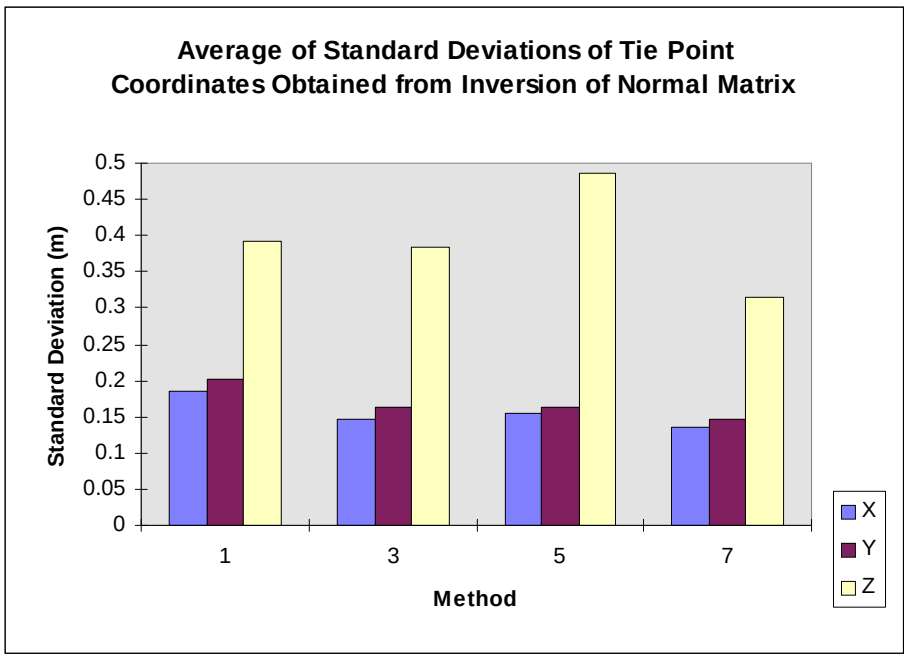

Figure 4. 52. Standard Deviations of All Tie and Pass Points

To determine whether incorporating additional self-calibration parameters would improve the results, self-calibration block adjustments were carried out using three

models for formulating additional parameters, namely: conventional radial and decentring distortion model (method 7-1), Brown's formulation (method 7-2), and harmonic functions (method 7-3). For this purpose, six control points were used and cross strips were also included in the adjustment. Figure 4. 53 shows the RMSE of check points when additional parameters were applied. It can be seen that the conventional model for additional parameters offered better results (method 7-1) compared to the results obtained from the other two methods. Comparing Figure 4. 53 and Figure 4. 51 show that an improvement of 30 mm in Z was feasible when applying additional parameters.

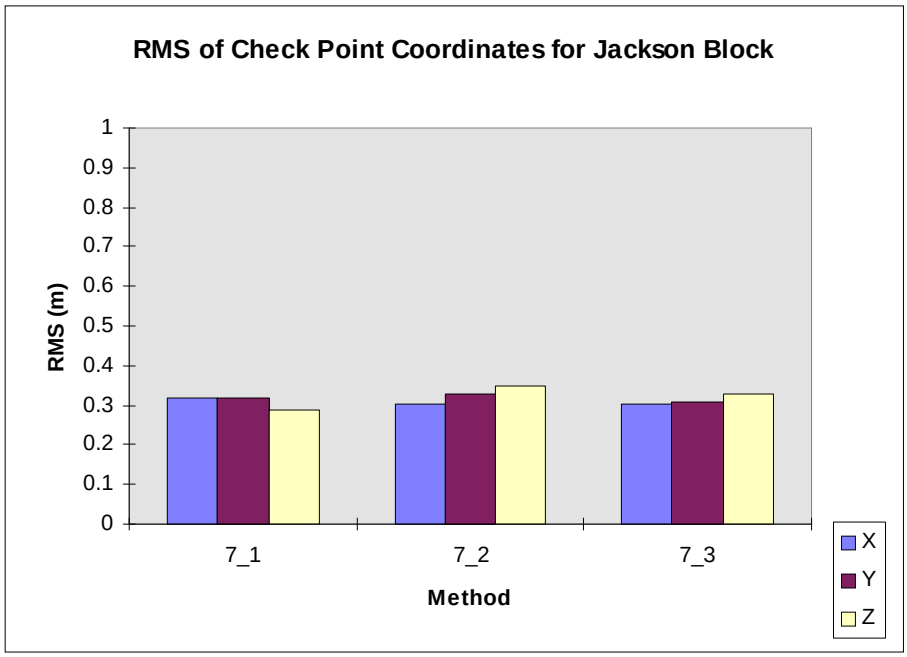

Figure 4.53. RMSE of Check Points (Additional Parameters included in The Adjustment)

To assess change in focal length from laboratory calibrated value, and the focal length obtained from self-calibration block adjustment, Figure 5. 54 shows this value for various methods. There is a 50 μm difference (1.2 m in Z in the object coordinate system)

between the focal length obtained from laboratory and the one obtained from Method 7-1.

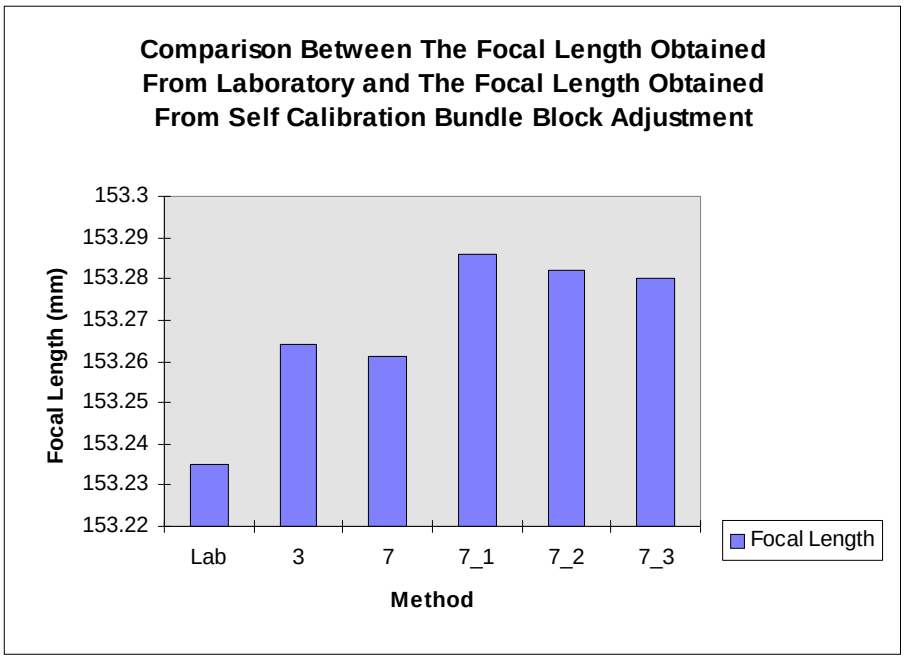

Figure 4. 54. Focal Length Obtained From Various Methods

In the reliability analysis, redundancy numbers and external reliability factors of image coordinates, GPS observations of exposure stations, and ground control points were extracted using the variance covariance matrix of residuals and weight matrix of observations. Figures 4. 55 - 4. 57 show the redundancy numbers for these three types of observations, and for various processing methods. Redundancy numbers for both x and y image coordinates obtained from Methods 6, 7, and 8 (GPS-assisted) are better than those obtained from Methods 4 and 5 (conventional block adjustment) confirming that incorporating GPS coordinates of the camera exposure stations into the photogrammetric block improves the reliability of image coordinates. Redundancy numbers for image coordinates obtained from method 2 or 3 (4 ground control points included) and those of

Method 1 (no ground control point) are almost the same, therefore, including ground control points in the GPS-photogrammetric block has little impact on the reliability of image coordinates. Redundancy numbers of GPS coordinates of the camera exposure stations are the same for all processing methods (Figure 4. 56). This was expected due to the fact that GPS exposure station coordinates were assigned the same precision for all methods. Including cross strips in a GPS photogrammetric block adjustment improves not only the accuracy of the block but the reliability of the ground control points as well (Figure 4. 57).

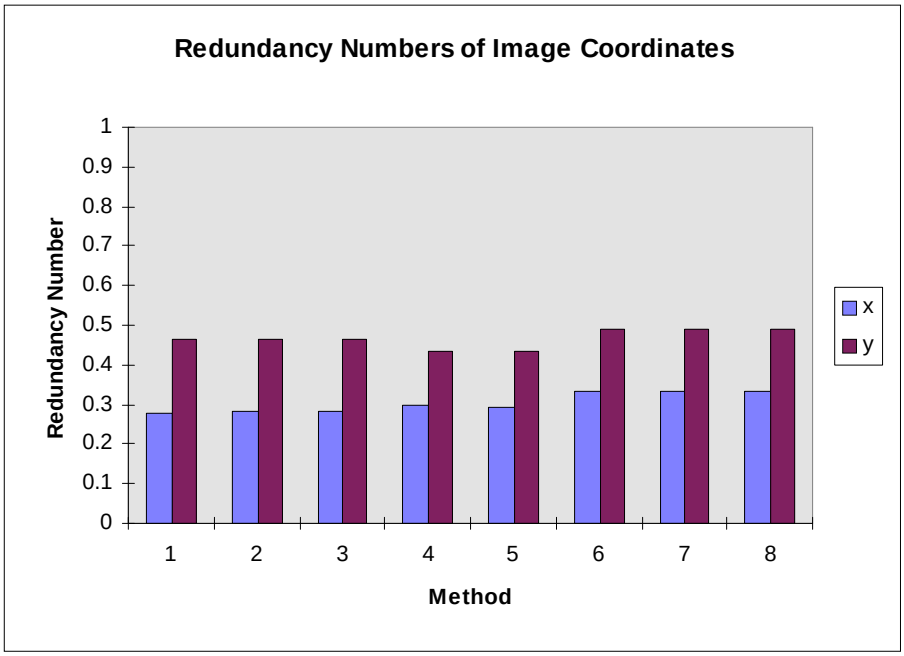

Figure 4. 55. Reliability Analysis of Image Points

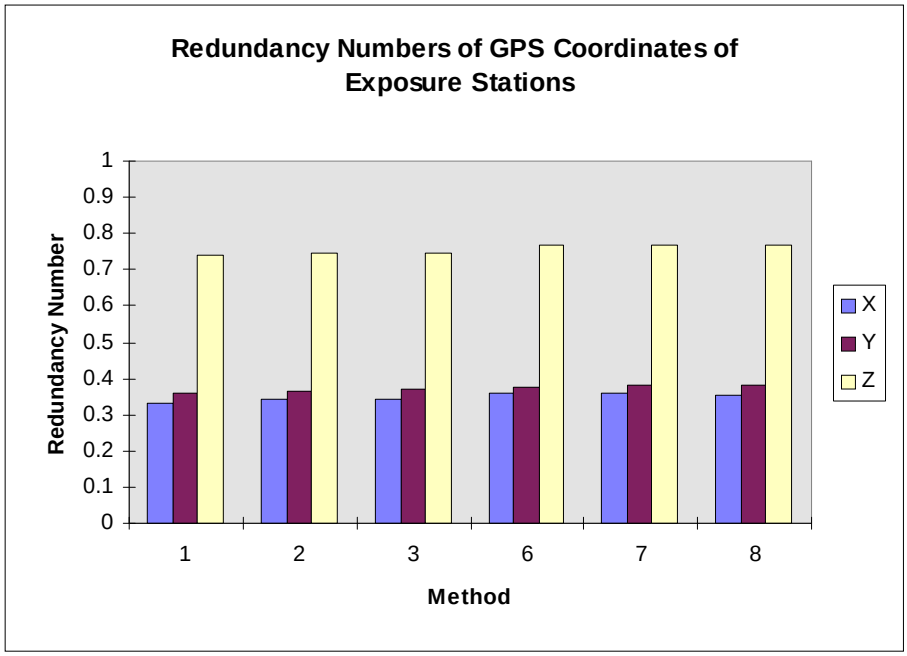

Figure 4. 56. Reliability Analysis of GPS Camera Exposure stations

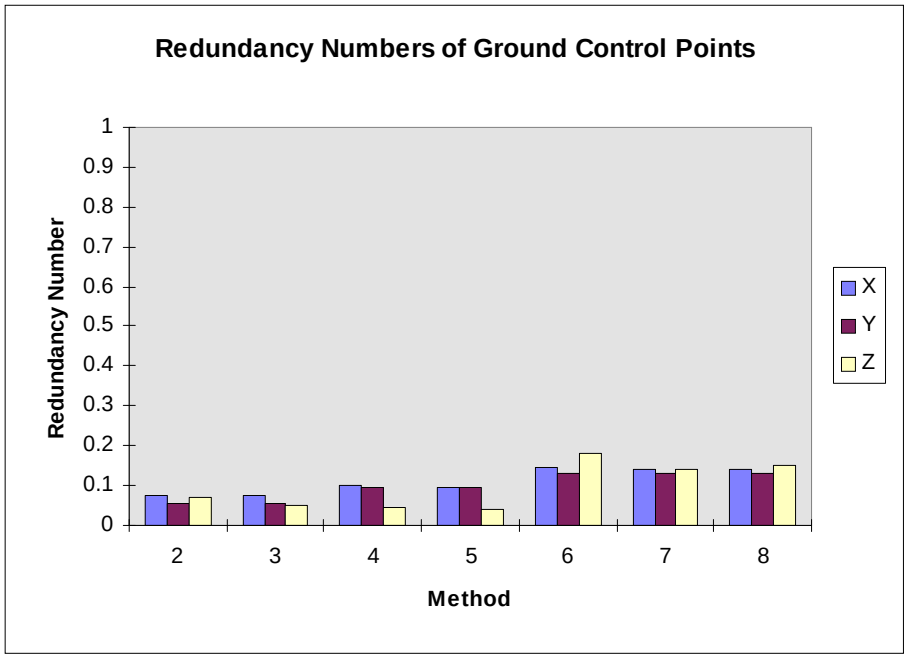

Figure 4. 57. Reliability Analysis of Ground Control Points

The external reliability factors of image coordinates, GPS coordinates of the exposure stations, and ground control points are shown in Figures 4. 58 - 4. 60. From the

external reliability point of view, Methods 6. 7, or 8 offered better results when compared to other methods.

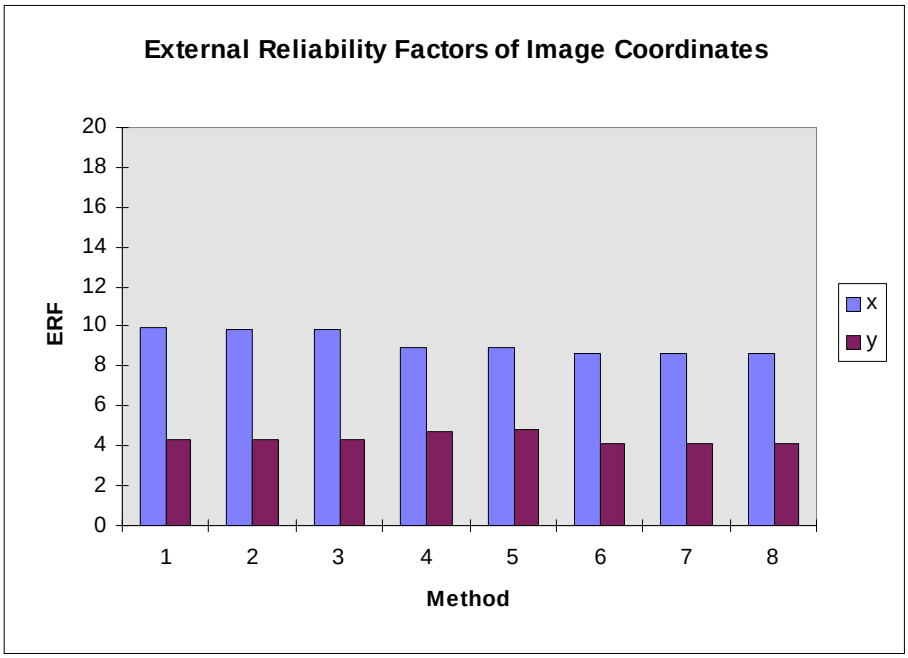

Figure 4. 58. External Reliability Factors of Image Points

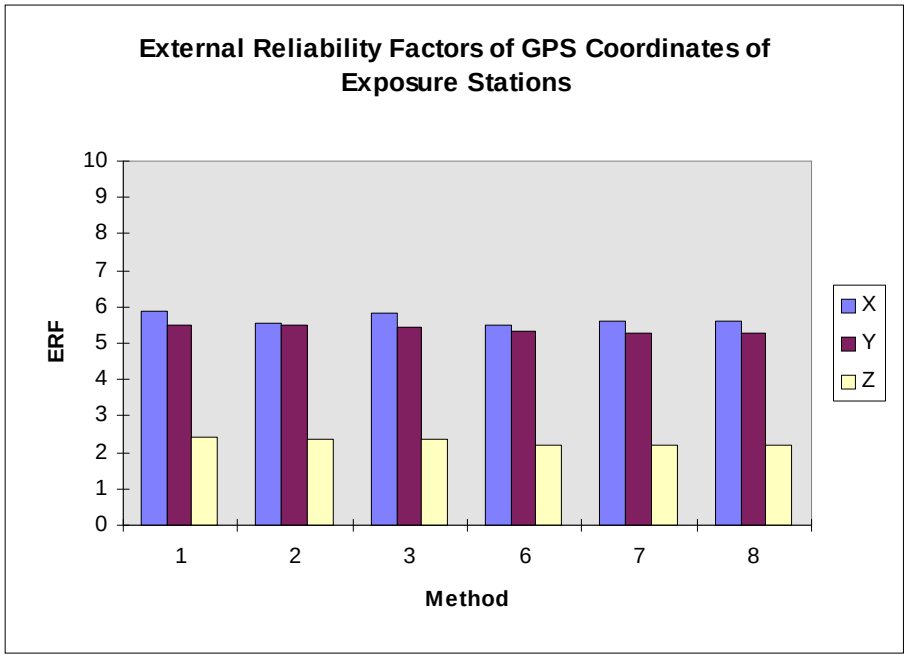

Figure 4. 59. External Reliability Factors of GPS Data

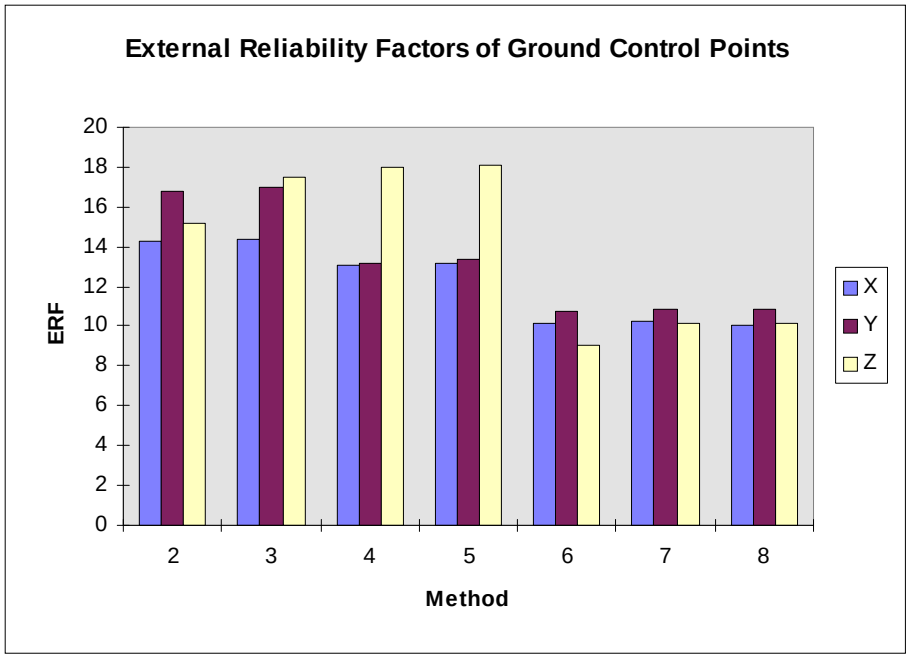

Figure 4. 60 External Reliability Factors of Ground Control Points

REFERENCES

Ackermann , F.E. (1966), *On the Theoretical Accuracy of Planimetric Block Triangulation*, *Photgrammetria*, Vol. 21, pp. 145-170.

Ackermann, F.E. (1974), *Accuracy of the Statoscope Data: Results from OPEEPE test Oberschwaben*, ISP Symposium, Commission III, Stuttgart, Germany.

Ackermann, F.E. (1975), *Results of Recent Test in Aerial Triangulation*, **Photogrammetric Engineering and Remote Sensing**, Vol. 41, No. 1, pp. 91-99.

Ackermann, F.E. (1984), *Utilization of Navigation Data for Aerial Triangulation*, Commission III, ISPRS Congress, Rio de Janeiro.

Ackermann, F.E. (1992), *Operational Rules and Accuracy Models for GPS Aerial Triangulation*, **International Archives of Photogrammetry and Remote Sensing**, Washington D.C., pp. 691-700.

Ackermann, F.E. (1994), *On the Status and Accuracy Performance of GPS Photogrammetry*, **Proceedings of Mapping and Remote Sensing Tools for the 21st Century**, Washington D.C., August 26-29, pp 80-90.

Ackermann, F.E. and H. Schade (1993), *Application of GPS for Aerial Triangulation*, **Photogrammetric Engineering and Remote Sensing**, Vol 59, No. 11, pp.1625-1632.

Alobaida, A., (1993), *Design and Simulation of a Real-Time Mapping Satellite for the Kingdom of Saudi Arabia*, Ph.D. Dissertation, Department of Geodetic Science and Surveying, The Ohio State University.

Baarda, W., 1968, *A Testing Procedure for Use in Geodetic Networks*, Netherlands Geodetic Commission, Publications on Geodesy, New Series, Vol. 2, No. 5, Delft, Netherlands.

Blais, J.A.R. (1976), *SPACE-M; Spatial Photogrammetric Adjustment for Control Extension using Independent Models*, Commission III, ISPRS Congress, Helsinki, Finland.

Blais, J.A.R. and M.A. Chapman (1984), *The Use of Auxiliary Airborne Sensor Data in SPACE-M Photogrammetric Block Adjustment*, **The Canadian Surveyor**, Vol. 38, No. 1, pp. 3-14.

Brown, D.C. (1966), *Decentring Distortion of Lenses*, **Photogrammetric Engineering**, Vol. 32, No.3, pp. 444-462.

Brown, D.C. (1976), *The Bundle Adjustment: Progress and Prospects*, **XIIIth international congress for photogrammetry**, Helsinki, Finland.

Brown, D.C. (1979), *Establishment of Photogrammetric Control by Satellite Doppler Positioning*, **Proceedings of the international Symposium on Current Trends in the Development, Execution, and use of Aerial Triangulation**, Brisbane, Queensland.

Burman H., and K. Toleg à rd (1994), Empirical Results of GPS Supported Block Triangulation, OEEPE Publication.

Cannon, M.E. (1991), *Airborne GPS/INS with an Application to Aerotriangulation*, **Ph.D. Dissertation,** Department of Geomatics Engineering, University of Calgary, Calgary.

Chapman, M.A. (1994), *Lecture Notes on Digital Stereo Image Matching*, Department of Geomatics Engineering, University of Calgary, Calgary.

Colomina, I. (1993), *A Note on the Analysis of Aerial Triangulation with GPS Aerial Control*, **Photogrammetric Engineering and Remote Sensing**, Vol 59, No. 11, pp. 1619-1624.

Corten, F.L. (1960), *Survey Navigation and Determination of Camera Orientation Elements*, **Photogrammetria**, Vol 15., pp. 251-281.

Corten, F.L. and F.J. Heimes (1976), *Integrated Flight and Navigation System*, Commission I, ISPRS Congress, Helsinki, Finland.

Curry, S. and K. Schuckman (1993), *Practical Considerations for the Use of Airborne GPS for Photogrammetry*, **Photogrammetric Engineering and Remote Sensing**, Vol 59, No. 11, pp.1611-1617.

Ebadi, H. and M.A. Chapman (1995), *An Experience on GPS Assisted Aerotriangulation*, **Proceedings of the 7th international conference on Geomatics**, June 13-15, Ottawa.

Ebner, H. (1972), *Theoretical Accuracy Models for Block Triangulation*, Bildmessung Und Luftbildesen, Vol 40, pp. 214-221.

Ebner, H. (1976), *Self Calibrating Block Adjustment*, Invited Paper of Commission III, ISP Congress, Helsinki, Finland.

El Hakim, S.F. (1979), *Potentials and Limitations of Photogrammetry for Precision Surveying*, **Ph.D. Dissertation,** Department of Geodesy and Geomatics Engineering, University of New Brunswick, Fredericton.

Faig, W. (1976), *Independent Model Triangulation with Auxiliary Vertical Control*, Commission III, ISPRS Congress, Helsinki, Finland.

Faig, W. (1979), *Canadian Experiences in the Adjustment of Large Photogrammetric Blocks with Auxiliary Vertical Control*, **Proceedings of the international Symposium on Current Trends in Aerial Triangulation,** Brisbane, Queensland.

Faig, W. (1985), *Lecture Notes on Aerial Triangulation and Digital Mapping*, **Monograph 10**, School of Surveying, The University of New South Wales, Kensington, N.S.W., Australia.

Faig, W. and T.Y. Shih (1989), *Should One Consider Combining Kinematic GPS with Aerial Photogrammetry?*, **Photogrammetric Engineering and Remote Sensing**, Vol. 55, No. 12, pp. 1723-1725.

Förstner, W., 1985, *The Reliability of Block Triangulation*, **Photogrammetric Engineering and Remote Sensing,** Vol. 51, pp. 1137-1149.

Fraser, C. S. (1995), *Observational Weighting Considerations in GPS Aerial Triangulation*, **Photogrammetric Record**, 15(86), pp. 263-275.

Frieβ, P.(1987), *The NAVSTAR Global Positioning System for Aerial Photogrammetry*, **Proceedings of the 41st photogrammetric week at Stuttgart University**, Stuttgart, Germany.

Frieβ, P. (1991), *GPS Supported Aerial Triangulation, Empirical Results*, **Proceedings of the 2nd international workshop on high precision navigation**, Dummler, Verlag, Bonn, Germany, pp. 7-18.

Frieβ, P. (1992), *Experience with GPS Supported Aerial Triangulation*, **Proceedings of ISPRS**, Commission I, Vol. 29, Part B1, Washington D.C., pp. 299-305.

Gelb, A. (1974), *Applied Optimal Estimation*, **The MIT Press,** Cambridge, Mass, U.S.A.

George, A. and J. Liu, (1995), *Computer Solution Of Sparse Linear Systems*, Publication of The Computer Science Department, University Of Waterloo, Canada.

Greening, W. J., B. A. Chaplin, D. G. Sutherland, and D. E. DesRoche (1994), *Commercial Applications of GPS-Assisted Photogrammetry*, Proceedings of the Fourth GPS/GIS Conference, Washington, D.C., pp. 391-402

Grüen, A. (1978), *Experience with Self Calibrating Bundle Adjustment*, ASP annual meeting, Washington D.C.

Hanson, R.H., (1978), *A Posteriori Error Propagation*, Proceedings Of The Second International Symposium On Problems Related To The Redefinition Of North American Geodetic Networks, Washington, D.C., National Geodetic Information Centre, NOAA, pp. 427-445.

Jacobsen, K. (1996), *A New Approach of Combined Block Adjustment Using GPS-Satellite Constellation*, **Proceedings of the International Congress on Photogrammetry and Remote Sensing**, Commission III, Vienna, Austria, Vol. XXXI, Part B3, pp. 355-359

Jenning, A., (1977), *Matrix Computation For Engineers And Scientists*, John-Wiley & Sons, New York, N.Y.

King, J.P., (1970), *An Automatic Reordering Scheme For Simultaneous Equations Derived From Network Systems*, International Journal For Numerical Methods in Engineering, Vol. 2, pp. 523-533.

Krakiwsky, E .J. (1990), *The Method of Least Squares: A Synthesis of Advances*, UCGE Report No. 10003, Department of Geomatics Engineering, University of Calgary.

Lachapelle, G., Cannon, M.E., and H. Schade (1993), *An Accuracy Analysis of Airborne Kinematic Attitude Determination with the NAVSTAR Global Positioning System*, **SPN**, pp. 90-95.

Lapine, L., (1991), Analytical Calibration of the Airborne Photogrammetric System Using A Priori Knowledge of the Exposure Station Obtained from Global Positioning System Technique, Ph.D. Dissertation, Department of Geodetic Science and Surveying, The Ohio State University, Publication No. 9111738, Ann Arbor, MI 48109

Li, D. and S. Jie (1989), *Quality Analysis of Bundle Block Adjustment with Navigation Data*, **Photogrammetric Engineering and Remote Sensing**, Vol. 55, No. 12, pp. 1743-1746.

Lucas, J.R. (1987), *Aerotriangulation without ground control*, **Photogrammetric Engineering and Remote Sensing**, Vol. 53, No. 3, pp. 311-314.

Milbert, D.G., (1984), *Heart Of Gold: Computer Routines For Large, Sparse, Least Squares Computations*, NOAA Technical Memorandum NOS NGS-39.

Molenaar, M. (1984), *The Connection of Aerotriangulation Blocks and Ground Control Reconsidered*, Commission III, ISPRS Congress, Rio de Janeiro, pp. 721-736.

Moniwa, H. (1977), *Analytical Photogrammetric System with Self Calibration and its Applications*, **Ph.D. Dissertation**, Department of Geodesy and Geomatics Engineering, University of New Brunswick, Fredericton.

Schut, G.H. (1968), *Formation of Strips from Independent Models*, **Photogrammetric Engineering**, Vol 34., No. 7., pp. 690-695.

Salmenpera, H., Anderson, J.M., and A. Savolainen (1974), Efficiency of The Extended Mathematical Model In Bundle Adjustment, Bildmessung Und Luftbildwesen, Vol. 6.

Schwarz, K.P., Chapman, M.A., Cannon, M.E., and P. Gong (1993), *An Integrated INS/GPS Approach to the Georeferencing of Remotely Sensed Data*, **Photogrammetric Engineering and Remote Sensing**, Vol. 55, No. 12, pp. 1667-1674.

Vani′ček , P., E. J. Krakiwsky, M. R. Craymer, Y. Gao, and P. S. Ong, 1991, Robustness Analysis, Technical Report No. 156, Department of Geodesy and Geomatics Engineering, University of New Brunswick, Canada.

Zarzycki, J.M. (1972), *The Use of Auxiliary Data in Aerial Triangulation*, Commission III, ISPRS Congress, Ottawa.

APPENDIX A

GAP (GENERAL ADJUSTMENT PROGRAM)

A. 1 Introduction/Overview

GAP is an integrated GPS, photogrammetric, and geodetic adjustment program developed for this research. It can be used to adjust a geodetic network (e.g., distances, directions, azimuths), a photogrammetric block (e.g., image coordinates, exterior orientation parameters) or a combined geodetic photogrammetric block. It can also incorporate GPS positions of the exposure stations into the block adjustment.

GAP was originally developed in Standard FORTRAN 77 and then upgraded to FORTRAN 90. One of the important features of FORTRAN 90 is that it allows dynamic memory allocation. The routines of this program are highly transportable; no machine dependent features and no operating system calls are embedded in the code.

A. 2 Sparse Matrix Solution

The bundle block adjustment usually requires the solution of large system of non-linear equations with sparse structured and symmetric coefficient matrices. It can be shown that normal equations for a least squares problem are symmetric. The first objective is to exploit the structure of normal equations by storing only the upper (or

lower) triangular portion of normal matrix N (Equation 3. 36). The unknown parameters, X, can be ordered such that the non-zero elements of N will fall in a diagonal band whose width is small compared to the dimension of the system. Figure A. 1. shows an example of this band storage structure.

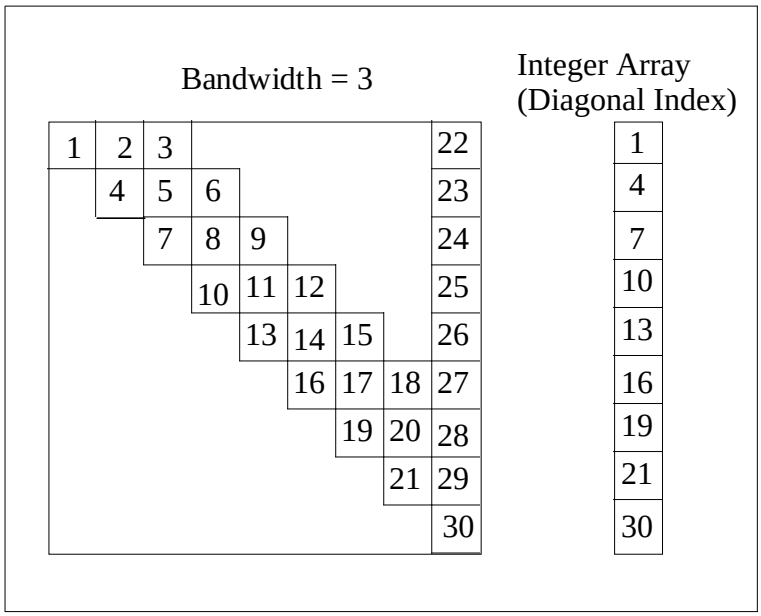

Figure A. 1. Fixed Bandwidth Storage Structure (from Milbert, 1984)

Here, all non-zero elements fit into a bandwidth of three. This structure can be described by storing the array indices of the diagonal elements in an integer array. If the bandwidth is one, the system is diagonal. Conversely, if the bandwidth is equal to the order of the normal matrix, then the system is full and sparse structure is not exploited. Greater savings in storage and execution times can be achieved by using a variable bandwidth (profile) structure (Jennings, 1977). Figure A. 2. shows this structure.

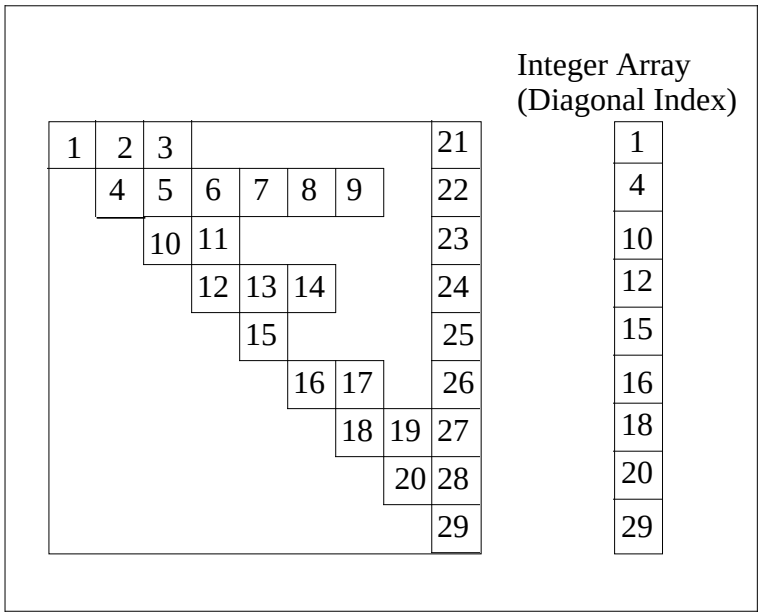

Figure A. 2. Variable Bandwidth Storage Structure (from Milbert, 1984)

The structure is again described by an index array. GAP is able to process large least squares system by exploiting the sparse non-zero structure of a problem. Speed in execution is attained by using a static data structure (Milbert, 1984) meaning that the rows of the system are stored end-to-end in a single array. The price paid for this rapid processing is that the structure of each least squares problem should be known before the equations are accumulated and solved. GAP consists of two modules: the first module performs the analysis of the structure of a least squares problem stored in an integer array, while the second module solves the normal equations using the predetermined structure. The elements of the normal equations are saved in a real array to further improve storage. The first module carries out the following tasks:

* Initialization of integer array to hold the address of the diagonal elements,

* Accumulation of connectivity information based on graph theory (George and Liu, 1995),
* Analysis of the structure and minimization of the bandwidth of normal equations.

King's algorithm (King, 1970) was used to reorder the unknowns. He applied this algorithm to simultaneously solve the equations derived from network systems.

Once a structure has been determined, the least squares problem is ready to be solved. The observation equations (e.g., image coordinates, exterior orientation parameters, GPS observations, ground control points) are accumulated one at a time into the normal equations. After all the observations have been processed, the system is solved using a cholesky factorization approach. A singularity can be detected by using a small positive, singularity tolerance.

In addition to the solution vector $\hat{X}$ of a least squares solution, statistics information (e.g., variances of unknowns) which is the diagonal elements of $\sum \hat{x}$ can be obtained by inverting the normal matrix, N. Hanson (1978) showed that the inverse elements of the normal equations can be computed within the profile in place at no greater cost than computing only the diagonal elements of the inverse. Variances of the adjusted observations and variances of the residuals can also be derived to carry out the reliability analysis.

Data abstraction and modularity which are important factors for structured programming have been considered in developing the GAP. Data abstraction separates logical view of the data from the internal storage structures, while modules perform specific tasks and make a minimum number of assumptions about processes in other parts of the program (Milbert, 1984). The modules were designed as subprograms sharing common variables in order to allow the user ease in discarding routines not needed for a particular application.

A. 3 Program Organization

The main flowchart of the program is shown in Figure A. 3. All observations (photo coordinates, control points, exterior orientation parameters) are treated as weighted observations with appropriate weights. Therefore, to solve for orientation angles, high standard deviations must be assigned to these angles. On the other hand, to constrain the positions of exposure stations (e.g., GPS data), low standard deviations should be considered for these positions.

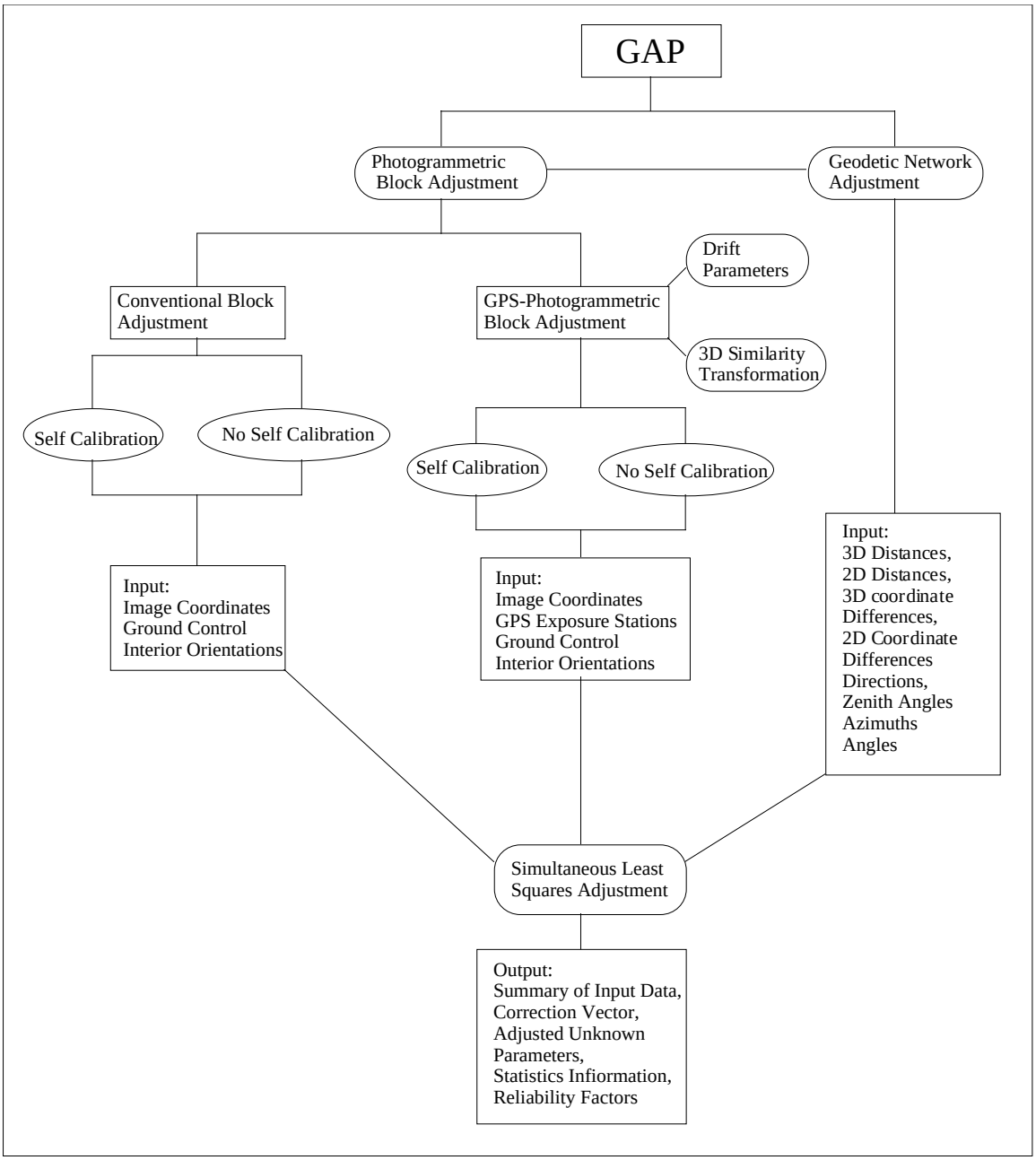

Figure A.3. Flowchart of GAP

Due to the huge number of unknowns for a large block of photography, the "KING" reordering scheme (King, 1970) was adopted to minimize the bandwidth of the normal equations and reduce the memory and CPU requirements. GAP can be run in both

conventional block adjustment mode in which all 6 exterior orientation elements are solved as unknowns using ground control points and GPS assisted block adjustment mode where coordinates of exposure stations are constrained using GPS data.

In GPS assisted aerial triangulation, the antenna should be located directly over the camera for best results. In this case, there is a Z shift (Z coordinate in GPS_OFFSET), otherwise, the camera should be locked in place during the flight or the crab angle should be recorded whenever changed. The standard deviations of exposure stations should be selected in such a way that they reflect the accuracy of GPS camera stations.

A. 4 Advanced Program Features

GAP also supports self-calibration bundle block adjustment. This means that the interior orientation and additional parameters can also be estimated to further improve the accuracy. There are 4 interior orientation parameters: the camera constant, the principal point coordinates, and the y-axis scale factor for the case of a CCD camera. GAP permits photowise, blockwise, or stripwise solution of these parameters. It is necessary to include standard deviations for these parameters when applying self calibration. Principal point coordinates are difficult to estimate in a self-calibration mode with aerial photography due to a high correlation with the camera leveling angles. Thus, their standard deviations should be set to small values. The y-axis scale factor is used when there is a scale

difference between the x and y photo axes. This is normally applicable to CCD cameras but may be useful to improve the results of conventional block adjustment.

GAP can also solve for GPS drift parameters by including the GPS exposure time of each photo and an index vector in order to apply them on stripwise basis. It is important that the GPS be processed in a special way to take advantage of the drift and offset parameters being solved for each strip. It is also necessary to add cross strips to the block to make it possible to solve for these extra parameters (6 per strip) with a minimum ground control configuration (4 GCPs).

GAP can also perform reliability analysis in which the redundancy numbers, internal reliability factors, and external reliability factors of various observations are computed based on standardized residuals. The statistical information pertaining to the adjustment parameters can be obtained by setting the appropriate flag in the input file. This requires that the least squares normal matrix be inverted.